

---

# **THE ROLE OF VASCULAR NADPH OXIDASE ENZYMES IN INFLUENZA MORBIDITY**

---

A thesis submitted to the Faculty of Medicine Nursing and Health Sciences



For the degree of Doctor of Philosophy  
Keshia Sarah Hendricks  
May 2018

Department of Pharmacology  
Biomedicine Discovery Institute  
Monash University  
Melbourne, Victoria  
Australia

**Copyright Notice**

© Keshia Hendricks (2018).

I certify that I have made all reasonable efforts to secure copyright permissions for third-party content included in this thesis and have not knowingly added copyright content to my work without the owner's permission.

## Contents

Copyright Notice .....	2
Declaration .....	5
Acknowledgements.....	6
Conference Abstracts.....	7
Abbreviations .....	8
Units of measurement .....	12
Summary .....	13
<b>Chapter One: General Introduction.....</b>	<b>15</b>
The Global Burden of Influenza Infection .....	16
A Double-Edged Sword: The Host Response to Influenza Virus Infection .....	20
Viral Entry and Replication.....	21
The First Line of Defence: The Toll-Like Receptors .....	24
Reactive Oxygen Species: Key contributors to the inflammatory response.....	26
Structure and Function of the NADPH oxidases .....	28
The Role of the NADPH oxidases in Inflammatory Disorders .....	32
Implicating the NADPH Oxidases in Influenza pathology .....	35
Emerging Evidence for a Role of the Endothelial Cells in Influenza Pathology.....	38
Nox4 Oxidase: Friend or Foe? .....	39
Cardiovascular Complications of Influenza Infection.....	40
Rationale .....	43
References.....	45
<b>Chapter Two: Influenza-Induced Endosomal Superoxide Production in Endothelial Cells .....</b>	<b>60</b>
Abstract .....	61
Introduction .....	62
Methods.....	65
Results .....	72
Discussion.....	84
References.....	89
<b>Chapter Three: Determining the effect of toll-like receptor activation on vascular tone .....</b>	<b>92</b>
Abstract .....	93
Introduction .....	94
Method.....	97
Results .....	99
Discussion.....	109
References.....	113

<b>Chapter Four: Endothelial Nox4 oxidase negatively regulates airway neutrophil infiltration and alleviates influenza virus pathology</b> .....	117
Abstract .....	118
Introduction .....	119
Methods.....	122
Results.....	128
Discussion.....	146
References.....	150
<b>Chapter Five: General Discussion</b> .....	154
Summary of Major Findings.....	155
Chapter 2: Influenza infected induces Nox2-dependent endosomal ROS production ....	157
Chapter 3: Activation of TLR3 and TLR7 leads to vascular relaxation through distinct pathways .....	160
Chapter 4: Endothelial Nox4 oxidase negatively regulates airway neutrophil infiltration and alleviates influenza virus pathology. ....	161
Expanding the paradigm: Influenza and the Vasculature .....	162
Pharmacological Intervention .....	163
Future directions.....	164
Concluding Remarks.....	164
References.....	166
Appendix .....	168

## Declaration

This thesis contains no material which has been accepted for the award of any other degree or diploma at any university or equivalent institution and that, to the best of my knowledge and belief, this thesis contains no material previously published or written by another person, except where due reference is made in the text of the thesis.

**Student signature:**

A solid black rectangular box redacting the student's signature.

**Date:** 31/07/2018

The undersigned hereby certify that the above declaration correctly reflects the nature and extent of the student's contributions to this work.

**Main Supervisor signature:**

A solid black rectangular box redacting the main supervisor's signature.

**Date:** 31/07/2018

## Acknowledgements

First of all, I would like to thank my supervisor, Dr Stavros Selemidis. Without the encouragement and support I received from him, and without his contagious enthusiasm for science, this thesis would never have been completed.

I would like to acknowledge the facilities, scientific and technical assistance of Monash Micro Imaging and the Monash Histology Platform (Monash University, Clayton Campus Australia). I would also like to acknowledge Dr Bradley Broughton for picking up the pigs' hearts and for his invaluable advice on immunocytochemistry. I would like to thank Assoc Prof John Stambas and Prof Patrick Reading, for providing the virus, Prof Ajay Shah, for providing the Nox4 transgenic mice, and Dr Hitesh Peshavariya, for providing the Nox2<sup>-/-</sup> MLEC. I would like to thank Dr Chrishan Samuel and Krupesh Patel for their assistance with the differential cell staining, and Dr Barbra Kemp-Harper, for her assistance with the organ bath studies.

I would like to thank the Monash Pharmacology Department, including researchers past and present, for providing a supportive and friendly environment to work in. They were always willing to help, full of encouragement and advice, and always good for a laugh. I would like to give some very special thanks to the other members of OXIB. In particular, I'd like to thank Dr Eunice To, Ray Luong, Jonathan Erlich, Felicia Liong who all assisted with the animal experiments in chapter 4. You're all brilliant researchers and I can't wait to see what you come up with next.

Last of all, I would like to thank my family, Dad, Papa and Saby, for always being there for a me. I love you all heaps. An extra big thanks to Mum. I hope I've made you proud.

### Conference Abstracts

Hendricks, K, To, E, Vlahos, R, Broughton, B, Peshavariya, H, Selemidis, S (2016a). Influenza A virus causes vascular endothelial cell oxidative stress via NOX2 oxidase. *Eur. Respir. J.* **48**:

Hendricks, KS, To, EE, Broughton, B, Peshavariya, H, Vlahos, R, Selemidis, S (2016b). Influenza A virus (IAV) causes vascular endothelial cell oxidative stress via Nox2 NADPH oxidase. *Respirology* **21**: 21–100.

## Abbreviations

-/-	Knockout
AAL-R	Sphingosine-1-phosphate analogue
AKT	Protein kinase B
ALI	Acute lung injury
ANOVA	Analysis of variance
Apocynin	4-hydroxy-3-methoxyacetophenone/ acetovanillone
BaCl <sub>2</sub>	Barium chloride
BALF	Bronchoalveolar lavage fluid
C57BL6/J	Wild-type mouse
Ca <sup>2+</sup>	Calcium ion
CCL	CC chemokine ligand, chemokine with two adjacent cysteines
CD31	cluster of differentiation 31
cDNA	copy DNA
cGMP	Cyclic guanosine monophosphate
CO <sub>2</sub>	Carbon dioxide
CT	cycle threshold
CXCL	Chemokine (C-X-C motif) ligand, two N-terminus cysteines are separated by an amino acid
DAPI	4',6-diamidino-2-phenylindole
DMEM	Dulbecco's Modified Eagle's Medium
DMSO	Dimethyl sulfoxide
DNA	Deoxyribonucleic acid
DPI	Diphenyleneiodonium
Duox	Dual oxidase
EBM-2	Endothelial basal medium 2

EDHF	Endothelial-Derived Hyperpolarising Factor
EEA1	Early endosome antigen 1
EGM-2	Endothelial growth medium 2
eNOS	Endothelial nitric oxide synthase
ERK	Extracellular regulated kinase
FAD	Flavin adenine dinucleotide
FBS	Foetal bovine serum
Gp91ds-tat	Glycoprotein 91 double-stranded-tat
GTP	Guanosine triphosphate
H(number)N(number)	Influenza strain subtype referring to the specific haemagglutinin and neuraminidase components
H <sub>2</sub> O <sub>2</sub>	Hydrogen peroxide
HMEC	Human microvascular endothelial cell
HO1	Heme oxygenase 1
IFN	Interferon
IL	Interleukin
IRF	Interferon regulatory factor
JAK	Janus kinase
K <sup>+</sup>	Potassium ion
K <sub>ir</sub> channels	Inwardly rectifying potassium channel
K <sub>max</sub>	Maximum contraction in response to KPSS
KPSS	High potassium physiological salt solution
L-NAME	N(G)-Nitro-L-arginine methyl ester
L012	8-amino-5-chloro-7-phenylpyrido[3,4-d]pyridazine- 1,4(2H,3H)dione
LPS	Liposaccharides
M2	Matrix 2 Protein

MLEC	Mouse lung endothelial cell
MLCK	Myosin light chain kinase
mRNA	Messenger ribonucleic acid
MyD88	Myeloid differentiation primary response 88
NADPH	Nicotinamide adenine dinucleotide phosphate
NF-κB	Nuclear factor κB
NO	Nitric oxide
Nox	NADPH oxidase
NOXA2	Nox adaptor 2
NOXO1	Nox organiser 1
O <sub>2</sub>	Molecular oxygen
O <sub>2</sub> <sup>•-</sup>	Superoxide
OH <sup>•</sup>	Hydroxyl radical
ONOO <sup>-</sup>	Peroxynitrite
PBS	Phosphate buffered saline
PEG	Polyethylene glycol
Poly I:C	Polyinosine polycytidylic
PTP	Protein tyrosine phosphatase
RIG-I	retinoic acid-inducible gene I
RNA	Ribonucleic acid
ROS	Reactive oxygen species
RT-PCR	Real-time polymerase chain reaction
siRNA	Small interfering RNA
SK <sub>Ca</sub>	Small conductance calcium-activated potassium channels
SOD	Superoxide dismutase
STAT	Signal transducer and activator of transcription

TG	Transgenic
TLR	Toll-like Receptor
TNF	Tumour necrosis factor
TRAIL	Tumor necrosis factor-related apoptosis-inducing ligand
TRAF	TNF receptor-associated factor
TRIF	Toll/interleukin-1 receptor-domain-containing adapter-inducing interferon- $\beta$
TYK	Tyrosine kinase
U46619	thromboxane A2 agonist
WHO	World Health Organisation

## Units of measurement

ms	millisecond
$\mu$ s	microsecond
ns	nanosecond
g	gram
mg	milligram
$\mu$ g	microgram
ng	nanogram
cm	centimetre
mm	millimetre
nm	nanometre
$\mu$ l	microliter
M	molar
mM	millimolar
$\mu$ M	micromolar
U	units
MOI	multiplicity of infection
PFU	plaque forming units
pH	negative logarithm of hydrogen ion concentration
RLU	relative light units
rpm	rotations per minutes
SEM	standard error of the mean
%	percentage
$^{\circ}$ C	degrees Celsius
$K_m$	concentration of substrate at which half maximal velocity is observed

## Summary

Every year, up to half a million people lose their lives to influenza infection. Australia recently experienced the worst seasonal influenza epidemic since the 2009 Swine Flu pandemic. Due to antigenic drift, the vaccine was ineffective, particularly for the H3N2 strains. There is a constant search for more innovative treatments, particularly treatments that don't contribute to viral resistance.

Influenza is characterised by an exaggerated inflammatory response, oxidative stress, cardiovascular dysfunction, and lung damage. While most of the literature focuses on the primary cellular targets of influenza infection, epithelial cells and macrophages, recent evidence has implicated the endothelium in influenza-induced inflammation. The mechanisms by which the endothelium contributes to influenza pathology are unknown. Thus, this thesis examined the role of the endothelium in influenza pathology.

Recent studies have shown that the reactive oxygen species (ROS) generating Nox2-containing nicotinamide adenine dinucleotide phosphate (NADPH) oxidase exacerbates influenza-induced inflammation, and that the toll-like receptor (TLR) 3 and TLR7 activation drive Nox2 activity in endosomes; specific subcellular compartments of the cell. Chapter 2 of the present thesis demonstrated influenza A virus internalising into human microvascular endothelial cells (HMEC) *via* endocytosis, and showed influenza infecting endothelial cells *in vivo*. It was the first demonstration of influenza-induced endosomal ROS production in endothelial cells and demonstrated that TLR3 activation resulted in an increase in endosomal ROS production in endothelial cells. Chapter 2 was also the first demonstration that TLR3-induced expression of cytokines interleukin (IL) 6, chemokine (C-X-C motif) ligand (CXCL) 10 and tumour necrosis factor (TNF) $\alpha$  is Nox2-dependent, and that TLR3-induced expression of interferon (IFN)  $\beta$  was Nox2-independent.

The endothelium also plays an important role in regulating vascular tone. Hypotension is a common sign of cardiopulmonary insufficiency in influenza patients. Chapter 3 examined the effect of TLR3

and TLR7 activation on vascular tone. It was the first demonstration of TLR7 activation causing relaxation through apamin-sensitive potassium channels on the smooth muscle, and the first demonstration of TLR3 activation in the endothelium resulting in eNOS activation and relaxation.

While Chapter 2 showed that influenza infection in endothelial cells resulted in Nox2 activation, Nox4 is highly expressed in the endothelium and differs greatly from Nox2 in terms of structure, activation, function, and subcellular location. Nox4 has been shown to have a protective role against cardiovascular disease and ischemia, but its role in influenza infection is largely unknown. Utilising endothelial Nox4 overexpressing mice, Chapter 4 determined that endothelial Nox4 activity was protective against influenza morbidity, including airway inflammation, lung oedema, body weight, oxidative stress and viral titre.

In summary, this thesis has demonstrated three novel biological properties influenced by ROS. The first, that influenza infection results in a Nox2-dependent increase in endosomal ROS production in endothelial cells and that TLR3 induces cytokine production through Nox2-dependent and independent mechanisms. The second is that TLR3 and TLR7 activation induces relaxation of vascular smooth muscle through distinct pathways. Finally, that endothelial Nox4 is protective against influenza-induced morbidity. The pathways examined in this thesis provide a deeper understanding of influenza pathology that could lead to more innovative and beneficial treatments.

## **CHAPTER ONE:**

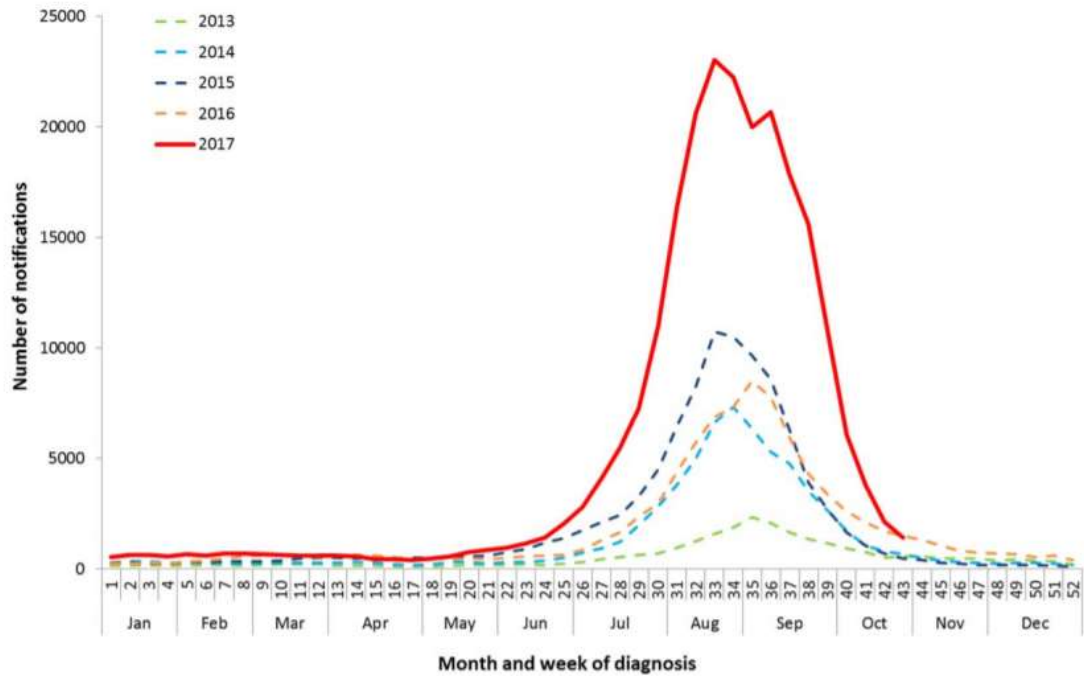
---

### **General Introduction**

---

### **The Global Burden of Influenza Infection**

Influenza continues to have an enormous global impact, despite advances in our understanding of the disease. Every year, the seasonal influenza epidemic results in up to half a million deaths worldwide, with three to five million people seriously ill (WHO, 2009). In addition to the seasonal influenza epidemics, there have been four major global pandemics in the last century. The first of these, the Spanish Flu of 1918, resulted in 50 to 100 million deaths (Johnson and Mueller, 2002). This was followed by the Asian Flu of 1957 and the Hong Kong Flu of 1968, the first known incidence of the H3N2 strain. The most recent, the 2009 H1N1 Swine Flu pandemic, resulted in up to 395 600 deaths, and up to 89 million people infected (Dawood *et al.*, 2012). While global incidents of influenza decreased in 2017, Australia had its worst influenza season since 2009 (Figure 1, Figure 2).



Source: NNDSS

**Figure 1.** Year by year comparison of confirmed influenza notification to the Australian National Notifiable Diseases Surveillance System (Graph taken from the Department of Health and Aging, 2017).

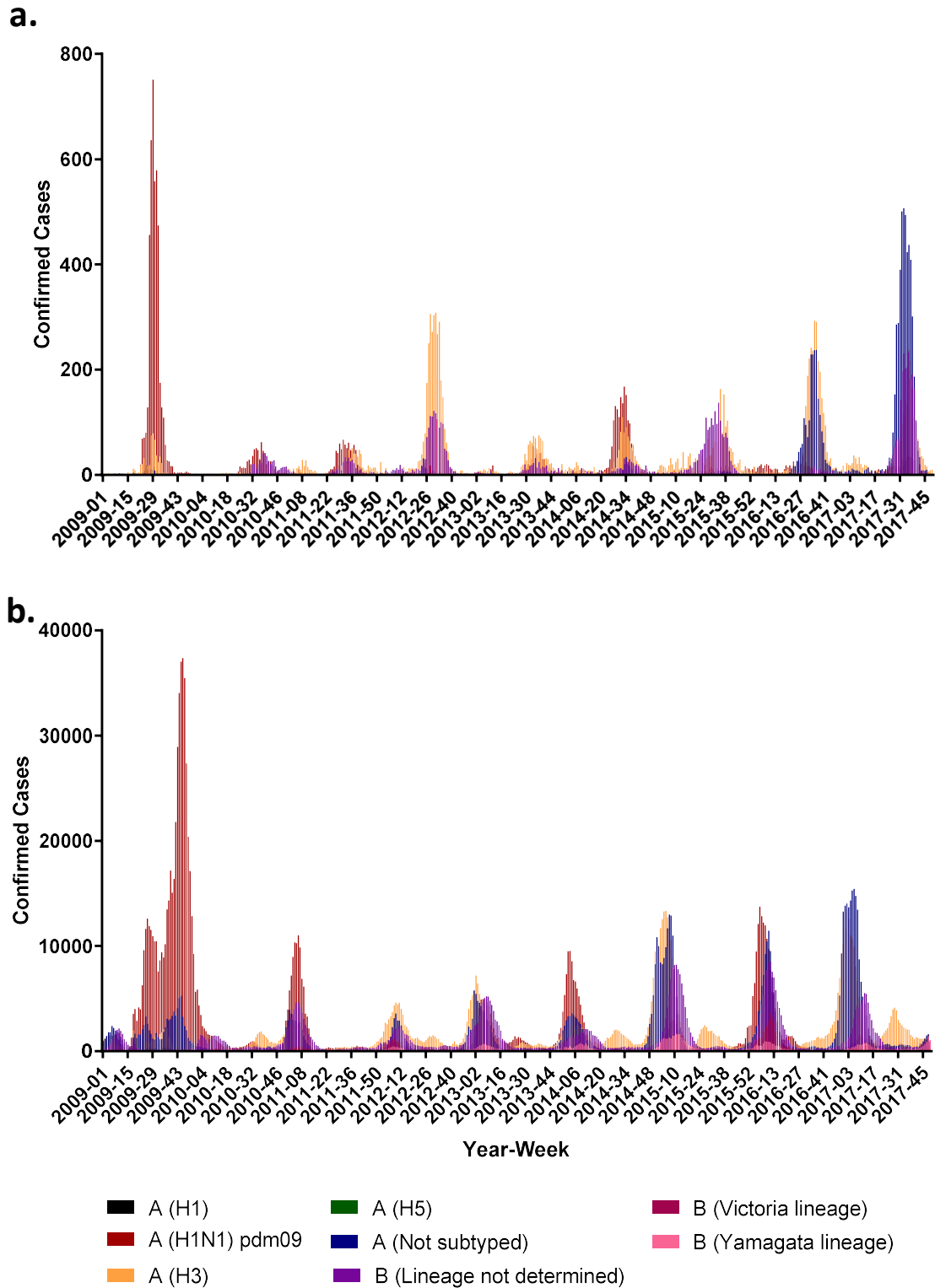


**Figure 2.** Number of influenza positive cases by subtype A. in Australia and B. all countries participating in the WHO surveillance program, from the 5<sup>th</sup> of November 2007 until the 25<sup>th</sup> of September 2017 (WHO, 2017).

In 2017, there were, 233 453 laboratory-confirmed influenza cases, including 745 deaths (Department of Health and Aging, 2017). In terms of the economic cost, influenza costs the United States up to 87 billion dollars annually (Molinari *et al.*, 2007) and the Australian Health Care System 115 million dollars annually, excluding indirect costs on business (Newall and Scuffham, 2008).

The current recommended treatment for influenza infection are the neuraminidase inhibitors, zanamivir and oseltamivir. Neuraminidase is a viral surface protein that cleaves sialic acid and allows the release of the newly replicated virus from the host cell. The neuraminidase inhibitors prevent this from occurring (Reviewed by Moscona, 2005). Initial clinical trials and a subsequent review found that oseltamivir and zanamivir reduced the duration of symptoms (Monto *et al.*, 1999; Nicholson *et al.*, 2000; Heneghan, *et al.* 2016). While the clinical trials found that oseltamivir and zanamivir to be well tolerated, the review by Heneghan *et al.* found that oseltamivir increased the risk of nausea, vomiting and psychiatric events in adult patients, and nausea in children. There has also been some criticism of these clinical trials themselves (Jefferson *et al.*, 2014). The protective effects of the neuraminidase inhibitors against severe negative outcomes such as pneumonia, hospitalisation and death can be attributed to selection bias. Seriously ill patients either die before they can be treated or require other interventions, as a matter of urgency. Therefore, the effect of neuraminidase treatments on these patients cannot be determined. In addition, the effectiveness of these drugs decrease after 48 hours (Centers for Disease Control and Prevention, 2014), and are not at all effective in high-risk populations such as asthmatic children (Matheson and Harnden, 2007). While drug resistance to the neuraminidase inhibitors is low, it is beginning to pose a problem (Leang *et al.*, 2013).

While zanamivir and oseltamivir are to some degree effective means of preventing influenza infection (Jackson *et al.*, 2011), vaccines are the preferred method of prophylaxis. However, there are many issues regarding their use, both social and due to the vaccine, itself. Vaccinations must be renewed and readministered annually due to antigenic drift (Carrat and Flahault, 2007). In 2017, the

vaccination used in Australia was comprised of an A/Michigan/45/2015 (H1N1) pdm09-like virus, an A/Hong Kong/4801/2014 (H3N2)-like virus, a B/Brisbane/60/2008-like virus (of the B/Victoria/2/87 lineage) and a B/Phuket/3073/2013-like virus (of the B/Yamagata/16/88 lineage), as was recommended by the World Health Organisation (WHO, 2016). In 2017, antigenic drift resulted in low effectiveness of the influenza vaccine, particularly for the H3 strains (Sullivan *et al.*, 2017). Overall, the vaccine was about 33% effective, 10% effective against Influenza A strains, and only 3-4% effective against the H3 strains. Another issue with the influenza vaccine is simply poor compliance. During the Swine Flu pandemic many were choosing not to get vaccinated for reasons including fear of potential side effects, and underestimating the seriousness of the illness (SteelFisher *et al.*, 2010). Due to these limitations, there is a pressing need for more innovative treatments. Many of the limitations of these treatments, the effectiveness of the vaccine, the risk of resistance to the neuraminidase inhibitors, stem from the ever-changing molecular and structural components of the virus. A potential solution is to target the host response, rather than the virus itself.

### **A Double-Edged Sword: The Host Response to Influenza Virus Infection**

The current paradigm is that pulmonary epithelial cells and alveolar macrophages are the primary targets of influenza A virus infection. Epithelial cells in the upper respiratory tract are the first cells to be infected (Bender and Small Jr, 1992). In response to infection, these cells produce proinflammatory cytokines such as interleukin (IL) 6 and IL8, tumour necrosis factor (TNF)  $\alpha$ , the production of which results in fever (Stefflerl *et al.*, 1996), apoptosis (Reviewed by Rath and Aggarwal, 1999) and inflammation, and chemokines such as ligand CCL5, (Matsukura *et al.*, 1996; Seo and Webster, 2002). Alveolar macrophages play a vital role in viral clearance, as they protect epithelial cells from infection (Cardani *et al.*, 2017). Depleting macrophages resulted in decreased TNF $\alpha$  expression and an increase in mortality in pigs infected with a circulating strain of H1N1 (Kim *et al.*, 2008). Macrophages are also susceptible to influenza infection (Hofmann *et al.*, 1997), and produce chemokines and cytokines as a result (Chan *et al.*, 2012). The production of chemokines and

cytokines by macrophages results in the infiltration of monocytes, neutrophils and T-cells *via* the vascular endothelium (La Gruta *et al.*, 2007).

The host immune response is critical for viral clearance. However, an excessive immune response may be hindering host recovery. Severely ill influenza patients display an excessive immune response, also known as a cytokine storm. Autopsies of patients who died during the 2009 Swine Flu pandemic showed evidence of lung pathology including haemorrhages, oedema, diffuse alveolar damage, alveolar fibrinous exudate, necrotising bronchiolitis, and an aberrant immune response (Mauad *et al.*, 2010). Another cohort of patients in Mexico showed that severely ill patients were more likely to present with acute respiratory distress syndrome, which is characterised by excessive lung inflammation and oedema (Domínguez-Cherit *et al.*, 2009).

Immune regulation has had mixed success in treating this influenza-induced cytokine storm. For example, anti-inflammatory agents, such as the corticosteroids, have been shown to be ineffective in treating influenza (Delaney *et al.*, 2016). Patients treated with corticosteroids spent longer ventilated than patients who were not, and there was no differences in mortality, or occurrence of secondary infections.

One study treated influenza-infected mice with a sphingosine analogue, AAL-R, an immunoregulatory drug which targets the sphingosine-1-phosphate receptor found on endothelial cells and lymphocytes. These mice showed an increase in survival compared to oseltamivir alone, and an even greater improvement was observed with a combination of the two (Walsh *et al.*, 2011). Targeting specific cellular pathways activated by the virus might prove to be the most effective strategy for treating influenza infection.

### **Viral Entry and Replication**

To understand how influenza A virus triggers an inflammatory response, it is important to consider how the virus interacts with host cells (Figure 3). Influenza A is a member of the family *Orthomyxoviridae*, and consists of a lipid layer and a matrix protein layer, surrounding eight

segments of single stranded RNA wrapped in nuclear protein (Luo, 2012). Influenza stains are categorised by their surface proteins, haemagglutinin and the neuraminidase (i.e. H1N1, H3N2). The hemagglutinin binds to the sialic acid residues of cells and the virus internalises into subcellular compartments called endosomes *via* endocytosis (Lakadamyali *et al.*, 2004), both dependent and independent of clathrin (Sieczkarski and Whittaker, 2002). This results in a fall in endosomal pH from 6 to 5, leading to viral uncoating and viral capsule fusion with the endosome membrane (Li *et al.*, 2014). The influenza nucleoprotein is then trafficked to the nucleus. The negative sense RNA needs to be converted to positive sense RNA before it can be transcribed. Replicated nucleoprotein is trafficked out of the nucleus, viral mRNA is translated by the host ribosomes, then the neuraminidase, hemagglutinin and M2 ion channels are trafficked to the plasma membrane (Reviewed by Samji, 2009). The newly created virus is then released from cells when neuraminidase cleaves sialic acid (Varghese *et al.*, 1992). The initial internalisation of the virus into the cell *via* endocytosis is the beginning of the host's defence against infection.

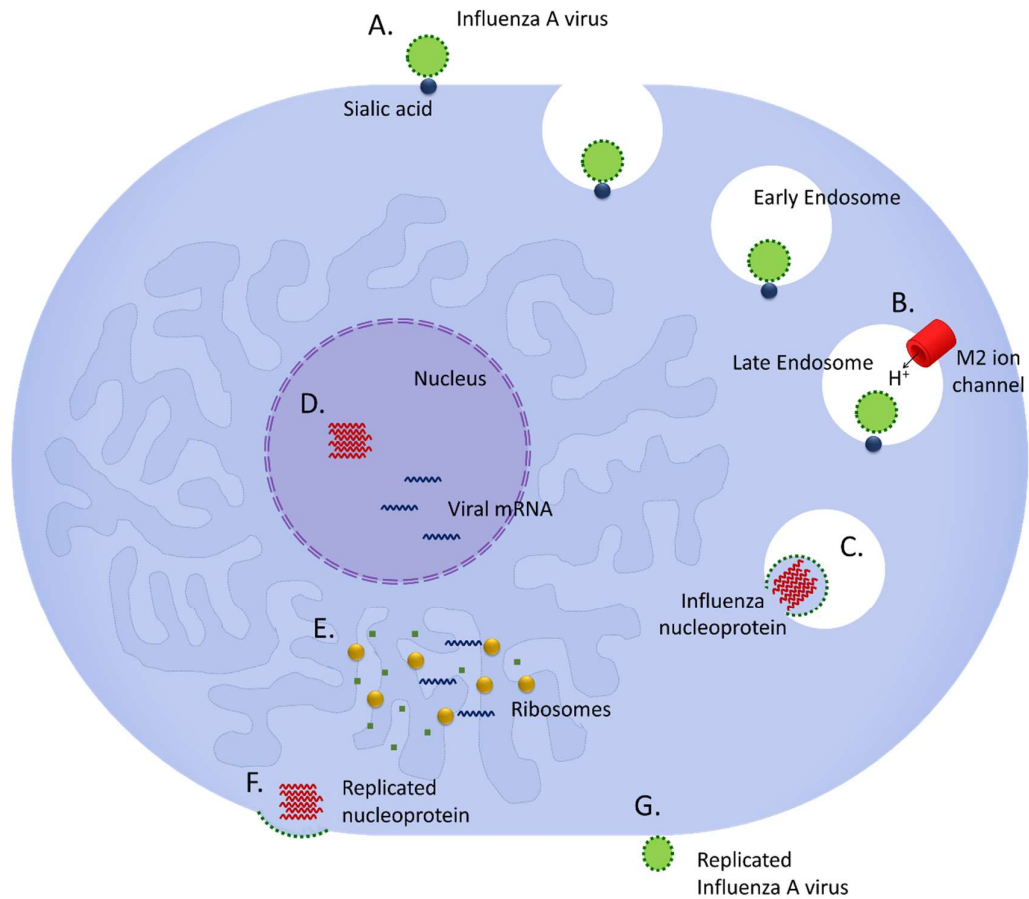


**Figure 3.** A schematic representation of viral entry and replication. **A.** The hemagglutinin protein on the cell surface of influenza A virus binds to sialic acid and internalises into cells *via* endocytosis. **B.** The early endosome containing the virus matures into a late endosome. The pH inside the late endosome drops from 6 to 5. **C.** The virus capsule then fuses with the membrane, resulting in the release of influenza nucleoprotein from the endosome. **D.** The nucleoprotein is then trafficked to the nucleus. Influenza nucleoprotein consists of negative sense RNA which must be converted to positive sense RNA to replicate. **E.** Viral mRNA is then translated into protein by the host cell ribosomes. **F.** Replicated viral nucleoprotein is trafficked from the nucleus to the side of the cell through exportin 1. Hemagglutinin, neuraminidase and the M2 ion channel are trafficked to the plasma membrane, which is used to make the new viral capsule. **G.** Neuraminidase cleaves sialic acid from the glycoproteins and glycolipids, resulting in the release of the newly formed virus from the cell. This process is blocked by the neuraminidase inhibitors.

### The First Line of Defence: The Toll-Like Receptors

The toll-like receptors (TLR) are a family of pathogen recognition receptors (PRRs) which, depending on subtype, can recognise bacterial components (TLR1, TLR4, TLR5), single stranded viral RNA (TLR7, TLR8), double stranded RNA (TLR3), and viral DNA (TLR9) (Blasius and Beutler, 2010). When activated, they cause the transcription of proinflammatory cytokines. TLR3, TLR7, TLR8 and TLR9 are trafficked from the endoplasmic reticulum to endosomes and function from within these specific subcellular compartments.

TLR7 is responsible for the detection of single stranded RNA and has been shown to play a crucial role in influenza-induced inflammatory signalling. TLR7 activation has been shown to be critical in the recruitment of neutrophils in response to influenza infection (Wang *et al.*, 2008). In these experiments, influenza-infected TLR7<sup>-/-</sup> mice had less neutrophil infiltration and a decrease in production of CCL2, which plays an important role in neutrophil infiltration (Xue, *et al.* 2007).

Paradoxically, while the activation of host inflammatory cells is crucial for the host antiviral defence, it has also been shown to enhance viral replication. The subsequent infiltration of monocytes, neutrophils and dendritic cells after activation of TLR7 has also been shown to be necessary for influenza replication (Pang *et al.*, 2013). The immune cells responsible for clearing the virus also become infected and thus, increase the viral load. It should be noted that the mice in this experiment were infected with 10<sup>6</sup> PFU of the highly pathogenic PR8 influenza virus, a much higher dose than typically used in mouse models. Another study found TLR7 to be protective in mice infected with the highly pathogenic H7N7 strain (Kaminski *et al.*, 2012).

TLR7 induces cytokine production through pathways dependent to the adaptor protein myeloid differentiation primary response 88 (MyD88). The activation of TLR7 results in the production of type I interferons such as IFN $\alpha$  through the IRF7 pathway, and the activation of the inflammatory protein complex nuclear factor  $\kappa$ -light-chain-enhancer of activated B cells (NF- $\kappa$ B) (Reviewed by Kawai and Akira, 2010). Active NF- $\kappa$ B signalling was shown to be necessary for influenza to infect cells (Nimmerjahn *et al.*, 2004), and NF- $\kappa$ B induction of TNF-related apoptosis-inducing ligand (TRAIL)

mediated apoptosis was shown to be integral for viral replication (Wurzer *et al.*, 2004). Inhibiting NF- $\kappa$ B has been shown to decrease viral replication of the avian flu strain H5N1 and a decrease in pro-inflammatory cytokine expression (Ehrhardt *et al.*, 2013).

Dendritic cells have been shown to respond to influenza A virus independently of TLR7 (Barchet *et al.*, 2005). The other toll-like receptors also play a role in detecting and responding to influenza virus. TLR3, TLR8 and TLR9 were all found to be upregulated, in addition to TLR7, in the monocytes and dendritic cells of hospitalised influenza patients (Lee *et al.*, 2013). Swine Flu patients in India showed an upregulation of inflammatory cytokines with increasing severity, as well as upregulation of TLR3, TLR4 and TLR7 (Arankalle *et al.*, 2010). Autopsies of Swine Flu patients also showed an increase in TLR3 expression (Mauad *et al.*, 2010).

TLR3 induces cytokine production through a TIR-domain-containing adapter-inducing interferon- $\beta$  (TRIF)-dependent pathway (Yamamoto *et al.*, 2003). TLR3 activation results in NF- $\kappa$ B (Alexopoulou *et al.*, 2001) activation, IFN $\beta$  activation through IRF3, and activation of the nucleotide-binding oligomerization domain, leucine rich repeat and pyrin domain containing 3 (NLRP3) inflammasome (Rajan *et al.*, 2010). Unlike TLR7, TLR3 is thought to be activated primarily by double stranded RNA. During replication, influenza has been shown to produce double stranded RNA (Pons, 1967; Majde, 2000). This was contested by a later study, which did not find a detectable amount of double stranded RNA in influenza infected cells (Weber *et al.*, 2006). However, TLR3 activation has been shown to play a crucial role in influenza A virus pathology. TLR3 knockout (TLR3<sup>-/-</sup>) mice were protected against influenza A virus infection (Le Goffic *et al.*, 2006). Infected TLR3<sup>-/-</sup> mice had reduced production of IL-6, and CCL5 compared to infected wild type (WT) mice. There was also an improvement in lung lesions and survival in the TLR3<sup>-/-</sup> mice compared to the WT mice. Paradoxically, viral load in the infected knockout mice was increased compared to the WT. TLR3 and the cytosolic dsRNA sensor retinoic acid-inducible gene I (RIG-I) were also shown to contribute to influenza-induced inflammatory cytokine production in epithelial cells (Le Goffic *et al.*, 2007), and were both

required for interferon (IFN)  $\beta$ , IFN  $\lambda$ 1, IFN  $\lambda$ 2/3 and interferon induced CXCL10 expression in response to influenza infection (Wu *et al.*, 2015). These studies all suggest that targeting TLR3 activation could prove helpful in treating influenza-induced inflammation.

### **Reactive Oxygen Species: Key contributors to the inflammatory response**

One of the hallmarks of a heightened inflammatory state is oxidative stress (Reviewed by Chatterjee, 2016). Oxidative stress is characterised by a persistent elevation in the production of reactive oxygen species (ROS) that overwhelms the endogenous antioxidant processes that metabolise them (Reviewed by Seis 2018). ROS are highly reactive molecules that have an unpaired valence electron. While ROS play an important role in cell signalling and the inflammatory response (Chen, *et al.* 2008), excessive production of ROS results in cell damage through the oxidation of lipids and proteins (Reviewed by Seis 2018). ROS include oxidants such as superoxide, hydrogen peroxide, hydroxyl radicals and peroxynitrite (Figure 4). The Hydroxyl radical is the most unstable of these and has a half-life of only  $10^{-9}$  seconds (Pryor, 1986). While the half-life of superoxide or hydrogen peroxide cannot be accurately calculated without knowledge of concentrations of superoxide dismutase, which catalyses the dismutation of superoxide into hydrogen peroxide; catalase, a peroxidase which catalyses the conversion of hydrogen peroxide into water, and the concentration of other substrates, they're estimated to be about  $10^{-6}$  seconds and  $10^{-3}$  seconds, respectively (Karuppanapandian *et al.*, 2011)

Superoxide has a free electron and a negative charge, which limits its ability to pass through plasma membrane without an ion channel (Hawkins *et al.*, 2007). In contrast, hydrogen peroxide is a two-electron oxidant. It is less reactive than superoxide and can pass through plasma membrane. Its effects are regulated by the presence of catalase and other antioxidant enzymes (Branco *et al.*, 2004). Nitric oxide is an important molecule in cell signalling but readily reacts with superoxide to produce peroxynitrite, which is extremely reactive and results in apoptosis (Li *et al.*, 2005). Another important factor that influences the actions of Nox4, and which accounts for its distinct activity

profile, is its subcellular localisation. ROS are highly reactive and thus their ultimate targets are generally at sites nearby their site of production (Chen *et al.*, 2008). For example, endothelial Nox4 is primarily localised to the endoplasmic reticulum and the nucleus and this location brings Nox4 in close proximity to the protein tyrosine phosphatase 1B (PTP1B) that influences its activity (Frangioni *et al.*, 1992).

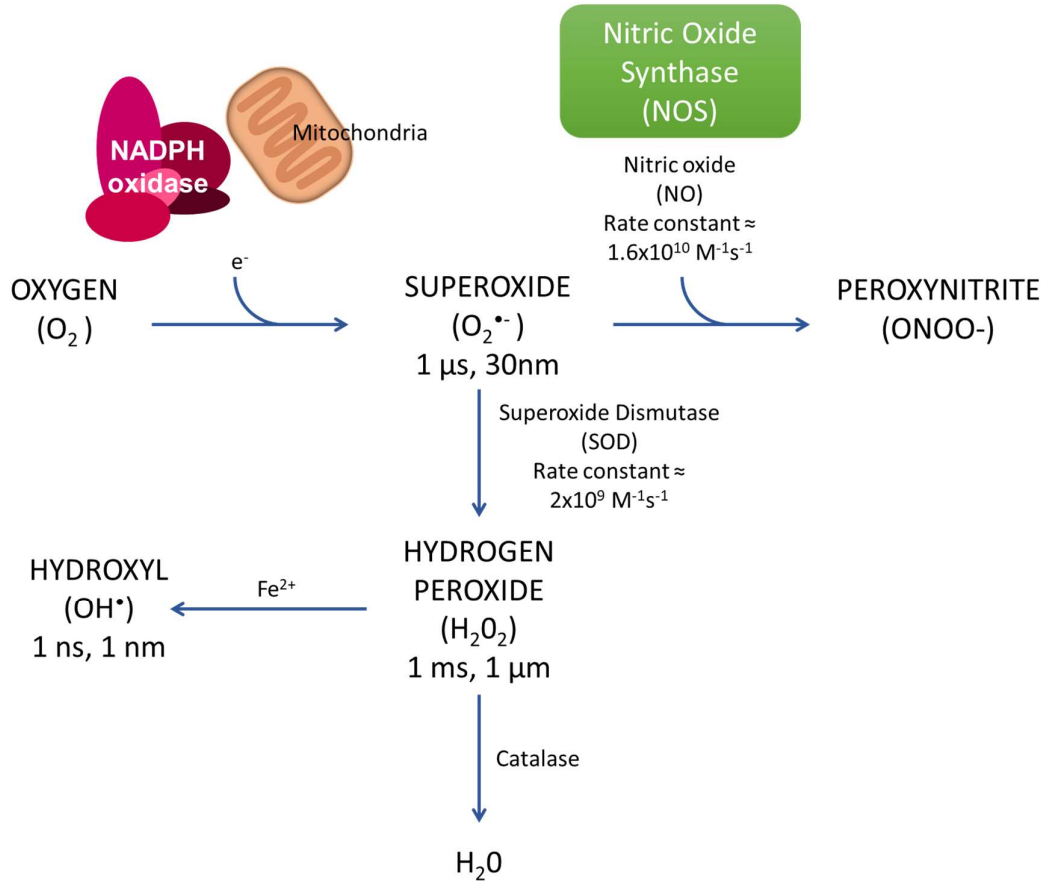


**Figure 4.** Sources of ROS and common reactions, including approximate rate constants, their approximate half-life and mobility (Karuppanapandian *et al.*, 2011; Forman and Fridovich, 1973; Nauser and Koppenol, 2002).

Oxidative stress has also been linked to influenza morbidity. Treating mice infected with a potentially lethal dose of influenza with superoxide dismutase, which converts superoxide into hydrogen peroxide (Figure 4), was shown to improve survival (Oda *et al.*, 1989). Superoxide and peroxynitrite have also been shown to exacerbate influenza infection (Akaike *et al.*, 1996). Imai *et al.*, (2008) infected mice with inactivated H5N1 avian influenza. These had impaired lung function, severe oedema, thickening of the alveolar wall, alveolar bleeding, and alveolar inflammation. These mice also showed signs of oxidative stress, measured as oxidised phospholipids. Imai, et al. (2008) also found that mice deficient in p47<sup>phox</sup>, which is important for ROS production, had less severe oedema, lung pathologies and oxidative stress. More recently, ROS has been shown to contribute to influenza-induced cytokine production in macrophages (Ye *et al.*, 2015). These studies all demonstrate an important role for ROS in influenza pathology, but considering the rapid nature of these ROS reactions, the enzymatic source and the localisation of the ROS production is critical for understanding and targeting these pathways.

### **Structure and Function of the NADPH oxidases**

ROS production can arise inadvertently as a by-product of many processes within the cell. The best example is ROS production that occurs within the mitochondrial electron transport chain during cellular respiration (Reviewed by Turrens, 2003). ROS is also produced as a by-product of the conversion of xanthine to uric acid by xanthine oxidase, which has been linked to cardiovascular disease and inflammation (Dawson and Walters, 2006; Miesel and Zuber 1993). However, there are enzymes with the specific and primary function of ROS production. The NADPH (nicotinamide adenine dinucleotide phosphate) oxidases are a family of membrane-bound enzymes that are specialised ROS generating enzymes, which consist of multiple subunits (Reviewed by Panday, *et al.* 2015). NADPH oxidases catalyse the reaction of NADPH into NADP<sup>+</sup>, and in doing so, provide electrons that are shuttled to molecular oxygen, which then gives rise to superoxide anion.

There are seven identified members of the NADPH oxidase enzyme family (Figure 5). Each member of this family is defined by either a distinct catalytic Nox subunit, i.e. Nox1, Nox2, Nox3, Nox4 and Nox5, or Duox catalytic subunit i.e. Duox1 and Duox2. p22<sup>phox</sup> has two functions; one, to form a stable heterodimer with the catalytic subunits Nox1, Nox2, Nox3 or Nox4, and two, to bind to the cytosolic subunits for Nox1, Nox2 or Nox3 (Reviewed by Bedard and Krause, 2007). p47<sup>phox</sup> and NOXO1 are the organiser subunits, and when bound to Nox2 or Nox1 and Nox3 respectively, allow for the recruitment of the activator subunits, p67<sup>phox</sup> or NOXA2. Nox4 oxidase only requires p22<sup>phox</sup> to stabilise that catalytic subunit and is constitutively active. In contrast, Nox5 oxidase does not require p22<sup>phox</sup>. Nox5 has an “EF-hand” motif and thus, allows for activation by cytosolic calcium.

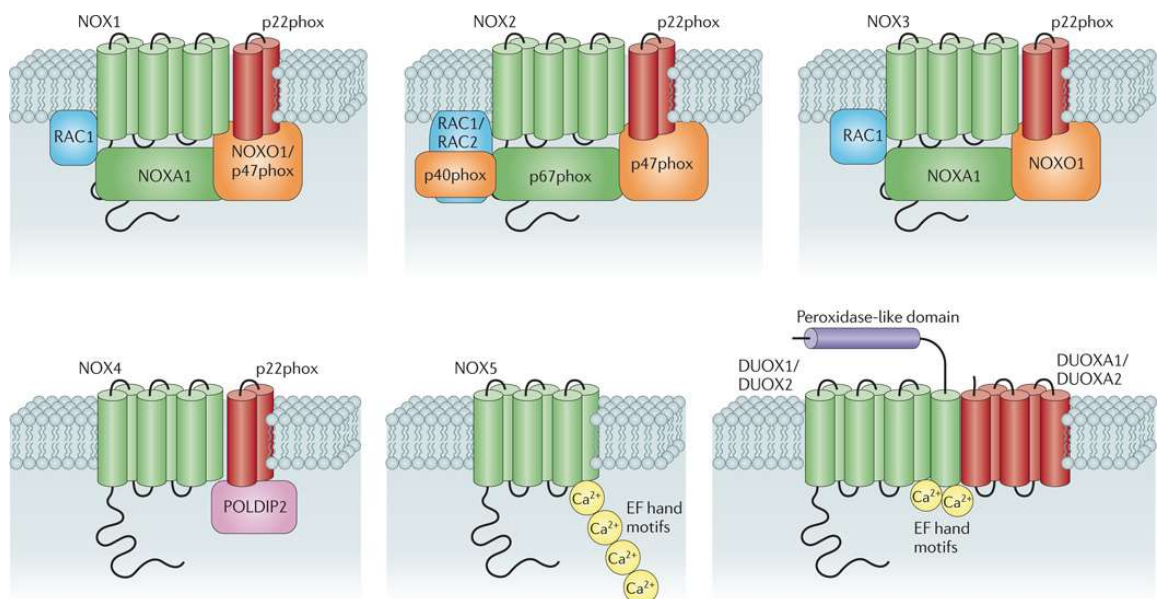


**Figure 5.** The various isoforms of the NADPH Oxidase enzymes. (Image taken from Drummond, *et al.* 2011)

Due to its unique structure, Nox4 plays a very different role to the other NADPH oxidases. While Nox1, Nox2, and Nox3 have been shown to produce superoxide as their primary product, Nox4 directly produces hydrogen peroxide, a more stable species of ROS, which also has the capacity to permeate plasma membrane (Takac *et al.*, 2011). This is due to its extended E loop, which is thought to slow the release of superoxide, allowing for a collision between two superoxide molecules before they can be released (Takac *et al.*, 2011) (Figure 6). The E loop also contains a highly conserved histidine that could potentially accelerate protons, resulting in the dismutation of superoxide. Superoxide has a negative charge and cannot readily pass through membranes, whereas hydrogen peroxide has the capacity to permeate cell membranes to a certain degree. These properties influence the molecular targets of ROS. For example, the extracellular signal regulated kinase (ERK) 1/2 phosphorylation is attenuated when Nox4 is modified to produce superoxide instead of hydrogen peroxide (Takac *et al.*, 2011). Nox4 activity is also modulated by Poldip 2, which binds to p22phox and drives Nox4 activity (Lyle, *et al.* 2009). Another important factor that influences the actions of Nox4, and which accounts for its distinct activity profile is its subcellular localisation. ROS are highly reactive and thus their ultimate targets are generally at sites nearby their site of production. As stated previously, endothelial Nox4 is primarily localised to the endoplasmic reticulum and the nucleus and this location brings Nox4 in close proximity to the protein tyrosine phosphatase 1B (PTP1B) that influences its activity (Chan, *et al.* 2008; Frangioni *et al.*, 1992).

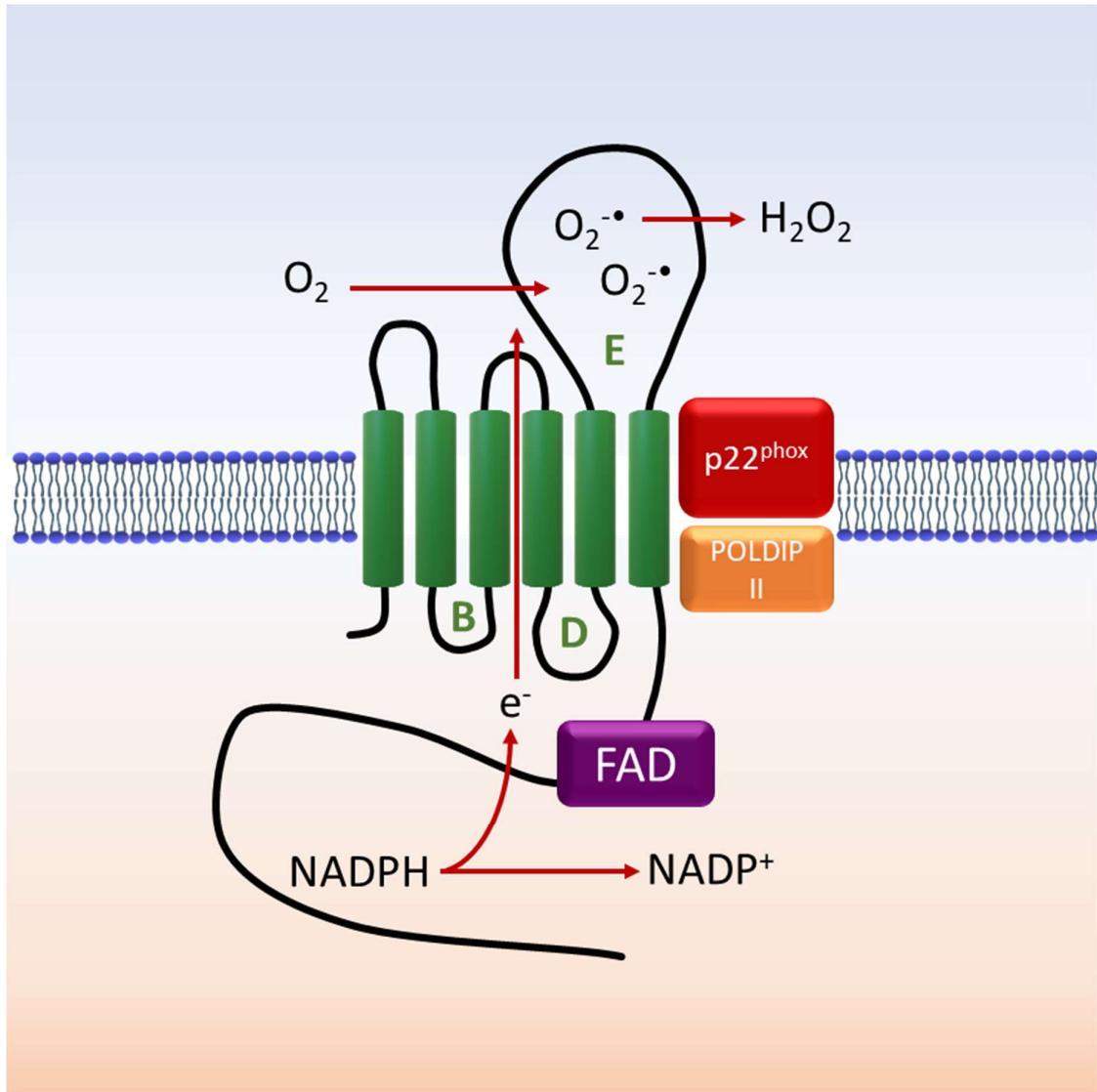


**Figure 6.** Structure of the Nox4 Oxidase complex. The electron from NADPH goes from flavin adenine dinucleotide (FAD), through the Nox heme groups and then forms superoxide with oxygen on the other side of the membrane. The unique B loop and C terminus allow Nox4 to be constitutively active. POLDIP 2 was shown to modulate Nox4-dependent hydrogen peroxide production. The Nox4 E loop has two features which result in the production of hydrogen peroxide rather than superoxide. The E loop is extended, which is thought to slow the release of superoxide and allow for a collision and contains a highly conserved histidine which can accelerate protons to form hydrogen peroxide.

## The Role of the NADPH oxidases in Inflammatory Disorders

Nox2 oxidase, or otherwise referred to as the phagocytic NADPH oxidase, was the first NADPH oxidase to be identified and initially characterised by its role in the bactericidal actions of immune cells. Deficiency in the genes encoding the Nox2 protein or any of the regulatory subunits of the Nox2 oxidase complex results in chronic granulomatous disease, which is characterised by an impaired ability to fight bacterial infection (Segal *et al.*, 2000). While the Nox2 oxidase is necessary for immune cells to mount an antibacterial response, it is also known to contribute to oxidative stress in a number of disorders and inflammatory signalling pathways.

Nitric oxide synthase (NOS) produces nitric oxide (NO) in cells, an important chemical in cell signalling. Nox2 oxidase and NOS were shown to form peroxynitrite, which caused cell death in microglia in a model of ischemic stress (Li *et al.*, 2005). Nox2 knockout mice had a smaller infarct volume and improved vascular recovery compared to wild type mice in a model of stroke (Walder *et al.*, 1997; McCann *et al.*, 2014). PTP1B is localised to the endoplasmic reticulum (Frangioni *et al.*, 1992), and has been shown to inhibit a number of inflammatory signalling molecules including janus kinase 2 (JAK 2), tyrosine kinase 2 (TYK2) (Myers *et al.*, 2001), signal transducer and activator of transcription 5a and 5b (STAT 5a/5b) (Aoki and Matsuda, 2000) and STAT6 (Lu *et al.*, 2008).

Atherosclerosis, the build-up of fatty plaques in blood vessels, has been considered an inflammatory disorder for many years. Influenza vaccination has been shown to be protective against acute coronary syndromes in patients with atherosclerosis (Madjid *et al.*, 2005). One of the major hallmarks of atherosclerosis is oxidative stress. Nox2 deletion resulted in improved NO bioavailability and a decrease in the amount of atherosclerotic plaques formed in ApoE<sup>-/-</sup> mice on a high fat diet (Judkins, *et al.* 2009). Specifically targeting Nox2 oxidase with the inhibitor Nox2 gs-tat also resulted in improvement of atherosclerotic plaques (Quesada *et al.*, 2016). Superoxide derived from Nox2 oxidase oxidises low density lipoproteins, which in turn stimulates macrophages (Lee *et al.*, 2014).

Aside from Nox2, other NADPH oxidases have been implicated in inflammatory disorders. Hydrogen peroxide produced by Nox4 oxidase has been shown to oxidise cysteine 215 on the active site of PTP1B and inactivate it (Chen *et al.*, 2008). While its role in influenza pathology is unknown, inhibiting PTP1B has been shown to exacerbate asthma-induced inflammation (Berdnikovs *et al.*, 2013) and lipopolysaccharide (LPS)-induced pulmonary oedema in mouse models (Grinnell *et al.*, 2012).

Diabetes is another condition that is considered a risk factor for becoming seriously ill during influenza infection. During the Swine Flu pandemic, patients with diabetes were three times as likely to be hospitalised (Allard *et al.*, 2010). While the mechanisms for this increase in severity are unclear, patients with hyperglycaemia are much more susceptible to infection (Reviewed by Hulme *et al.*, 2017). As with influenza infection, ROS plays a large role in the progression of diabetes. Diabetic mice showed signs of oxidative stress in both the endothelium and the smooth muscle of the aorta, and Nox1 expression was increased in these mice (Wendt *et al.*, 2005). Inhibiting Nox1 oxidase prevented oxidative stress in endothelial cells exposed to hyperglycaemic conditions (Gray *et al.*, 2013)

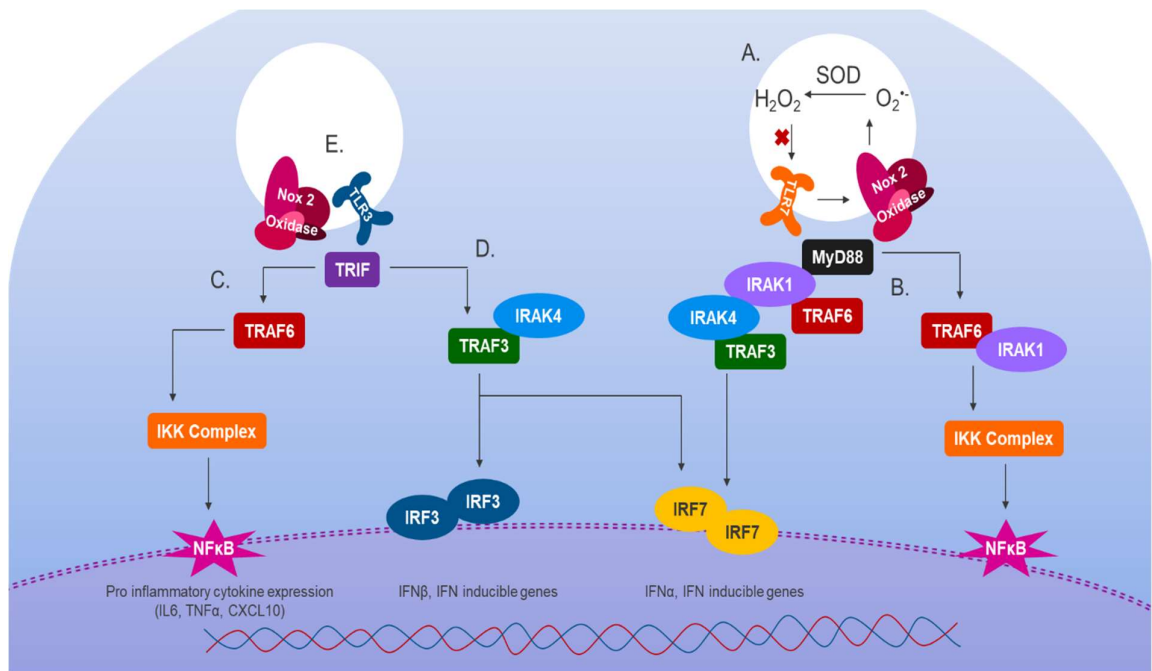


**Figure 7.** Toll-like receptor 3 and 7 signalling pathways. **A.** TLR7 activation drives Nox2-dependent endosomal superoxide production. TLR7 is then deactivated by hydrogen peroxide. **B.** TLR7 activation results in an increase in proinflammatory cytokine expression through MyD88, which activates NF- $\kappa$ B and IRF7. **C.** TLR3 results in NF- $\kappa$ B activation through a TRIF-TRAF6 dependent pathway. **D.** TLR3 activation results in an increase IFN $\beta$  expression though a TRIF-TRAF3-IRF3 dependent pathway. **E.** A physical association between Nox2 and TLR3 was shown to be necessary for TLR3 induced cytokine expression.

### **Implicating the NADPH Oxidases in Influenza pathology**

Due to the large role that the NADPH oxidases play in inflammatory disorders, more recent studies have examined their role in influenza-induced inflammation and pathology. A potential mechanism *via* which influenza infection could cause oxidative stress is through the interaction of certain TLRs with the NADPH oxidases. TLR4 is responsible for the detection of LPS found on the surface of bacteria. TLR4 has been shown to form a physical association with Nox4 oxidase, and that association was shown to be necessary for LPS-induced ROS production and activation of NF- $\kappa$ B (Park *et al.*, 2004). While TLR4 has been shown to be upregulated in influenza patients, its impact on influenza pathology is likely limited outside the context of secondary bacterial infections.

As stated previously, TLR3 is upregulated in influenza patients and is associated with influenza-induced inflammation. TLR3 has also been shown to interact with the p47phox subunit of Nox2 oxidase. This is critical for an oxidative burst response that is essential for TLR3-induced activation of IRF3, NF- $\kappa$ B and STAT1 in macrophages (Yang *et al.*, 2013).

Previous studies by our lab have shown that Nox2 deletion is protective against influenza infection, resulting in a decrease in lung oxidative stress, peri-bronchial inflammation, viral titre, and in CCL2 production (Vlahos *et al.*, 2011). In contrast, Nox1 oxidase has been shown to be protective against influenza infection (Selemidis *et al.*, 2013). Influenza-infected Nox1 knockout mice lost more weight, showed more signs of oxidative stress and had more peri-bronchial and perivascular inflammation than the infected wildtype mice. This highlights the importance of the specific source of ROS production in influenza pathology when selecting drug targets for potential treatments. Our lab further explored the mechanisms behind Nox2-dependent ROS production, and also found that influenza A virus infection and treatment with TLR7 agonists, but not TLR3 agonists, was shown to drive Nox2-dependent superoxide production in macrophages (To *et al.*, 2014). While this process has been shown in macrophages, potential differences in other cell types have not been explored.

Due to the reactive nature of ROS, the location of their production determines their cellular targets (Figure 8). Nox2 has been localised to endosomes, endoplasmic reticulum and the perinuclear region (Van Buul *et al.*, 2005). Nox4 has been localised to endoplasmic reticulum and in the nucleus (Kuroda *et al.*, 2005), but not in endosomes. Endosomal ROS has been shown to be involved in inflammatory signalling. Endosomal Nox2 superoxide production activates NF- $\kappa$ B through induction of TNF $\alpha$  (Li *et al.*, 2009). In this same study, endosomal superoxide production was shown to be necessary for the recruitment of TNF receptor-associated factor TRAF 2 to the endosome.

Given the role of endosomal ROS in immune signalling, the fact that Nox2 deletion ameliorates influenza-induced inflammation and that, as previously stated, influenza internalises into cells *via* endocytosis, our group sought to study the pathways involved in endosomal ROS in the context of influenza. Influenza infection and TLR7 activation resulted in a Nox2-dependent increase in endosomal ROS production in macrophages (To *et al.*, 2017). This study also shows a negative feedback loop, in which TLR7 is then deactivated by hydrogen peroxide, which oxidises a specific cysteine on TLR7, c98. While the role of endosomal ROS production in influenza-induced inflammation in macrophages has been explored in this study, other cell types have not been examined.

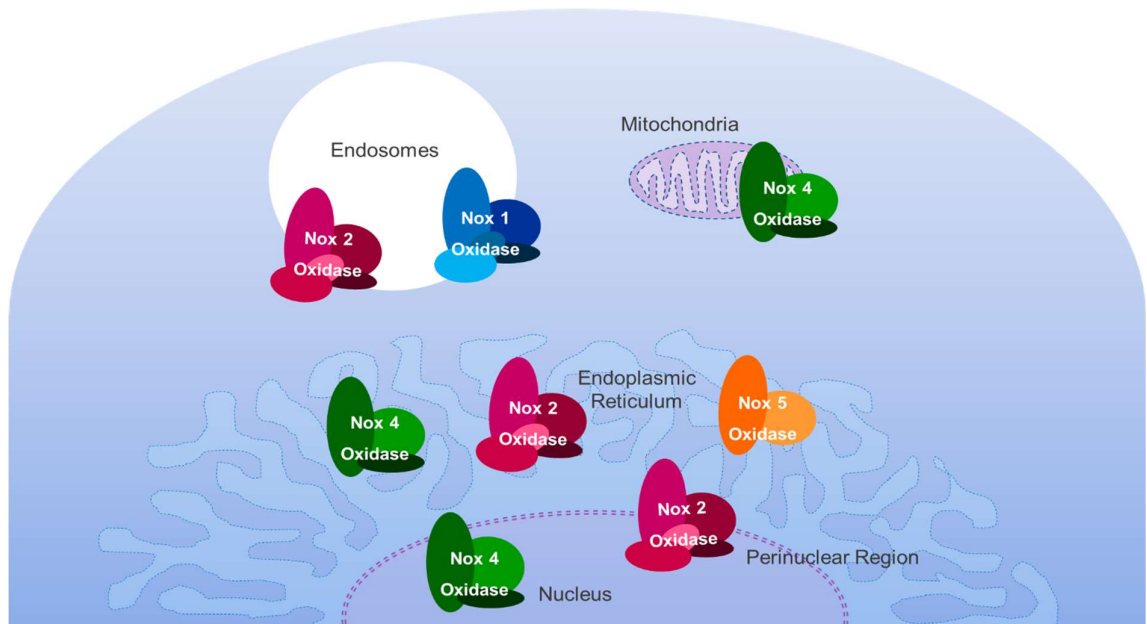


**Figure 8.** The subcellular locations of the NADPH Oxidase enzymes. Nox2 has been shown to be present in endosomes, the endoplasmic reticulum, and the perinuclear region. Nox1 has been localised to endosomes. Nox5 has been localised to the endoplasmic reticulum. Nox4 has been localised to mitochondria, the endoplasmic reticulum, and the nucleus.

### Emerging Evidence for a Role of the Endothelial Cells in Influenza Pathology

While most of the literature examines the role of epithelial cells and macrophages in influenza pathology, recent evidence suggests that lung endothelial cells may play a larger role than originally thought. Endothelial cells exposed to influenza A virus *in vitro* have shown an increase in apoptosis and degradation of claudin-5, a membrane protein important for the formation of tight junctions and the endothelial monolayer preventing fluid entering the lungs (Armstrong *et al.*, 2012). These processes could contribute to the pulmonary oedema frequently seen in seriously ill patients. Endothelial cells have also been implicated in the damaging influenza-induced cytokine storm (Teijaro *et al.*, 2011). Specifically targeting endothelial cells with a sphingosine analogue in lymphocyte-deficient mice has also been shown to decrease cytokine production and improve survival. How the endothelium regulates influenza-induced inflammation, or the potential involvement of endothelial NADPH oxidase in influenza pathology, is unknown.

While TLR7 has been shown to have a crucial role in influenza pathology in macrophages and dendritic cells, TLR7 activation had no effect on CXCR3 ligand induction and TLR7 expression was undetected by RT-PCR in human microvascular endothelial cells (Loos *et al.*, 2006). TLR3, however, is highly expressed in the endothelium and plays an important role in influenza pathology. As previously stated, TLR3 was shown to play a role in influenza-inflammation derived from the epithelium (Le Goffic *et al.*, 2006), and TLR3 expression increases in influenza infections (Mauad *et al.*, 2010). Activation of TLR3 in endothelial cells by the agonist polyinosine polycytidylic (poly I:C) has been shown to result in apoptosis, an increase in production of IL-8 and CXCL10, and increases in oxidative stress (Zimmer *et al.*, 2011). It has also been shown to result in impaired endothelial vasodilation and reduced regrowth of the endothelium following injury. Given the role TLR3 plays in influenza pathology, the interactions between TLR3 and Nox2, and the effect of TLR3 activation in endothelial cells, this pathway could be involved in influenza pathogenesis.

### **Nox4 Oxidase: Friend or Foe?**

As discussed, Nox4 oxidase differs from Nox2 oxidase in terms of structure, mode of activation and function. In endothelial cells, Nox4 is highly expressed; 100 times more than Nox2 (Van Buul *et al.*, 2005). Nox4 is also localised at the endoplasmic reticulum, whereas Nox2 has been localised to plasma membrane, endosomes and the perinuclear region. Nox4 is also constitutively active, whereas Nox2 requires the assembly of cytosolic subunits.

Epithelial Nox2 and Nox4 were shown to regulate distinct kinase pathways in response to stimulation with either insulin, TNF $\alpha$ , or angiotensin II (Anilkumar *et al.*, 2008). JNK activation increased in HEK293 cells with overexpressed Nox2, while p38 mitogen-activated protein kinases, protein kinase B, and glycogen synthase kinase 3  $\beta$  phosphorylation increased in HEK293 cells overexpressing Nox4. Unlike Nox2, Nox4 was shown to be protective against atherosclerosis (Gray *et al.*, 2016). In a mouse model examining atherosclerosis in the context of diabetes, Nox4<sup>-/-</sup> mice had an increase in atherosclerotic plaques, reduced hydrogen peroxide production, increased macrophage accumulation and an increase in fibrillar collagen. Nox4 was also downregulated in patients with atherosclerosis, and diabetes, and in mice with atherosclerosis. Deleting Nox4 resulted in increases in oxidative stress, increases in atherosclerotic plaques and inflammatory cytokine expression. Nox4 has also been shown to have a protective effect against ischemic stress (Schröder *et al.*, 2012b). Nox4<sup>-/-</sup> mice treated with angiotensin II in a model of hypotension had increased inflammation and endothelial dysfunction compared to the WT mice.

While Nox4 has been shown to have a protective role in atherosclerosis and ischemic stress, there are very little data on Nox4 in influenza or lung disorders. In contrast to what was seen in vascular diseases, Nox4 was found to exacerbate fibrosis in a bleomycin-induced lung fibrosis mouse model (Sato *et al.*, 2016). It has also been thought to exacerbate LPS-induced oedema in a mouse model of bacterial acute lung injury (Grinnell *et al.*, 2012). To date, only one study has examined the role of Nox4 in influenza infection. Viral replication in cultured epithelial cells was found to be dependent on

Nox4-induced hydrogen peroxide (Amatore *et al.*, 2015). Amatore *et al.* (2015) also found that Nox4 was upregulated in these cells. However, the Nox4 antibody used in their western blot experiments was found to be ineffective (Altenhöer, *et al.* 2012). Due to the abundance of Nox4 in the endothelium and many studies implicating the endothelium in influenza pathology, examining the role of endothelial Nox4 in an *in vivo* model could give us a better understanding of the mechanism involved in influenza-induced inflammation.

### **Cardiovascular Complications of Influenza Infection.**

While the role of the endothelium in the inflammatory response is critical, it has many other functions that could contribute to influenza pathology. Many swine flu patients also presented with heart failure (Brown *et al.*, 2011). Of the many deaths that occurred during the swine flu pandemic, 83 000 of them were due to cardiovascular complications (Dawood *et al.*, 2012). Influenza vaccination was shown to reduce the risk of hospitalisation due to stroke or cardiovascular disease (Nichol *et al.*, 2003) and protective against myocardial infarction (Smeeth *et al.*, 2004).

Cardiopulmonary insufficiency is characterised by heart failure and pulmonic regurgitation.

Hypotension, along with breathing difficulties, coughing up blood and chest pain, is a sign of cardiopulmonary insufficiency in influenza patients, which is a potentially fatal complication (WHO, 2010). There is very little research examining the role of cardiopulmonary insufficiency or the cardiovascular effects of influenza.

A major function of the endothelium is to regulate vascular tone. The endothelium induces relaxation in the vasculature through the nitric oxide pathway (Palmer *et al.*, 1987), and the elusive endothelial-derived hyperpolarising factor (EDHF) (Reviewed by Ozkor and Quyyumi, 2011), which result in relaxation of vascular smooth muscle. Relaxation of vasculature can also occur through multiple different potassium channels on the smooth muscle itself (Figure 8). ROS have varied effects on vascular tone. Hydrogen peroxide has been shown to cause endothelium-dependent relaxation of the vasculature (Yang *et al.*, 1998). Superoxide production decreases the bioavailability of nitric oxide

and would thus, result in an increase in vascular tone. There is some evidence that superoxide itself directly causes relaxation of the vasculature (Wei *et al.*, 1996), but it's not well established. Low concentrations of peroxynitrite have been shown to result in the endothelium-dependent relaxation of cerebral blood vessels (Li *et al.*, 2005). The effect of influenza-induced ROS production on vascular tone is unknown.

Hypotension is a known side effect of oral imiquimod treatment, suggesting that TLR7 activation may have an effect on vascular tone (Aldara product sheet, 2014). TLR7 activation has been shown to cause airway relaxation (Drake, *et al.* 2013). This study did not find TLR7 on airway smooth muscle. However, Kvarnhammar *et al.*, (2013) found that TLR7 was expressed on smooth muscle cells, suggesting that the smooth muscle could be involved. Treatment with TLR3 agonists has been shown to result in hypotension (Reviewed by Christopher and Wong, 2011). The mechanisms behind toll-like receptor-induced hypotension, including whether or not these effects are endothelium-dependent, have not been studied, and the implications for changes in vascular tone in influenza pathology have not been considered. Given the very serious cardiovascular complications associated with influenza infection, much more research into this area is required.

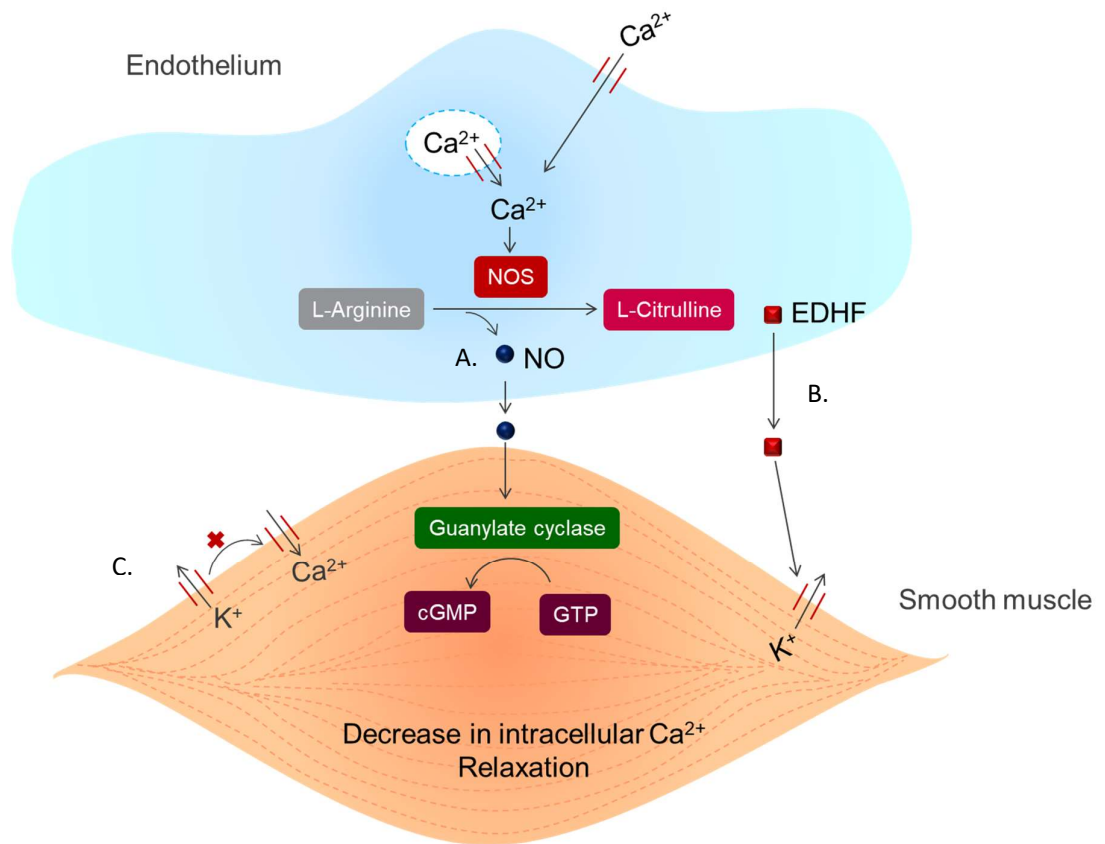


**Figure 9.** Pathways involved in vascular smooth muscle relaxation. A. Nitric oxide derived from the endothelium diffuses through the membrane and causes relaxation of the smooth muscle by activating guanylate cyclase. B. Endothelial-Derived Hyperpolarising Factor (EDHF) causes smooth muscle relaxation through the opening of potassium channels, but the pathways involved remain poorly understood. C. Activating potassium channels directly on the smooth muscle also results in relaxation.

## Rationale

Influenza is a massive global burden and due to the limitations of current treatments there is an urgent need for new therapies. Hospitalised influenza patients had an excessive immune response, resulting in lung damage. Recent studies have implicated the endothelial cell in influenza A virus inflammation. However, there are many questions about influenza-induced inflammation left unanswered. The mechanisms through which endothelial cells contribute to influenza-induced inflammation are unknown. While NADPH oxidases are known to play a role in influenza pathology, the role of endothelial NADPH oxidases remain unstudied. Studies into the mechanisms by which endosomal ROS regulates inflammation have only scratched the surface. While vascular inflammation has been considered to underpin influenza morbidity, the role of the vasculature in regulating tone has been largely unexplored. Therefore, this thesis explores the potential role of the vasculature in influenza pathology, including TLR-NADPH oxidase signalling in endosomes; the mechanisms involved in TLR-induced hypotension, and the potentially protective or detrimental effects of vascular Nox4 oxidase (Figure 9). Thus, this thesis consists of three studies.

### Study 1: Examining the role of endothelial Nox2 oxidase in influenza A virus pathology.

*Aim 1:* To determine if influenza internalises into endothelial cells *via* endocytosis, *in vivo* and *in vitro*.

*Aim 2:* To determine if influenza A virus infection or TLR activation in endothelial cells results in a Nox2 oxidase-dependent increase in endosomal ROS production.

*Aim 3:* To establish if TLR3-and TLR7- induced cytokine production in endothelial cells is Nox2 oxidase-dependent.

Study 2: Determining the effect of TLR activation on vascular tone.

*Aim:* To determine if TLR3 and TLR7 activation results in a change in vascular tone and to examine the mechanisms involved.

Study 3: Examining the role of endothelial Nox4 oxidase in influenza A virus pathology

*Aim:* To investigate the role of endothelial Nox4 in influenza A virus-induced inflammation and morbidity.

## References

- Akaike, T, Noguchi, Y, Ijiri, S, Setoguchi, K, Suga, M, Zheng, YM, *et al.* (1996). Pathogenesis of influenza virus-induced pneumonia: involvement of both nitric oxide and oxygen radicals. *Proc. Natl. Acad. Sci. U. S. A.* **93**: 2448–2453.
- Alexopoulou, L, Czopik Holt, A, Medzhitov, R, Flavell, RA (2001). Recognition of double-stranded RNA and activation of NF-kappa B by Toll-like receptor 3. *Nature* **413**: 732–738.
- Aldara product sheet (2014) iNova Pharmaceuticals
- Allard, R, Leclerc, P, Tremblay, C, Tannenbaum, T-N (2010). Diabetes and the severity of pandemic influenza A (H1N1) infection. *Diabetes Care* **33**: 1491–1493.
- Altenhöfer, S, Kleikers, PWM, Radermacher, KA, Scheurer, P, Hermans, JJR, Schiffers, P, *et al.* (2012). The NOX toolbox: Validating the role of NADPH oxidases in physiology and disease. *Cell. Mol. Life Sci.* **69**: 2327–2343.
- Amatore, D, Sgarbanti, R, Aquilano, K, Baldelli, S, Limongi, D, Civitelli, L, *et al.* (2015). Influenza virus replication in lung epithelial cells depends on redox-sensitive pathways activated by NOX4-derived ROS. *Cell. Microbiol.* **17**: 131–145.
- Anilkumar, N, Weber, R, Zhang, M, Brewer, A, Shah, AM (2008). Nox4 and nox2 NADPH oxidases mediate distinct cellular redox signaling responses to agonist stimulation. *Arterioscler. Thromb. Vasc. Biol.* **28**: 1347–1354.
- Aoki, N, Matsuda, T (2000). A cytosolic protein-tyrosine phosphatase PTP1B specifically dephosphorylates and deactivates prolactin-activated STAT5a and STAT5b. *J. Biol. Chem.* **275**: 39718–39726.
- Arankalle, V a, Lole, KS, Arya, RP, Tripathy, AS, Ramdasi, AY, Chadha, MS, *et al.* (2010). Role of host immune response and viral load in the differential outcome of pandemic H1N1 (2009) influenza virus infection in Indian patients. *PLoS One* **5**: e13099

- Armstrong, SM, Wang, C, Tigdi, J, Si, X, Dumpit, C, Charles, S, *et al.* (2012). Influenza infects lung microvascular endothelium leading to microvascular leak: role of apoptosis and claudin-5. *PLoS One* **7**: e47323.
- Barchet, W, Krug, A, Cella, M, Newby, C, Fischer, JAA, Dzionek, A, *et al.* (2005). Dendritic cells respond to influenza virus through TLR7- and PKR-independent pathways. *Eur. J. Immunol.* **35**: 236–242.
- Bedard, K, Krause, K-H (2007). The NOX Family of ROS-Generating NADPH Oxidases: Physiology and Pathophysiology. *Physiol. Rev.* **87**: 245–313.
- Bender, B, Small Jr, P (1992). Influenza: pathogenesis and host defense. *Semin. Respir. Infect.* **7**: 38–45.
- Berdnikovs, S, Abdala-Valencia, H, Cook-Mills, JM (2013). Endothelial cell PTP1B regulates leukocyte recruitment during allergic inflammation. *Am. J. Physiol. Lung Cell. Mol. Physiol.* **304**: L240–249.
- Blasius, AL, Beutler, B (2010). Intracellular Toll-like Receptors. *Immunity* **32**: 305–315.
- Branco, MR, Marinho, HS, Cyrne, L, Antunes, F (2004). Decrease of H<sub>2</sub>O<sub>2</sub> Plasma Membrane Permeability during Adaptation to H<sub>2</sub>O<sub>2</sub> in *Saccharomyces cerevisiae*. *J. Biol. Chem.* **279**: 6501–6506.
- Brown, SM, Pittman, J, Miller III, RR, Horton, KD, Markewitz, B, Hirshberg, E, *et al.* (2011). Right and left heart failure in severe H1N1 influenza A infection. *Eur. Respir. J.* **37**: 112–118.
- Cardani, A, Boulton, A, Kim, TS, Braciale, TJ (2017). Alveolar Macrophages Prevent Lethal Influenza Pneumonia By Inhibiting Infection Of Type-1 Alveolar Epithelial Cells. *PLoS Pathog.* **13**: 1–25.
- , F, Flahault, A (2007). Influenza vaccine: the challenge of antigenic drift. *Vaccine* **25**: 6852–6862.
- Centers for Disease Control and Prevention (2012). Influenza Antiviral Medications: Summary for

Clinicians.

Chan, RWY, Leung, CYH, Nicholls, JM, Peiris, JSM, Chan, MCW (2012). Proinflammatory cytokine response and viral replication in mouse bone marrow derived macrophages infected with influenza H1N1 and H5N1 viruses. *PLoS One* **7**: e51057.

Chatterjee, S (2016). Oxidative Stress, Inflammation and Disease. In: Dziubla, T, Butterfield, DA (eds). *Oxidative Stress and Biomaterials*. Elsevier Inc: Philadelphia. pp 35-58.

Chen, K, Kirber, MT, Xiao, H, Yang, Y, Keaney, JF (2008). Regulation of ROS signal transduction by NADPH oxidase 4 localization. *J. Cell Biol.* **181**: 1129–1139.

Christopher, ME, Wong, JP (2011). Use of Toll-Like Receptor 3 Agonists Against Respiratory Viral Infections. *Antiinflamm. Antiallergy. Agents Med. Chem.* **10**: 327–338.

Dawood, FS, Iuliano, D, Reed, C, Meltzer, MI, Shay, DK, Cheng, P-Y, *et al.* (2012). Estimated global mortality associated with the first 12 months of 2009 pandemic influenza A H1N1 virus circulation: a modelling study. *Lancet Infect. Dis.* **12**: 687–695.

Dawson, J, Walters, M (2006) Uric acid and xanthine oxidase: Future therapeutic targets in the prevention of cardiovascular disease? *British Journal of Clinical Pharmacology.* **62**: 633-644

Delaney, JW, Pinto, R, Long, J, Lamontagne, F, Adhikari, NK, Kumar, A, *et al.* (2016). The influence of corticosteroid treatment on the outcome of influenza A(H1N1pdm09)-related critical illness. *Crit. Care* **20**: 75.

Department of Health and Aging (2017). Australian Influenza Surveillance Report - 2017 Season Summary

Domínguez-Cherit, G, Lapinsky, SE, Macias, AE, Pinto, R, Espinosa-Perez, L, la Torre, A de, *et al.* (2009). Critically ill patients with 2009 influenza A (H1N1) in Mexico. *JAMA* **302**: 1880–1887.

Dostert, C, Pétrilli, V, Bruggen, R Van, Steele, C, Brooke, T (2008). Innate Immune Activation Through

- Nalp3 Inflammasome Sensing of Asbestos and Silica. *Science*. **320**: 674–677.
- Drake, MG, Scott, GD, Proskocil, BJ, Fryer, AD, Jacoby, DB, Kaufman, EH (2013). Toll-like receptor 7 rapidly relaxes human airways. *Am. J. Respir. Crit. Care Med.* **188**: 664–672.
- Ehrhardt, C, Rückle, A, Hrncius, ER, Haasbach, E, Anhlan, D, Ahmann, K, *et al.* (2013). The NF- $\kappa$ B inhibitor SC75741 efficiently blocks influenza virus propagation and confers a high barrier for development of viral resistance. *Cell. Microbiol.* **15**: 1198–1211.
- Forman, HJ, Fridovich, I (1973) Superoxide Dismutase: A Comparison of Rate Constants. *Archives of Biochemistry and Biophysics*. **158**: 396-400.
- Frangioni, J V, Beahm, PH, Shifrin, V, Jost, CA, Neel, BG (1992). The nontransmembrane tyrosine phosphatase PTP-1B localizes to the endoplasmic reticulum via its 35 amino acid C-terminal sequence. *Cell* **68**: 545–560.
- Gray, SP, Marco, E Di, Kennedy, K, Chew, P, Okabe, J, El-Osta, A, *et al.* (2016). Reactive Oxygen Species Can Provide Atheroprotection via NOX4-Dependent Inhibition of Inflammation and Vascular Remodeling. *Arterioscler. Thromb. Vasc. Biol.* **36**: 295–307.
- Gray, SP, Marco, E Di, Okabe, J, Szyndralewicz, C, Heitz, F, Montezano, AC, *et al.* (2013). NADPH Oxidase 1 plays a key role in diabetes mellitus-accelerated atherosclerosis. *Circulation* **127**: 1888–1902.
- Grinnell, KL, Chichger, H, Braza, J, Duong, H, Harrington, EO (2012). Protection against LPS-induced pulmonary edema through the attenuation of protein tyrosine phosphatase-1B oxidation. *Am. J. Respir. Cell Mol. Biol.* **46**: 623–632.
- Hawkins, BJ, Madesh, M, Kirkpatrick, CJ, Fische, AB (2007). Superoxide Flux in Endothelial Cells via the Chloride Channel-3 Mediates Intracellular Signaling. *Mol. Biol. Cell* **18**: 2002–2012.

- Heneghan, CJ, Onakpoya, I, Jones, MA, Doshi, P, Del Mar, CB, Hama, R, Thompson, MJ, Spencer, EA, Mahtani, KR, Nunan, D, Howick, J, Jefferson, T (2018). Neuraminidase inhibitors for influenza: a systematic review and meta-analysis of regulatory and mortality data. *Cochrane Database Syst. Rev.* **20(42)**:1-242.
- Hofmann, P, Sprenger, H, Kaufmann, A, Bender, A, Hasse, C, Nain, M, *et al.* (1997). Susceptibility of mononuclear phagocytes to influenza A virus infection and possible role in the antiviral response. *J Leukoc Biol* **61**: 408–414.
- Hulme, KD, Gallo, LA, Short, KR (2017). Influenza virus and glycemic variability in diabetes: A killer combination? *Front. Microbiol.* **8**..
- Imai, Y, Kuba, K, Neely, GG, Yaghubian-Malhami, R, Perkmann, T, Loo, G Van, *et al.* (2008). Identification of oxidative stress and Toll-like receptor 4 signaling as a key pathway of acute lung injury. *Cell* **133**: 235–249.
- Jackson, RJ, Cooper, KL, Tappenden, P, Rees, A, Simpson, EL, Read, RC, *et al.* (2011). Oseltamivir, zanamivir and amantadine in the prevention of influenza: a systematic review. *J. Infect.* **62**: 14–25.
- Jefferson, T, Jones, MA, Doshi, P, Mar, CB Del, Hama, R, Thompson, MJ, *et al.* (2014). Neuraminidase inhibitors for preventing and treating influenza in healthy adults and children. *Cochrane Database Syst. Rev.*
- Johnson, N, Mueller, J (2002). Updating the accounts: global mortality of the 1918-1920 ‘Spanish’ influenza pandemic. *Bull. Hist. Med.* **76**: 105–115.
- Judkins, CP, Diep, H, Broughton, BRS, Mast, AE, Hooker, EU, Miller, AA, Selemidis, S, Dusting, GJ, Sobey, CG, Drummond, GR (2009) Direct evidence of a role for Nox2 in superoxide production, reduced nitric oxide bioavailability, and early atherosclerotic plaque formation in ApoE<sup>-/-</sup> mice. *Am J Physiol Heart Circ Physiol.* **298**: 24-32

- Kaminski, MM, Ohnemus, A, Cornitescu, M, Staeheli, P (2012). Plasmacytoid dendritic cells and toll-like receptor 7-dependent signalling promote efficient protection of mice against highly virulent influenza A virus. *J. Gen. Virol.* **93**: 555–559.
- Karuppanapandian, T, Moon, JC, Kim, C, Manoharan, K, Kim, W (2011). Reactive oxygen species in plants: Their generation, signal transduction, and scavenging mechanisms. *Aust. J. Crop Sci.* **5**: 709–725.
- Kawai, T, Akira, S (2010). The role of pattern-recognition receptors in innate immunity: update on Toll-like receptors. *Nat. Immunol.* **11**: 373–384.
- Kim, HM, Lee, Y-W, Lee, K-J, Kim, HS, Cho, SW, Rooijen, N van, *et al.* (2008). Alveolar Macrophages Are Indispensable for Controlling Influenza Viruses in Lungs of Pigs. *J. Virol.* **82**: 4265–4274.
- Kuroda, J, Nakagawa, K, Yamasaki, T, Nakamura, KI, Takeya, R, Kuribayashi, F, *et al.* (2005). The superoxide-producing NAD(P)H oxidase Nox4 in the nucleus of human vascular endothelial cells. *Genes to Cells* **10**: 1139–1151.
- Kvarnhammar, AM, Tengroth, L, Adner, M, Cardell, LO (2013). Innate Immune Receptors in Human Airway Smooth Muscle Cells: Activation by TLR1/2, TLR3, TLR4, TLR7 and NOD1 Agonists. *PLoS One* **8**: 1–10.
- La Gruta, NL, Kedzierska, K, Stambas, J, Doherty, PC (2007). A question of self-preservation: Immunopathology in influenza virus infection. *Immunol. Cell Biol.* **85**: 85–92.
- Lakadamyali, M, Rust, M, Zhuang, X (2004). Endocytosis of influenza viruses. *Microbes Infect.* **6**: 929–936.
- Leang, S, Deng, Y, Shaw, R, Caldwell, N, Iannello, P, Komadina, N, *et al.* (2013). Influenza antiviral resistance in the Asia-Pacific region during 2011. *Antiviral Res.* **97**: 206–210.
- Lee, N, Wong, CK, Hui, DSC, Lee, SKW, Wong, RYK, Ngai, KLK, *et al.* (2013). Role of human Toll-like

receptors in naturally occurring influenza A infections. *Influenza Other Respi. Viruses* **7**: 666–675.

Lee, SJ, Thien Quach, CH, Jung, K-H, Paik, J-Y, Lee, JH, Park, JW, *et al.* (2014). Oxidized Low-Density Lipoprotein Stimulates Macrophage <sup>18</sup>F-FDG Uptake via Hypoxia-Inducible Factor-1 Activation Through Nox2-Dependent Reactive Oxygen Species Generation. *J. Nucl. Med.* **55**: 1699–1705.

Le Goffic, R, Balloy, V, Lagranderie, M, Alexopoulou, L, Escriou, N, Flavell, R, *et al.* (2006). Detrimental contribution of the Toll-like receptor (TLR)3 to influenza A virus-induced acute pneumonia. *PLoS Pathog.* **2**: 526–535.

Le Goffic, R, Pothlichet, J, Vitour, D, Meurs, E, Chignard, M, Mustapha, S-T (2007). Influenza A Virus Activates TLR3-dependent Inflammatory and RIG-1-Dependent Antiviral Response in Human Lung Epithelial Cells. *J. Immunol.* **178**: 3368–3372.

Li, J, Baud, O, Vartanian, T, Volpe, JJ, Rosenberg, PA (2005). Peroxynitrite generated by inducible nitric oxide synthase and NADPH oxidase mediates microglial toxicity to oligodendrocytes. *Proc. Natl. Acad. Sci. U. S. A.* **102**: 9936–9941.

Li, Q, Harraz, MM, Zhou, W, Zhang, LN, Ding, W, Zhang, Y, *et al.* (2006). Nox2 and Rac1 Regulate H<sub>2</sub>O<sub>2</sub>-Dependent Recruitment of TRAF6 to Endosomal Interleukin-1 Receptor Complexes †. *Mol. Cell. Biol.* **26**: 140–154.

Li, Q, Spencer, NY, Oakley, FD, Buettner, GR, Engelhardt, JF (2009). Endosomal Nox2 facilitates redox-dependent induction of NF-kappaB by TNF-alpha. *Antioxid. Redox Signal.* **11**: 1249–1263.

Li, S, Sieben, C, Ludwig, K, Höfer, CT, Chiantia, S, Herrmann, A, *et al.* (2014). PH-ontrolled two-step uncoating of influenza virus. *Biophys. J.* **106**: 1447–1456.

Loos, T, Dekeyzer, L, Struyf, S, Schutyser, E, Gijssbers, K, Gouwy, M, *et al.* (2006). TLR ligands and cytokines induce CXCR3 ligands in endothelial cells: Enhanced CXCL9 in autoimmune arthritis.

*Lab. Investig.* **86**: 902–916.

Lu, X, Malumbres, R, Shields, B, Jiang, X, Sarosiek, KA, Natkunam, Y, *et al.* (2008). PTP1B is a negative regulator of interleukin 4-induced STAT6 signaling. *Blood* **112**: 4098–4108.

Luo, M (2012). Viral Molecular Machines. In *Advances in Experimental Medicine and Biology*, M.G. Rossmann, and V.B. Rao, eds. (Boston, MA: Springer US), pp 201–221.

Lyle, AN, Deshpande, NN, Taniyama, Y, Seidel-Rogol, B, Pounkova, LK, Du, P, *et al.* (2009). Poldip2, a novel regulator of Nox4 and cytoskeletal integrity in vascular smooth muscle cells. *Circ. Res.* **105**: 249–259.

Madjid, M, Awan, I, Ali, M, Frazier, L, Casscells, W (2005). Influenza and atherosclerosis: vaccination for cardiovascular disease prevention. *Expert Opin. Biol. Ther.* **5**: 91–96.

Majde, JA (2000). Viral Double-Stranded RNA, Cytokines, and the Flu. *J. Interf. Cytokine Res.* **272**: 259–272.

Matheson, N, Harnden, A (2007). Neuraminidase inhibitors for preventing and treating influenza in children. *Cochrane Database Syst Rev.*

Matsukura, S, Kokubu, F, Noda, H, Tokunaga, H, Adachi, M (1996). Expression of IL-6, IL-8, and RANTES on human bronchial epithelial cells, NCI-H292, induced by influenza virus A. *J. Allergy Clin. Immunol.* **98**: 1080–1087.

Mauad, T, Hajjar, L a, Callegari, GD, Silva, LFF da, Schout, D, Galas, FRBG, *et al.* (2010). Lung pathology in fatal novel human influenza A (H1N1) infection. *Am. J. Respir. Crit. Care Med.* **181**: 72–79.

McCann, SK, Disting, GJ, Roulston, CL (2014). Nox2 knockout delays infarct progression and increases vascular recovery through angiogenesis in mice following ischaemic stroke with reperfusion. *PLoS One* **9**: 1–13.

Miesel, R, Zuber, M (1993) Elevated levels of xanthine oxidase in serum of patients with

inflammatory and autoimmune rheumatic diseases. *Inflammation*. **17**(5): 551–561

Molinari, N-AM, Ortega-Sanchez, IR, Messonnier, ML, Thompson, WW, Wortley, PM, Weintraub, E, *et al.* (2007). The annual impact of seasonal influenza in the US: measuring disease burden and costs. *Vaccine* **25**: 5086–5096.

Monto, A, Fleming, D, Henry, D, de Groot, R, Makela, M, Klein, T, *et al.* (1999). Efficacy and safety of the neuraminidase inhibitor zanamivir in the treatment of influenza A and B virus infections. *J. Infect. Dis.* **180**: 254–261.

Moscona, A (2005). Neuraminidase inhibitors for influenza. *N. Engl. J. Med.* **353**: 1363–1373.

Myers, MP, Andersen, JN, Cheng, Tremblay, ML, Horvath, CM, Parisien, JP, *et al.* (2001). TYK2 and JAK2 are substrates of protein-tyrosine phosphatase 1B. *J. Biol. Chem.* **276**: 47771–47774.

Nauser, T, Koppenol, WH (2002). The Rate Constant of the Reaction of Superoxide with Nitrogen Monoxide: Approaching the Diffusion Limit. *J. Phys. Chem.* **106**: 4084–4086.

Newall, AT, Scuffham, P (2008). Influenza-related disease: the cost to the Australian healthcare system. *Vaccine* **26**: 6818–6823.

Nichol, KL, Nordin James, Mullooly, J, Lask Richard, Fillbrandt, K (2003). Influenza Vaccination and Reduction in Hospitalization for Cardiac Disease. *N Engl J Med* **348**: 1322–1332.

Nicholson, K, Aoki, F, Osterhaus, A, Trottier, S, Carewicz, O, Mercier, C, *et al.* (2000). Efficacy and safety of oseltamivir in treatment of acute influenza: a randomised controlled trial. *Lancet* **355**: 1845–1850.

Nimmerjahn, F, Dudziak, D, Dirmeier, U, Hobom, G, Riedel, A, Schlee, M, *et al.* (2004). Active NF- $\kappa$ B signalling is a prerequisite for influenza virus infection. *J. Gen. Virol.* **85**: 2347–2356.

Oda, T, Akaike, T, Hamamoto, T, Suzuki, F, Hirano, T, Maeda, H (1989). Oxygen radicals in influenza-induced pathogenesis and treatment with pyran polymer-conjugated SOD. *Science* **244**: 974–

976.

Ozkor, MA, Quyyumi, and AA (2011). Endothelium-Derived Hyperpolarizing Factor and Vascular Function. *Cardiol. Researcg Pract.* **2011**: 156146.

Palmer, RM, Ferrige, AG, Moncada, S (1987). Nitric oxide release accounts for the biological activity of endothelium-derived relaxing factor. *Nature* **327**: 524–526.

Panday, A, Sahoo, MK, Osorio, D, Batra, S (2015) NADPH oxidases: an overview from structure to innate immunity-associated pathologies. *Cellular and Molecular Biology.* **12**: 5-23

Pang, IK, Pillai, PS, Iwasaki, A (2013). Efficient influenza A virus replication in the respiratory tract requires signals from TLR7 and RIG-I. *Proc. Natl. Acad. Sci.* **110**: 13910–13915.

Park, HS, Jung, HY, Park, EY, Kim, J, Lee, WJ (2004). Cutting Edge: Direct Interaction of TLR4 with NADPH Oxidase 4 Isozyme Is Essential for Oxygen Species and Activation of NF- $\kappa$ B. *J. Immunol.* **173**: 3589–3593.

Pons, MW (1967). Some characteristics of double-stranded influenza virus ribonucleic acid. *Arch. Für Die Gesamte Virusforsch.* **22**: 203–209.

Pryor, WA (1986). Oxy-Radicals and Related Species: Their Formation, Lifetimes and Reactions. *Annu. Rev. Physiol.* **48**: 657–667.

Quesada, IM, Lucero, A, Amaya, C, Meijles, DN, Cifuentes, ME, Pagano, PJ (2016). HHS Public Access. **242**: 469–475.

Rajan, J V., Warren, SE, Miao, EA, Aderem, A (2010). Activation of the NLRP3 inflammasome by intracellular poly I:C. *FEBS Lett.* **584**: 4627–4632.

Rath, PC, Aggarwal, BB (1999). TNF-induced signaling in apoptosis. *J. Clin. Immunol.* **19**: 350–364.

Samji, T (2009). Influenza A: Understanding the viral life cycle. *Yale J. Biol. Med.* **82**: 153–159.

- Sato, N, Takasaka, N, Yoshida, M, Tsubouchi, K, Minagawa, S, Araya, J, *et al.* (2016). Metformin attenuates lung fibrosis development via NOX4 suppression. *Respir. Res.* **17**: 1–12.
- Schröder, K, Zhang, M, Benkhoff, S, Mieth, A, Pliquett, R, Kosowski, J, *et al.* (2012). Nox4 is a protective reactive oxygen species generating vascular NADPH oxidase. *Circ. Res.* **110**: 1217–25.
- Segal, BH, Leto, TL, Gallin, JI, Malech, HL, Holland, SM (2000). Genetic, biochemical, and clinical features of chronic granulomatous disease. *Med.* **79**: 170–200.
- Seis, H (2018). On the history of oxidative stress: Concept and some aspects of current development. *Current Opinion in Toxicology.* **7**:122-126.
- Selemidis, S, Seow, HJ, Broughton, BRS, Vinh, A, Bozinovski, S, Sobey, CG, *et al.* (2013). Nox1 oxidase suppresses influenza a virus-induced lung inflammation and oxidative stress. *PLoS One* **8**: e60792.
- Seo, SH, Webster, RG (2002). Tumor necrosis factor alpha exerts powerful anti-influenza virus effects in lung epithelial cells. *J. Virol.* **76**: 1071–6.
- Sieczkarski, SB, Whittaker, GR (2002). Influenza Virus Can Enter and Infect Cells in the Absence of Clathrin-Mediated Endocytosis Influenza Virus Can Enter and Infect Cells in the Absence of Clathrin-Mediated Endocytosis. *J. Virol.* **76**: 10455–10464.
- Smeeth, L, Ph, D, Thomas, SL, Ph, D, Hall, AJ, Ph, D, *et al.* (2004). Risk of myocardial infarction and stroke after acute infection or vaccination. *N. Engl. J. Med.* **351**: 2611–8.
- SteelFisher, G, Blendon, R, Bekheit, M, Lubell, K (2010). The public's response to the 2009 H1N1 influenza pandemic. *N. Engl. J. Med.* **65**: 1–6.
- Stefflerl, A, Hopkins, SJ, Rothwell, NJ, Luheshi, GN (1996). The role of TNF-alpha in fever: opposing actions of human and murine TNF-alpha and interactions with IL-beta in the rat. *Br. J.*

*Pharmacol.* **118**: 1919–24.

Sullivan, SG, Chilver, MB, Carville, KS, Grant, KA, Higgins, G, Komadina, N, *et al.* (2017). Low interim influenza vaccine effectiveness , Australia , 1 May to 24 September 2017. *Eurosurveillance* **678**: 1–7.

Takac, I, Schröder, K, Zhang, L, Lardy, B, Anilkumar, N, Lambeth, JD, *et al.* (2011). The E-loop is involved in hydrogen peroxide formation by the NADPH oxidase Nox4. *J. Biol. Chem.* **286**: 13304–13313.

Teijaro, JR, Walsh, KB, Cahalan, S, Fremgen, DM, Roberts, E, Scott, F, *et al.* (2011). Endothelial cells are central orchestrators of cytokine amplification during influenza virus infection. *Cell* **146**: 980–91.

To, EE, Broughton, BRS, Hendricks, KS, Vlahos, R, Selemidis, S (2014). Influenza A virus and TLR7 activation potentiate NOX2 oxidase-dependent ROS production in macrophages. *Free Radic. Res.* **48**: 940–947.

To, EE, Vlahos, R, Luong, R, Halls, ML, Reading, PC, King, PT, *et al.* (2017). Endosomal NOX2 oxidase exacerbates virus pathogenicity and is a target for antiviral therapy. *Nat. Commun.* **8**: 69.

Turrens, JF (2003). Mitochondrial formation of reactive oxygen species. *J. Physiol.* **552**: 335–344.

Van Buul, J, Fernandez-Borja, M, Anthony, E, Hordijk, P (2005). Expression and localization of NOX2 and NOX4 in primary human endothelial cells. *Antioxidants Redox Signal.* **7**: 308–317.

Varghese, JN, McKimmbreschkin, JL, Caldwell, JB, Kortt, AA, Colman, PM (1992). The Structure of the Complex Between Influenza-Virus Neuraminidase and Sialic-Acid, the Viral Receptor. *Proteins-Structure Funct. Genet.* **14**: 327–332.

Vlahos, R, Stambas, J, Bozinovski, S, Broughton, BRS, Drummond, GR, Selemidis, S (2011). Inhibition of Nox2 oxidase activity ameliorates influenza A virus-induced lung inflammation. *PLoS*

*Pathog.* **7**: e1001271.

Walder, CE, Green, SP, Darbonne, WC, Mathias, J, Rae, J, Dinauer, MC, *et al.* (1997). Ischemic stroke injury is reduced in mice lacking a functional NADPH oxidase. *Stroke* **28**: 2252–2258.

Walsh, K, Teijaro, J, Wilker, P (2011). Suppression of cytokine storm with a sphingosine analog provides protection against pathogenic influenza virus. *Proc. Natl. Acad. Sci.* **108**: 12018–12023.

Wang, JP, Bowen, GN, Padden, C, Cerny, A, Finberg, RW, Newburger, PE, *et al.* (2008). Toll-like receptor-mediated activation of neutrophils by influenza A virus. *Blood* **112**: 2028–34.

Weber, F, Wagner, V, Simon, B, Hartmann, R, Paludan, SR, Rasmussen, SB (2006). Double-Stranded RNA Is Produced by Positive-Strand RNA Viruses and DNA Viruses but Not in Detectable Amounts by Negative-Strand RNA Viruses Double-Stranded RNA Is Produced by Positive-Strand RNA Viruses and DNA Viruses but Not in Detectable Amounts by Neg. *J. Virol.* **80**: 5059–5064.

Wei, EP, Kontos, H a, Beckman, JS (1996). Mechanisms of cerebral vasodilation by superoxide, hydrogen peroxide, and peroxynitrite. *Am. J. Physiol.* **271**: H1262–H1266.

Wendt, MC, Daiber, A, Kleschyov, AL, Mülsch, A, Sydow, K, Schulz, E, *et al.* (2005). Differential effects of diabetes on the expression of the gp91phoxhomologues nox1 and nox4. *Free Radic. Biol. Med.* **39**: 381–391.

WHO (2009). Influenza Fact Sheet.

WHO (2010). WHO guidelines for pharmacological management of pandemic (H1N1) 2009 influenza and other influenza viruses

WHO (2016). Recommended composition of influenza virus vaccines for use in the 2017 southern hemisphere influenza season

WHO (2017). Global Surveillance Report.

Wu, W, Zhang, W, Duggan, ES, Booth, JL, Zou, MH, Metcalf, JP (2015). RIG-I and TLR3 are both required for maximum interferon induction by influenza virus in human lung alveolar epithelial cells. *Virology* **482**: 181–188.

Wurzer, WJ, Ehrhardt, C, Pleschka, S, Berberich-Siebelt, F, Wolff, T, Walczak, H, *et al.* (2004). NF- $\kappa$ B-dependent induction of tumor necrosis factor-related apoptosis-inducing ligand (TRAIL) and Fas/FasL is crucial for efficient influenza virus propagation. *J. Biol. Chem.* **279**: 30931–30937.

Yamamoto, M, Sato, S, Hemmi, H, Hoshino, K, Kaisho, T, Sanjo, H, *et al.* (2003). Role of Adaptor TRIF in the MyD88-Independent Toll-Like Receptor Signaling Pathway. *Science (80-. )*. **301**: 640–643.

Yang, C-S, Kim, J-J, Lee, SJ, Hwang, JH, Lee, C-H, Lee, M-S, *et al.* (2013). TLR3-triggered reactive oxygen species contribute to inflammatory responses by activating signal transducer and activator of transcription-1. *J. Immunol.* **190**: 6368–6377.

Yang, Z, Zheng, T, Zhang, A, Altura, BT, Burton M. Altura (1998). Mechanisms of hydrogen peroxide-induced contraction of rat aorta. *Eur. J. Pharmacol.* **344**: 169–181.

Xue, ML, Thakur, A, Cole, N, Lloyd, A, Stapleton, F, Wakefield, D, *et al.* (2007). A critical role for CCL2 and CCL3 chemokines in the regulation of polymorphonuclear neutrophils recruitment during corneal infection in mice. *Immunol. Cell Biol.* **85**: 525–531.

Ye, S, Lowther, S, Stambas, J (2015). Inhibition of Reactive Oxygen Species Production Ameliorates Inflammation Induced by Influenza A Viruses via Upregulation of SOCS1 and SOCS3. *J. Virol.* **89**: 2672–2683.

Zimmer, S, Steinmetz, M, Asdonk, T, Motz, I, Coch, C, Hartmann, E, *et al.* (2011). Activation of endothelial toll-like receptor 3 impairs endothelial function. *Circ. Res.* **108**: 1358–1366.



## **CHAPTER TWO:**

---

# **Influenza-Induced Endosomal Superoxide Production in Endothelial Cells**

---

## Abstract

Endothelial cells have been shown to contribute to influenza A virus-induced lung inflammation, but the mechanisms by which this occurs remain largely unknown. Influenza internalises into cells via endocytosis and activates TLRs, resulting in an inflammatory response. Interactions between TLRs and the ROS-generating NADPH oxidases have a critical role in inflammation. Endosomal ROS has been shown to play a critical role in inflammatory signalling. Recently, we have shown that Nox2-deficiency is protective against influenza-induced inflammation, and that endosomal, Nox2-dependent ROS production in influenza-infected macrophages is critical for TLR7 signalling. Thus, the aims of this study were: [1] to demonstrate influenza internalising into endothelial cells *via* endocytosis, [2] to determine if influenza infection causes an increase in endosomal ROS production, and [3] to examine ROS signalling in TLR-induced cytokine expression. Human microvascular endothelial cells (HMEC), and WT and NOX2<sup>-/-</sup> mouse lung endothelial cells (MLEC) were infected with influenza A virus strain X-31 (MOI 10) or treated with TLR3 agonist, poly I:C (100µg/ml) or TLR7 agonist imiquimod (10µg/ml). Confocal microscopy was used to localize early endosomes, influenza nucleoprotein and NOX2. OxyBURST fluorescence was used to detect endosomal ROS. Cytokine expression in poly I:C and imiquimod treated WT and NOX2<sup>-/-</sup> MLEC was determined using RT-PCR. This study demonstrated for the first time that influenza internalises into endothelial cells via endocytosis, both in an *in vivo* model and *in vitro*. It was the first demonstration of influenza and TLR3-induced endosomal ROS production in endothelial cells. This study also demonstrated that TLR3 induced expression of IL6, CXCL10 and TNFα was Nox2-dependent, but IFNβ expression was Nox2-independent. The Nox2-TLR3 pathway examined in this study could be involved in the endothelial derived cytokine storm associated with influenza infection. Understanding this process could yield potential treatments for seriously ill patients.

## Introduction

Influenza A virus infection is characterised by a severe and detrimental inflammatory response (Mauad *et al.*, 2010; Domínguez-Cherit, *et al.* 2009), and oxidative stress (Oda *et al.*, 1989). While previous findings suggest that pulmonary epithelial cells and alveolar macrophages are primarily responsible for mediating the inflammatory response to influenza, recent evidence suggests that endothelial cells may also play a hitherto unappreciated role. Influenza virus A (H3N2) can infect microvascular endothelial cell *in vitro* (Armstrong, *et al.* 2012). This is thought to result in increased permeability of the endothelial monolayer, which could lead to the pulmonary oedema seen *in vivo*. Targeting cytokine production specifically from endothelial cells in both wild type and lymphocyte-deficient mice resulted in a decrease in the expression of cytokines CCL2, CCL5 and CXCL10 mRNA compared to the influenza infected mice that were not treated and a significant improvement in survival (Teijaro *et al.*, 2011). This supports the concept that excessive cytokine production is responsible for much of the damage resulting from influenza infection and well as implicating pulmonary endothelial cells in instigating this response. These studies suggest that endothelial cells, not just epithelial cells and macrophages, play a crucial role in influenza induced acute lung injury and acute respiratory distress syndrome, and the excessive immune response associated with them. However, more work needs to be done *in vitro* to understand the potential mechanism involved with influenza infection of endothelial cells.

Given the role of ROS in modulating the inflammatory response and the role of immune dysregulation following influenza A infection, recent studies have attempted to find a link between ROS production (excessive or otherwise) and influenza infection. NADPH oxidases are responsible for the generation of ROS in cells. In addition to the role of Nox2 oxidase in the phagocytosis of microbes, NADPH oxidase also plays an integral role in modulating the immune response through redox signalling. ROS have been shown to interact with protein complexes including inflammasomes, nuclear factor kappa-light-chain-enhancer of activated B cells (NFκB) (Dostert *et al.*, 2008; Zhou *et al.*, 2011), toll-like receptors and the extracellular regulated kinases (ERK) (Pleschka, 2008) to name a

few. While ROS are important in immune related signalling, excessive ROS production (oxidative stress) can result in oxidation of key protein and lipids in the cell and is harmful to the cell. If superoxide reacts with nitric oxide, highly toxic peroxynitrite is formed. This excess production of ROS, including peroxynitrite, was found in mice with influenza-induced pneumonia (Akaike *et al.*, 1996). Consistent with the pathogenic role of ROS, Nox2<sup>-/-</sup> mice infected with H3N2 and H1N1 influenza A strains showed a reduction in viral titre, epithelial cell apoptosis, bronchoalveolar lavage fluid macrophages, peri-bronchial inflammation, superoxide and peroxynitrite production and CCL2 levels compared to the infected wild type mice (Vlahos, *et al.* 2011) . While it's clear that Nox2 plays a role in influenza-induced inflammation, the mechanisms remain largely undefined.

To fully understand the mechanisms of the host immune response to influenza A virus infection, a thorough understanding of viral entry and the interactions between the virus and the cell is imperative. Influenza has been shown to internalise into HeLa cells *via* endocytosis (Lakadamyali *et al.*, 2004). There is a drop in pH in the late endosome, which results in a conformational change of hemagglutinin, which then allows the virus to fuse to the late endosome and release the nuclear protein into the cytosol so that the virus can replicate (Luo, 2012). Intracellular toll-like receptors (TLR), such as TLR3, TLR7, TLR9 and TLR8, are trafficked from the endoplasmic reticulum to endosomes and their activation results in the transcription of proinflammatory cytokines (Blasius and Beutler, 2010). TLR7 is primarily responsible for detecting single stranded RNA, such as RNA from the influenza virus, and has been shown to be critical in the recruitment of neutrophils in response to influenza infection (Wang *et al.*, 2008). However, TLR3, TLR7, TLR8 and TLR9 were all found to be upregulated in the monocytes and dendritic cells of patients with influenza, suggesting a potential role for TLR3, TLR8 and TLR9 as well (Lee *et al.*, 2013). Despite being thought to be activated by double stranded RNA, TLR3 activation has been shown contribute to the influenza-induced inflammatory response (Le Goffic *et al.*, 2007).

Recent studies have linked redox signalling in the endosome with inflammation. Endosomal ROS produced by Nox2 oxidase has been shown to result in the production of NF- $\kappa$ B and TNF- $\alpha$  (Li *et al.*

2009). It has also been shown to regulate the assembly of the IL-1 receptor complex. TLR3, as stated previously, has been shown to be activated by influenza A virus infection and contributes to influenza induced-inflammation. TLR3 is primarily localised to early endosomes (Blasius and Beutler, 2010) and TLR3-dependent Nox2 oxidase activation contributes to the inflammatory response in macrophages in response to a TLR3 agonist, poly I:C (Yang *et al.*, 2013). Influenza infection has been shown to internalise into macrophages *via* endocytosis, resulting in a Nox2-dependent increase in endosomal ROS production (To *et al.*, 2017). In the same experiment, treatment with a TLR7 agonist also resulted in a Nox2-dependent increase in endosomal ROS production. Interestingly, hydrogen peroxide also deactivated TLR7 by oxidation of cysteine 98.

Given the role of Nox2 and the toll-like receptors in influenza-induced inflammation, the role of endothelial cells in influenza pathology, and the link between endosomal ROS and inflammation, it was hypothesised that endothelial cells infected with influenza A virus would drive an increase in endosomal ROS. Therefore, the aims of this study are to:

1. Determine if influenza A virus internalises into endothelial cells *via* endocytosis.
2. Establish if there is a Nox2-dependent increase in endosomal ROS in these cells.
3. Determine if TLR3 and TLR7 activation result in a Nox2-dependent increase in endosomal ROS production.
4. Determine if TLR-induced cytokine production in endothelial cells is Nox2-dependent.

## Methods

### *Virus*

The strain of virus used was the Hong Kong X-31 (H3N2), a low pathogenic, mouse-adapted strain of influenza A virus. The virus was supplied by A/Prof John Stambas (School of Medicine, Deakin University, CSIRO) at a concentration of  $7 \times 10^8$  plaque forming units (PFU)/ml. The virus was dissolved in phosphate buffered saline (PBS) and stored at  $-80^\circ\text{C}$  at a concentration of  $1 \times 10^7$  PFU/ml. When required, the virus was thawed out to  $37^\circ\text{C}$ . Multiplicity of infection (MOI) refers to the number of PFU per cell.

### *Cell Culture*

Human microvascular endothelial cells (HMEC), and wild type and Nox2 knock out mouse lung endothelial cells (MLEC) were used. They were cultivated in Endothelial Growth Media-2 (EGM-2) with 5% fetal bovine serum (FBS), and were incubated at  $37^\circ\text{C}$  with 5% carbon dioxide ( $\text{CO}_2$ ). The media was changed every two to three days and cells were split 1:2 when fully confluent using 0.12% trypsin. Before seeding the MLEC cells into flasks or onto coverslips, the flasks and coverslips were coated with  $1 \mu\text{g}/\text{ml}$  human fibronectin for twenty minutes.  $30 \mu\text{L}$  of suspended HMEC and MLEC were used for cell counting.  $10 \mu\text{L}$  of the cell suspension was mixed with  $10 \mu\text{L}$  trypan blue and transferred into a Countess<sup>®</sup> chamber slide. The cell viability and live cell count were obtained by a Countess<sup>®</sup> cell counter, which is an automated system. The cells were used if the viability was greater than 80%.

### *Fluorescence Microscopy*

Images were taken using Nikon C1 Upright confocal microscope with a x100 objective and running NIS Elements Software (Nikon, Tokyo, Japan), using the facilities, scientific and technical assistance of Monash Micro Imaging, Monash University, Victoria, Australia. Excitation lasers 405 nm, 488 nm, and 635 nm were used. Images were taken from random fields. This was achieved by lowering the objective onto different sections of the slide and ensuring the cells seen under the microscope had not been seen before.

To examine the co-localisation of influenza nucleoprotein and CD31, lung sections were obtained from 7-12-week-old male C57BL/6 mice that weighed approximately 25g. These mice were anaesthetized by methoxyflurane inhalation and then infected with X-31 (MOI  $1 \times 10^4$ ) *i.n.* and were euthanized by an *i.p.* injection of sodium pentobarbitone (360 mg/kg) three days post-infection. Mouse infections were performed by Professor Ross Vlahos (RMIT university). The sections had been fixed in 4% paraformaldehyde and processed in paraffin wax. The lungs were then cut into 3-5  $\mu\text{m}$  sections and mounted onto glass slides.

Deparaffinisation of the lung sections was done by submerging the slides in xylene for 10 minutes, and then in fresh xylene for another 10 minutes. They were then submerged for 2 minutes in 100% ethanol, 1 minute in 95% ethanol, 1 minute in 70% ethanol, 1 minute in 50% ethanol and 2 minutes in 0.01X PBS. The slides were then submerged in 10 mM citrate buffer, microwaved for 6 minutes on high and then allowed to cool to room temperature.

The slides were washed three times for 10 minutes with 0.01 M PBS and blocked with Mouse Ig blocking agent diluted in PBS for 4 hours. The slides were then incubated with mouse influenza A virus nucleoprotein antibody (1:100) and rabbit CD31 antibody (1:50) overnight at room temperature. Controls included lung sections of uninfected mice, and infected lung sections that were incubated with antibody diluent, with only the CD31 antibody, or with the nucleoprotein antibody. The slides were then washed vigorously in PBS five times for ten minutes, and then incubated with Alexa 488 goat anti-mouse antibody (1:200) and the Alexa 647 goat anti-rabbit antibody (1:500) for two hours at room temperature, in minimal light. After a final five PBS washes, the sections were then cover slipped with Vectorshield® mounting media with DAPI staining.

To examine early endosome antigen 1 (EEA1) co-localisation with influenza nucleoprotein and with Nox2,  $10^5$  HMEC for each group were grown on glass coverslips in EGM-2 media with 5% FBS. After 24 hours, the media was replaced with serum free EGM-2. The cells were infected with X-31 (MOI 10)

for 30 minutes, 1 hour and 3 hours, or incubated with a PBS vehicle. This was repeated for each biological replicate.

Cells were washed with PBS, fixed with 4% paraformaldehyde for 15 mins, and washed three times for 10 minutes with 0.01 M PBS. The cells were then incubated for ten minutes with antibody diluent for ten minutes (0.25% triton X) before washing out with PBS three times for five minutes. The cells were then incubated in 10% goat serum for 4 hours. After another three, 10 minute washes, the cells were incubated with primary antibody. When imaging influenza and early endosomes, cells were incubated with mouse influenza A virus nucleoprotein antibody (1:10 000) and rabbit EEA1 antibody (1:2000) for 1 hour at room temperature. When imaging Nox2 and early endosomes, cells that had been infected for 30 minutes were incubated with rabbit Nox2 antibody (1:500) and mouse EEA1 antibody (1:1000) overnight at 4°C. Controls included infected cells that were incubated with antibody diluent, with only the EEA1 antibody, or with either the nucleoprotein or Nox2 antibodies.

The cells were then washed five times and then incubated with Alexa 488 goat anti-mouse antibody (1:1000) and the Alexa 647 goat anti-rabbit antibody (1:1000 dilution for EEA1 imaging and 1:500 for Nox2 imaging) for two hours at room temperature, in minimal light. After a final five PBS washes, the coverslips were then mounted onto baked slides with Vectorshield® mounting media with DAPI staining.

To examine endosomal ROS production with OxyBURST,  $10^5$  WT MLEC and Nox2<sup>-/-</sup> MLEC were seeded onto glass coverslips in EGM-2. This was done by placing a glass coverslip at the bottom of a 24 well plate. After 24 hours, the media was replaced with serum free EBM-2 with ascorbic acid. Before each infection or treatment, cells were pretreated with 50 µg/ml OxyBURST green assay reagent (dihydro-2',4,5,6,7'-hexafluorofluorescein coupled with bovine serum albumin) for five minutes.

In minimal light, X-31 (MOI 10) diluted in PBS or a PBS vehicle was added to each well seeded with either WT MLEC and Nox2<sup>-/-</sup> MLEC for 30 minutes. For some experiments, before infection or PBS treatment, WT MLEC were also pre-treated with SOD (50u/ml).

Coverslips were then washed with PBS and then fixed with paraformaldehyde for 15 minutes. The coverslips were washed three times for 10 minutes with 0.01M PBS, and were then mounted onto baked slides with Vectorshield mounting media with DAPI staining.

#### *Real Time PCR*

$10^6$  WT and Nox2<sup>-/-</sup> MLEC were seeded into a 6-well plate and either treated with poly I:C (30-100 µg/ml) or imiquimod (3-10 µg/ml) or infected with X-31 (MOI 10). Infected or TLR agonist-treated WT MLEC were also pre-treated with catalase (1000 u/ml) for 30 minutes.

After 6 hours, the media was removed, 350µl of a Buffer RLT mixture containing 1% β-mercaptoethanol was added to each well, and the cells were scraped. The cells were then homogenised with a sonicator while on ice. The sample was then centrifuged in an Eppendorf 5424 (8.4 cm radius) at 14 000 rpm for 5 minutes. The supernatant was removed and combined with an equal amount of 70% RNase free ethanol, transferred to a spin column and spun at 10 000 rpm for 15 seconds. 700µl of Buffer RW1 was added to the spin column which was spun at 10 000 rpm for 15 seconds. DNase was mixed with Buffer RDD at a ratio of 1:7. 80µl of this mixture was added to the spin column and left at room temperature for 15 minutes. 500µl of Buffer RPE was added to the spin column which was spun at 10 000 rpm for 15 seconds. Another 500µl of Buffer RPE was added to the spin column which was spun at 10 000 rpm for 2 minutes. The spin column was run at 14 000 rpm for 1 minute with a new collection tube to remove residual flow through. The column was placed in an Eppendorf tube. 30µl of RNase free water was left to sit in the spin column for one minute and then it spun for 10 000 rpm for another minute to elute the RNA.

The RNA was quantified, and sample purity was ensured with a NanoDrop 1000 spectrophotometer. The RNA was then converted to cDNA with a reverse transcriptase kit. The mRNA expression of IL6, CXCL10, IFNβ and TNFα was then measured with real time PCR. 100 ng of cDNA was loaded into each well for IL6, CXCL10, IFNβ and TNFα, and 10 ng of cDNA was loaded into each well for the house keeping gene (either 18s for experiments with virus or poly I:C, or GAPDH for experiments with

imiquimod). The plate was run for two minutes at 50°C, one hour at 95°C, and alternating between 95°C for 15 seconds and 60°C for a minute for 40 cycles.

#### *Analysis and Statistics*

To quantify the OxyBURST fluorescence intensity, 20 images from each group were taken (with approximately 80-110 cells per group) from random fields. The intensity of the OxyBURST fluorescence was measured using the FIJI imaging program. This was done by setting the threshold so that only the OxyBURST fluorescence was measured. The threshold was kept constant between groups. The area of each cell was selected using the freeform tool, and the program calculated the area of fluorescence as percentage area. The percentage area for each group was then averaged over each repeated experiment and then normalised to the control. The data were analysed with a One-Way ANOVA, with a Sidak post hoc using GraphPad Prism.

To analyse the-real time PCR data, the baseline threshold was set at 200 RFU. Fold change in expression was calculated by finding the delta threshold cycle ( $\Delta$ CT) by subtracting the CT from the housekeeping gene CT for each treatment group, finding the  $\Delta\Delta$ CT by subtracting the  $\Delta$ CT for the control group from the  $\Delta$ CT for each treatment group, and finding the fold-change by squaring this value. The data was analysed with a Two-Way ANOVA. The data from the catalase experiments was analysed with a One-Way ANOVA.

#### *Chemicals and Drugs*

The 10mM citrate buffer was prepared by dissolving citric acid (Ajay Finechem) in distilled water, adjusting the pH to 6.0 and adding 0.5ml of Tween 20 (Sigma). It was then stored at -4 °C. The antibody diluent consisted of 0.25% Triton X-1000 (Sigma) dissolved in PBS and was stored at -4 °C.

<b>Chemicals</b>	<b>Manufacture</b>	<b>Storage temperature</b>
RNeasy minikit	Qiagen	-20°C
DNase and Buffer RDD	Qiagen	-20°C
High capacity cDNA reverse transcriptase kit	Applied Biosystems	-20°C
TaqMan® assay solution	Life Technologies	4°C
18S and GAPDH housekeeping primer (FAM)	Applied Biosystems	-20°C
IL6, CXCL10, IFNβ, TNFα and IL1β PCR primers (VIC)	Applied Biosystems	-20°C
Trypan blue	Invitrogen	Room temperature
β-mercaptoethanol	Sigma	4°C
EGM-2 supplements (0.2ml hydrocortisone, 2 ml human fibroblast growth factor, 0.5ml vascular endothelial growth factor, 0.5 ml R3 insulin-like growth factor-1, 0.5ml ascorbic acid, 0.5ml human endothelial growth factor, 25 ml FBS)	Lonza	-20°C
EMB-2 media	Lonza	4°C
Trypsin 0.12%	Sigma	-20°C
Imiquimod (1 mg/ml)	Invivogen	-20°C in endotoxin free water
Poly I:C (1 mg/ml)	Invivogen	-20°C in endotoxin free water
OxyBURST® (1mg/ml)	Molecular Probes	-20°C in PBS

Superoxide dismutase (30 000 u/ml)	Sigma	-20°C
Catalase (10 <sup>6</sup> u/m/)	Sigma	4°C
Influenza nucleoprotein antibody	BioRad	-20°C
Nox2 and EEA1 antibodies	AbCam	-20°C

## Results

### *Influenza internalisation into endothelial cells via endocytosis.*

Lung sections of male C57BL/6 mice that had been infected with X-31 (MOI  $1 \times 10^4$ ) for 3 days were labelled with a CD31 antibody, an IAV nucleoprotein antibody and DAPI. There was evidence of X-31 infection in CD31 positive cells (Figure 1). This suggests that endothelial cells, and not just epithelial cells and macrophages, are infected in these mice.

Triple-labelling with the EEA1 antibody, the nucleoprotein antibody and DAPI was used to examine influenza A virus internalising into endothelial cells, *in vitro*. There was evidence for constitutive endosomal activity in uninfected HMEC. After infection with X-31 (MOI 10), influenza A virus nucleoprotein labelling showed evidence of X-31 internalisation into HMEC as soon as 30 minutes and up to 3 hours after exposure. There was also evidence for influenza located elsewhere than early endosomes in infected cells, evidence for co-localisation of X-31 and early endosomes, and evidence for constitutive endosomal activity in X-31 infected groups (Figure 2).

### *Endothelial Nox2 superoxide production in influenza infected endothelial cells.*

Triple-labelling with the EEA1 antibody, the Nox2 antibody and DAPI was used to confirm if Nox2 oxidase was present in the endosomes of X-31 infected endothelial cells. There was evidence of co-localisation of EEA1 and Nox2 in both infected HMEC and the PBS control, showing that Nox2 oxidase is present in endosomes (Figure 3).

Endosomal superoxide production in response to infection was examined using the probe OxyBURST. There was an increase in OxyBURST fluorescence in WT MLEC infected with X-31 for 30 minutes compared to uninfected WT MLEC ( $p=0.04$ ). SOD treatment decreased the OxyBURST fluorescence due to X-31 infection in WT MLEC (Figure 4a, 4b.). There was a decrease in OxyBURST fluorescence in X-31 infected Nox2<sup>-/-</sup> MLEC compared to the X-31 infected WT MLEC ( $p<0.0001$ ) (Figure 4c, 4d).

#### *TLR3-induced Nox2 superoxide production in endothelial cells*

There was an increase in OxyBURST fluorescence in WT MLEC treated with the TLR3 agonist, poly I:C (100 µg/ml), for 30 minutes compared to the untreated WT MLEC ( $p=0.02$ ). There was a decrease in OxyBURST fluorescence in Nox2<sup>-/-</sup> MLEC treated with poly I:C, compared to WT MLEC treated with poly I:C ( $p=0.001$ ) (Figure 5a, 5b). There was no significant difference in OxyBURST fluorescence between WT MLEC treated with TLR7 agonist, imiquimod (10 µg/ml), for 30 minutes and untreated WT MLEC ( $p=0.94$ ). There was also no significant difference in fluorescence between Nox2<sup>-/-</sup> MLEC treated with imiquimod, and WT MLEC treated with imiquimod ( $p=0.25$ ) (Figure 5c, 5d).

#### *Effect of Nox2-derived ROS on TLR7-induced cytokine expression*

In MLEC treated with imiquimod (3-10 µg/ml), there was a significant increase in IL6 ( $p=0.002$ ), and CXCL10 expression (no asterisk shown in figure) ( $p=0.05$ ), but no significant effect of Nox2 deletion ( $p=0.14$ , and  $p=0.15$ , respectively). There was no effect of imiquimod treatment on IFNβ ( $p=0.42$ ) or TNFα expression ( $p=0.77$ ), and no effect of Nox2 deletion ( $p=0.40$ , and  $p=0.52$ , respectively) (Figure 6).

The study then examined the effect of hydrogen peroxide specifically on TLR7-induced cytokine production in endothelial cells. Interestingly, pre-treatment with catalase (1000 u/ml) resulted in a significant increase in IL6 ( $p=0.04$ ) and TNFα expression ( $p=0.002$ ) in imiquimod-treated MLEC, and a trend in increased CXCL10 ( $p=0.36$ ) and IFNβ expression ( $p=0.06$ ) (Figure 7).

#### *Effect of Nox2-derived ROS on TLR3-induced cytokine expression*

6-hour of poly I:C treatment (30-100 µg/ml) resulted in a significant increase in IL6 ( $p=0.002$ ), CXCL10 ( $p=0.0004$ ), IFNβ ( $p<0.0001$ ) and TNFα expression ( $p=0.0006$ ) in MLEC cells. Nox2 deletion resulted in a significant decrease in poly I:C induced IL6 ( $p=0.0003$ ), CXCL10 ( $p<0.0001$ ), and TNFα expression ( $p=0.0007$ ), but not in IFNβ expression ( $p=0.82$ ) (Figure 8).

Catalase pre-treatment resulted in increased poly I:C-induced (100  $\mu\text{g/ml}$ ) IL6 ( $p=0.009$ ) and TNF $\alpha$  expression ( $p=0.01$ ), and a trend in increased IFN $\beta$  expression ( $p=0.13$ ). Catalase pre-treatment had no significant effect on poly I:C-induced CXCL10 expression ( $p=0.41$ ) (Figure 9).

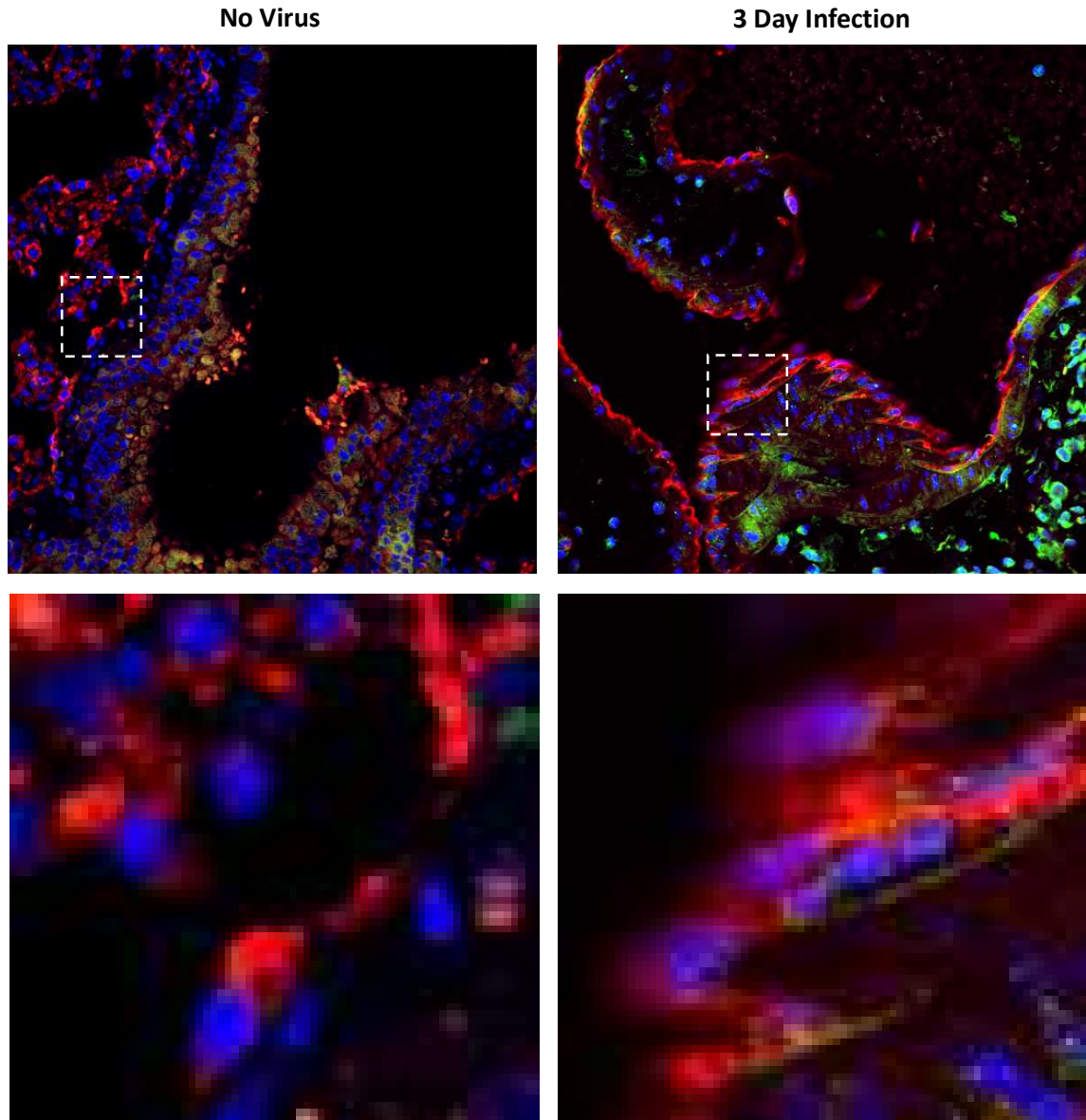


**Figure 1. Evidence for influenza A virus localised to endothelial cells in mice infected with X-31.**

Lung sections of male C57BL/6 mice that had been infected with X-31 ( $1 \times 10^4$  PFU) for 3 days (n=3) and uninfected mice (n=2). Endothelial cells were labelled with a CD31+ antibody with Alexa 647 goat anti-mouse as a secondary (shown in red), the virus was labelled with an influenza A virus nucleoprotein antibody with goat anti-rabbit Alexa 488 as a secondary (shown in green). DAPI was used to stain the nucleus (shown in blue). The images show influenza nucleoprotein in CD31 positive cells.

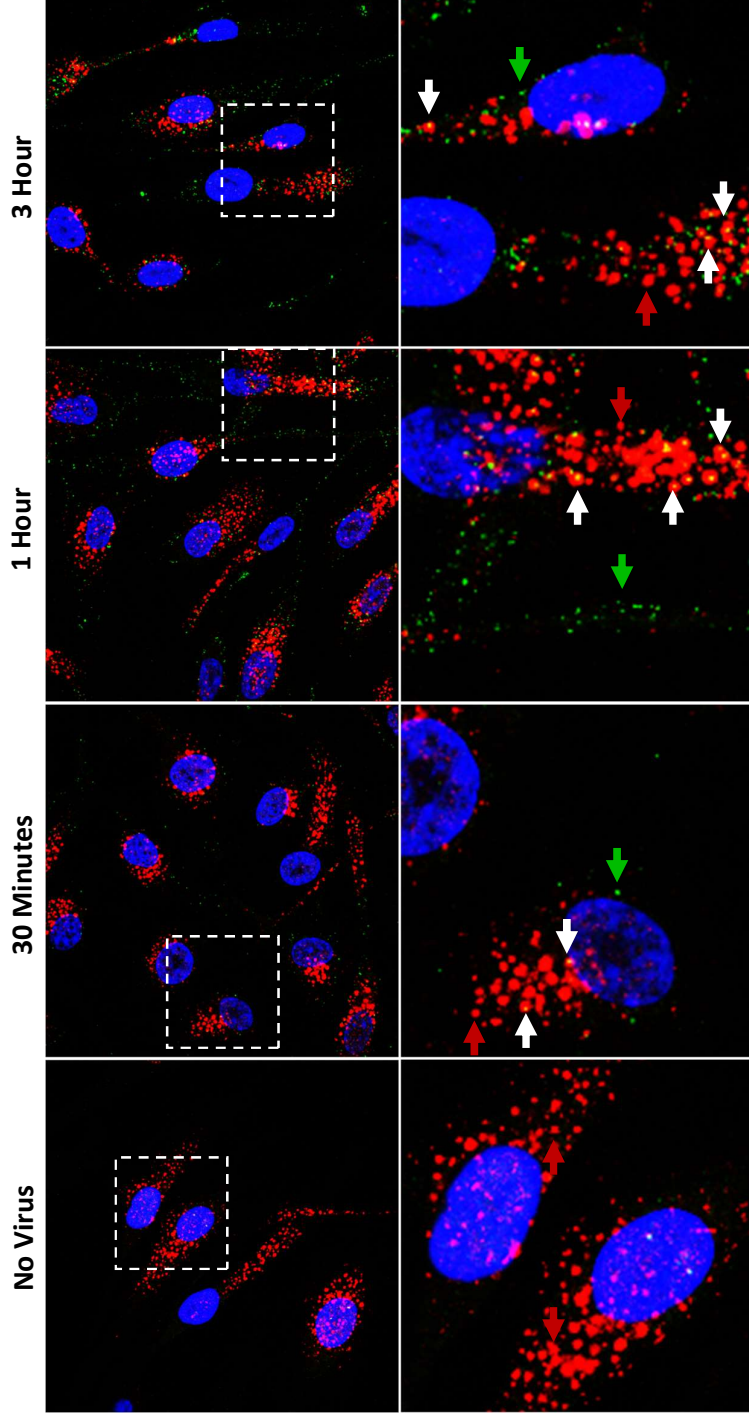


**Figure 2. Evidence of influenza A virus internalisation into endothelial cells via endocytosis.** HMEC were infected with X-31 (MOI 10) and labelled with an influenza A virus nucleoprotein antibody with goat anti-mouse Alexa 488 as a secondary (shown in green), and EEA1 with goat anti-rabbit Alexa 647 as a secondary (shown in red). DAPI was used to stain the nucleus (shown in blue). The control group showed evidence of constitutive endosomal activity, and no evidence of X-31 internalisation. Thirty minutes post infection, there was evidence of X-31 internalisation, as well as nuclear protein colocalisation with early endosomes. The white arrow highlights some evidence of X-31 and early endosome colocalisation, red arrows highlight examples of constitutive endosomal activity and green arrows highlight evidence of X-31 that isn't within an early endosome (n=4).

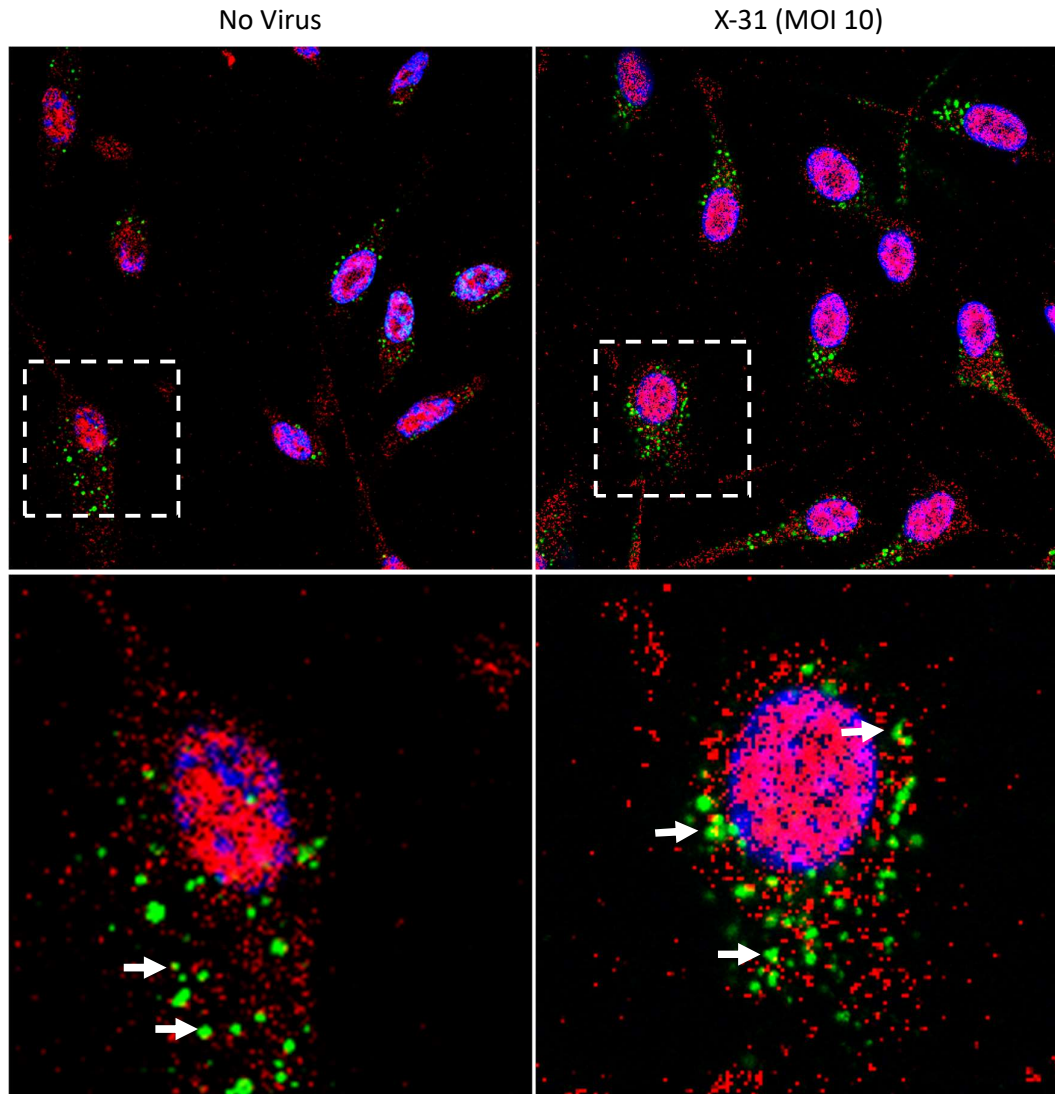


**Figure 3. Evidence that Nox2 is localised to the endosomes of endothelial cells.** HMEC infected with X-31 (MOI 10) for 30 minutes and labelled with a Nox2 antibody with Alexa 647 goat anti-mouse as a secondary (shown in red), and early endosomal antigen 1 antibody with goat anti-rabbit Alexa 488 as a secondary (shown in green). DAPI was used to stain the nucleus (shown in blue). The white arrow highlights some evidence of Nox2 and early endosome colocalisation (n=4).

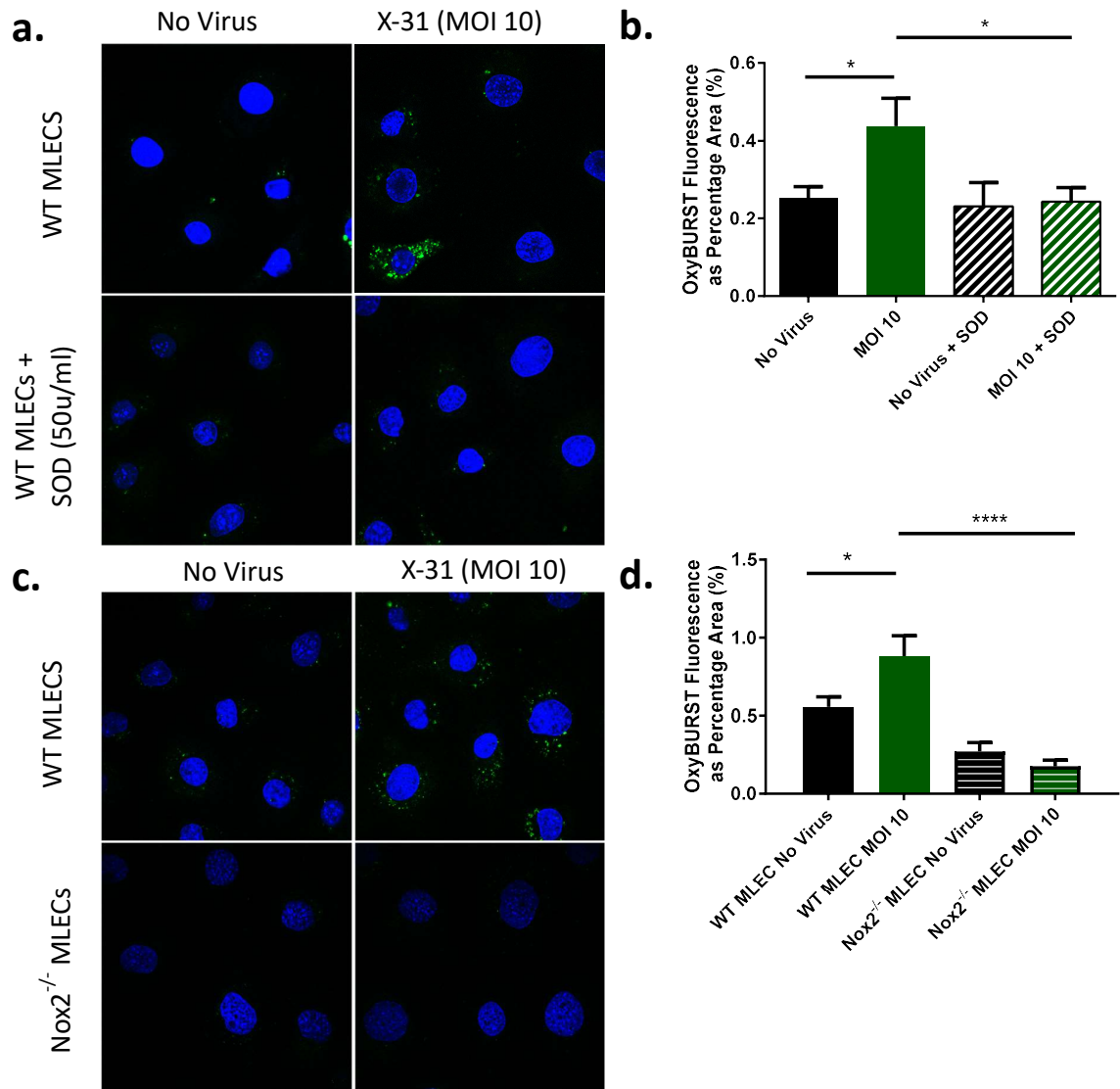


**Figure 4. Evidence that the increase in endosomal ROS production that occurs in endothelial cells after infection with influenza A virus is Nox2-dependent.** **A.** Images showing an increase in OxyBURST fluorescence (shown in green) in X-31-infected WT MLEC compared to an uninfected control, which was not seen in X-31-infected WT MLEC pretreated with SOD (50 u/ml) for 30 minutes (n=6). **B.** Quantified OxyBURST fluorescence in uninfected WT MLEC, X-31-infected WT MLEC, and X-31-infected WT MLEC pretreated with SOD, expressed as percentage area per cell. **C.** Images showing a decrease in OxyBURST fluorescence in X-31-infected Nox2<sup>-/-</sup> MLEC compared to X-31-infected WT MLEC (n=7). **D.** Quantified OxyBURST fluorescence in uninfected and X-31-infected WT and Nox2<sup>-/-</sup> MLEC, expressed as percentage area per cell. Data shown as mean±s.e.m and analysed using an ordinary one way ANOVA with a Sidak post hoc test (p<0.05 \*, p<0.01 \*\*, p<0.001 \*\*\*, p<0.0001 \*\*\*\*).

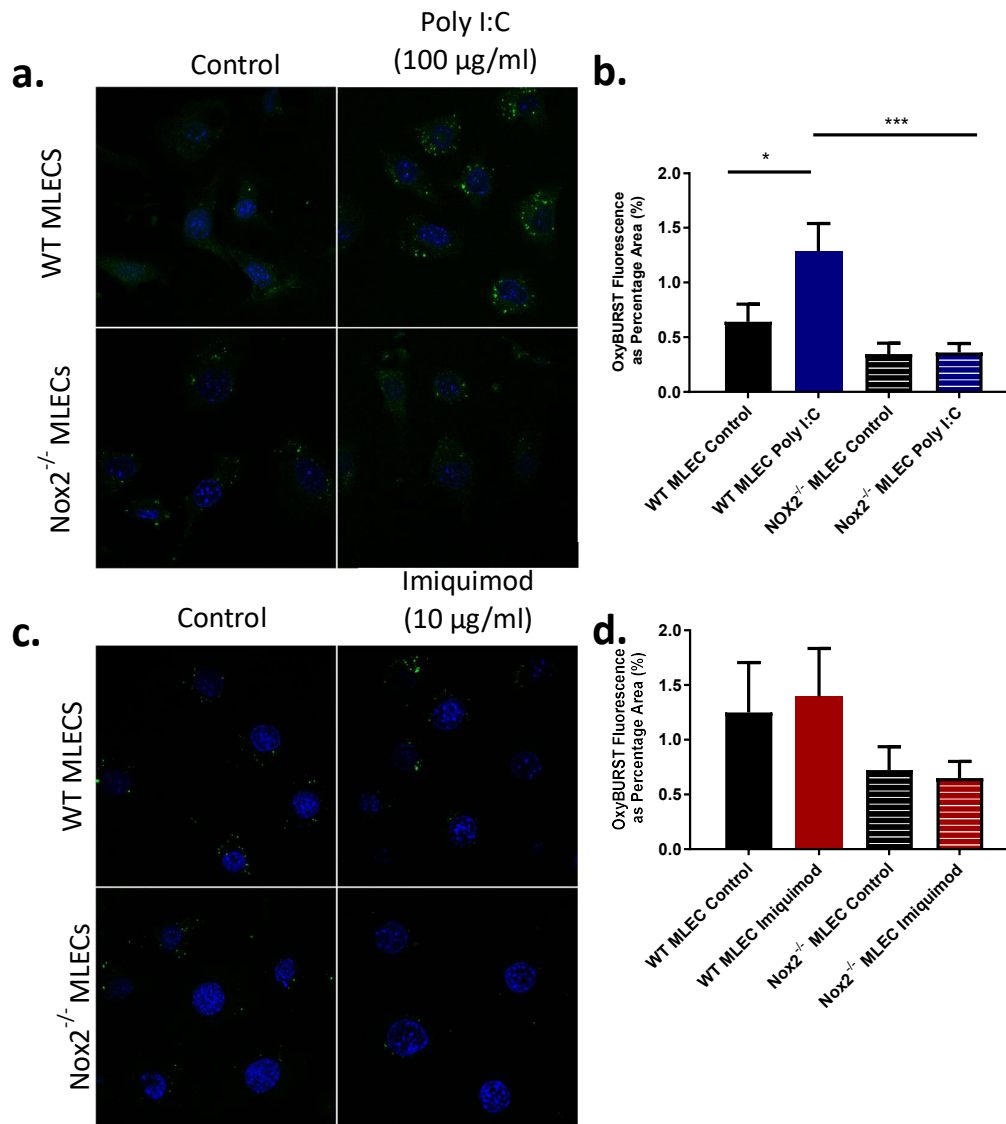


**Figure 5. Evidence that TLR3 activation results in a Nox2-dependent increase in endosomal ROS production.** **A.** Images showing an increase in OxyBURST fluorescence (shown in green) in WT MLEC treated with poly I:C (100 µg/ml) compared to the control and decrease in fluorescence in Nox2<sup>-/-</sup> MLEC treated with poly I:C compared to the poly I:C treated WT MLEC (n=8). **B.** Quantified OxyBURST fluorescence in WT and Nox2<sup>-/-</sup> MLEC, treated with poly I:C. **C.** Images showing no change in OxyBURST fluorescence in WT MLEC treated with TLR7 agonist, imiquimod (10 µg/ml), compared to the control, and no change in fluorescence in Nox2<sup>-/-</sup> MLEC treated with imiquimod compared to the imiquimod treated WT MLEC (n=7). **D.** Quantified OxyBURST fluorescence in WT and Nox2<sup>-/-</sup> MLEC treated with imiquimod, expressed as percentage area per cell. Data shown as mean±s.e.m and analysed using an ordinary one-way ANOVA with a Sidak post hoc test (p<0.05 \*, p<0.01 \*\*, p<0.001 \*\*\*, p<0.0001 \*\*\*\*).

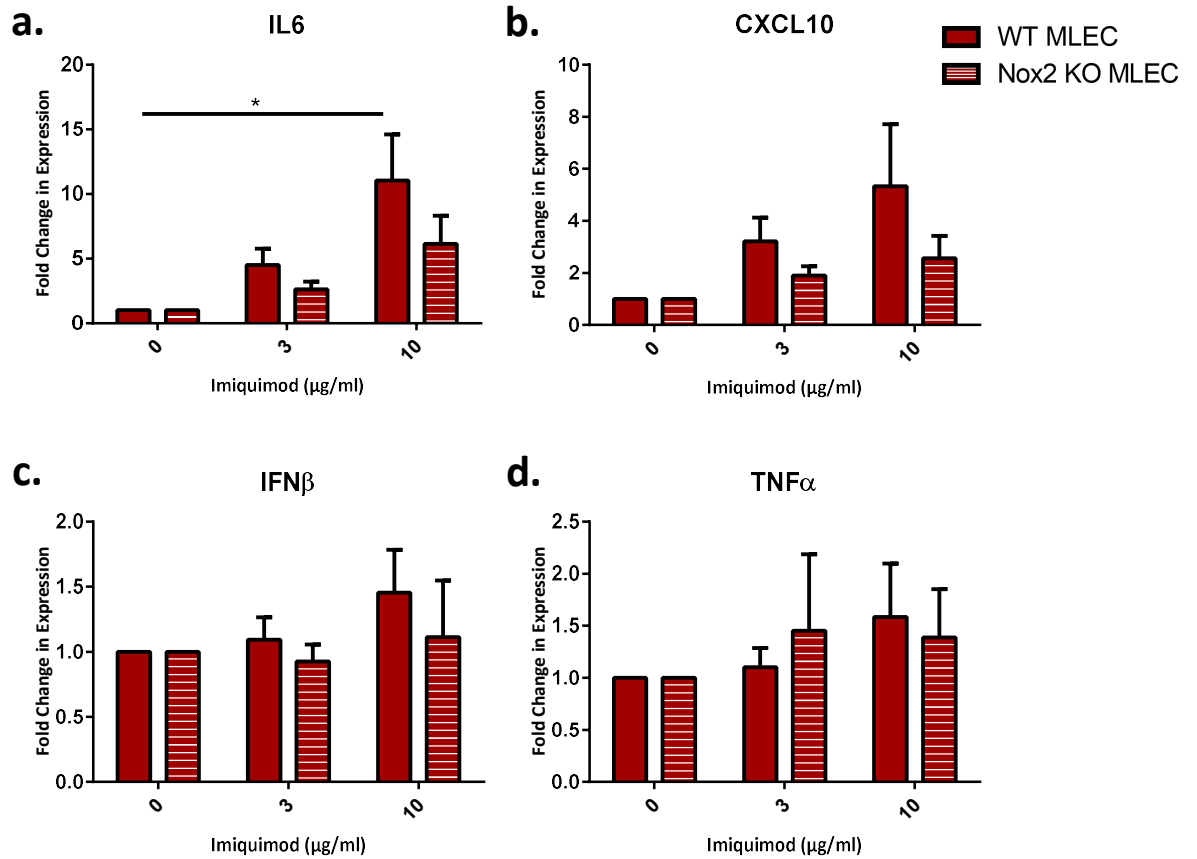


**Figure 6. Evidence that TLR7 activation does not result in a Nox2-dependent increase in cytokine expression in endothelial cells.**

WT and Nox2<sup>-/-</sup> MLEC mice were treated with imiquimod (3-10 μg/ml) for 6 hours. RT-PCR was used to determine the mRNA expression of **A. IL6**, **B. CXCL10**, **C. IFNβ** and **D. TNFα**.

GAPDH was used as a housekeeping gene. Data shown as mean±s.e.m fold change compared to the untreated cells and analysed using an ordinary two-way ANOVA with a Sidak post hoc test

(n=4, p<0.05 \*, p<0.01 \*\*, p<0.001 \*\*\*, p<0.0001 \*\*\*\*).

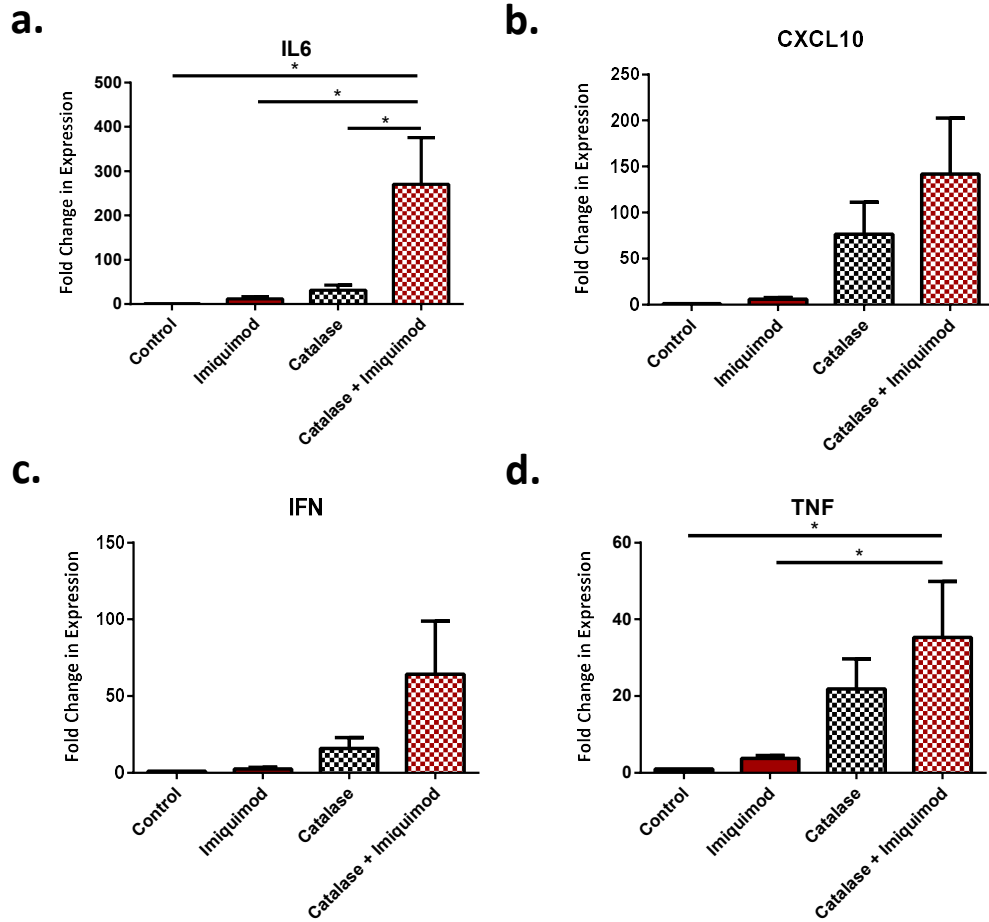


**Figure 7. Evidence that hydrogen peroxide has an inhibitory effect on cytokine expression in endothelial cells.** WT MLEC were pretreated with catalase (1000 u/ml) for 30 minutes, or untreated. Cells were then treated with imiquimod (10  $\mu$ g/ml) for 6 hours. mRNA expression of **A.** IL6 **B.** CXCL10 **C.** IFN $\beta$  and **D.** TNF $\alpha$  were measured with RT-PCR. GAPDH was used as a house keeping gene. Data shown as mean $\pm$ s.e.m and analysed using an ordinary two-way ANOVA with a Sidak post hoc test (n=7, p<0.05 \*, p<0.01 \*\*, p<0.001 \*\*\*, p<0.0001 \*\*\*\*).

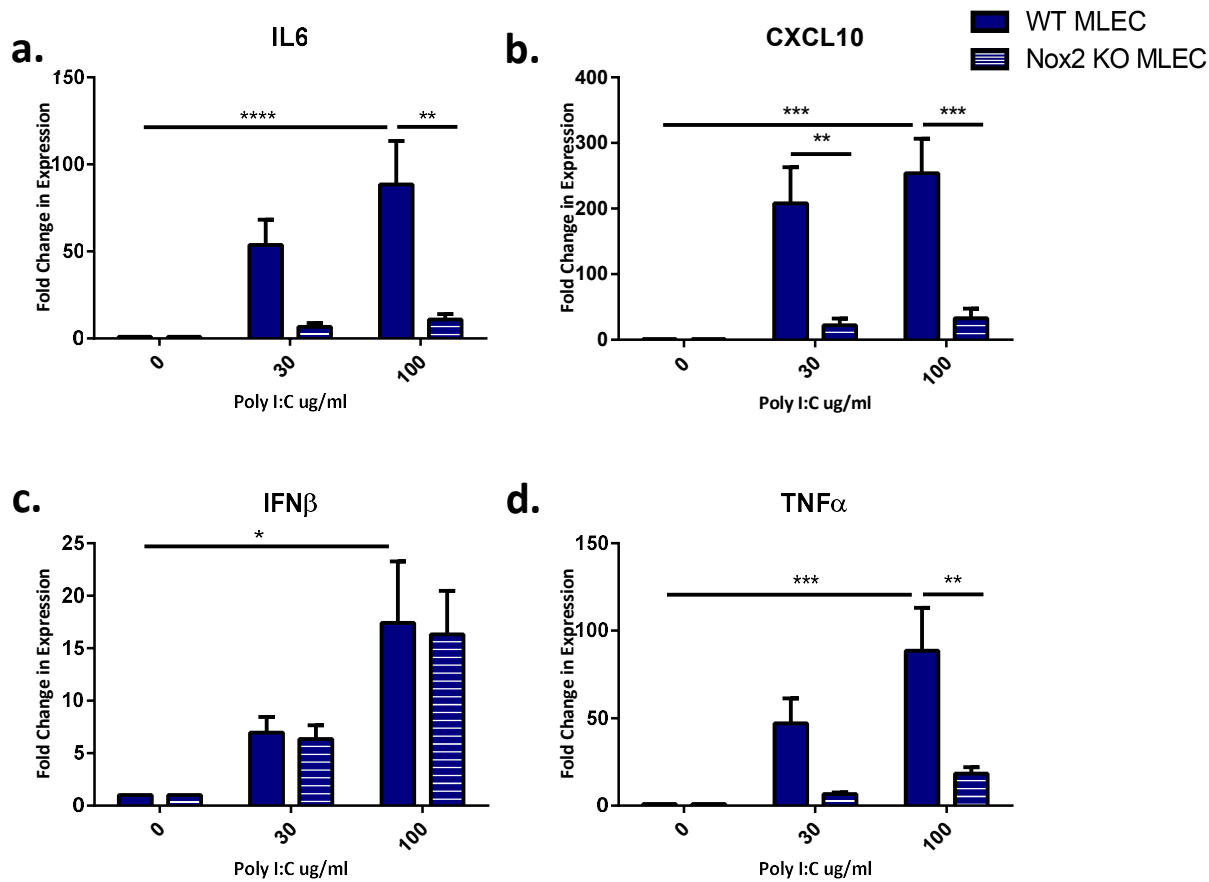


**Figure 8. Evidence that TLR3 activation results in a Nox2-dependent increase in IL6, TNFα and CXCL10 expression in endothelial cells.**

WT and Nox2<sup>-/-</sup> MLEC mice were treated with poly I:C (30-100 μg/ml) for 6 hours. RT-PCR was used to determine the mRNA expression of **A. IL6**, **B. CXCL10**, **C. IFNβ** and **D. TNFα**.

18S was used as a housekeeping gene. Data shown as mean±s.e.m fold change compared to the untreated cells and analysed using an ordinary two-way ANOVA with a Sidak post hoc test (n=5, p<0.05 \*, p<0.01 \*\*, p<0.001 \*\*\*, p<0.0001 \*\*\*\*).

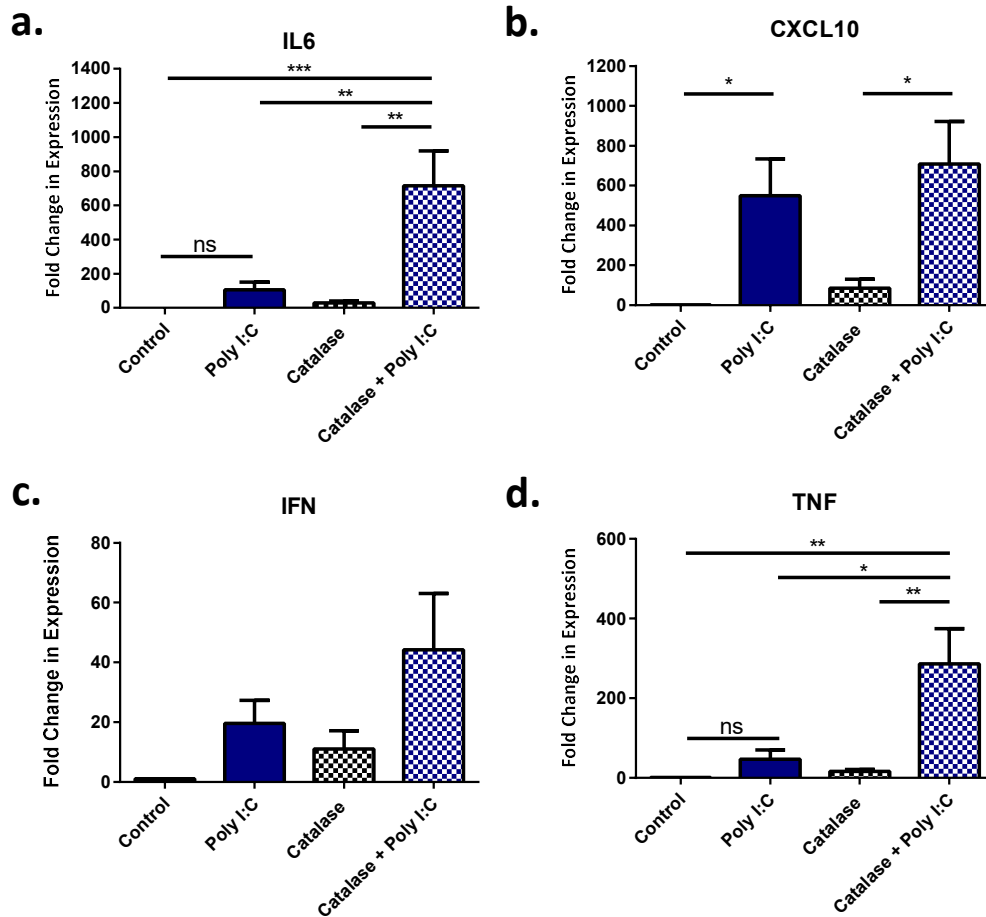


**Figure 9. Evidence that hydrogen peroxide has an inhibitory effect on TLR3-induced IL6 and TNF $\alpha$  expression in endothelial cells.**

WT MLEC were pretreated with catalase ( $1 \times 10^9$  u/ml) for 30 minutes, or untreated. Cells were then treated with poly I:C (100  $\mu$ g/ml) for 6 hours. mRNA expression of **A.** IL6 **B.** CXCL10 **C.** IFN $\beta$  and **D.** TNF $\alpha$  were measured with RT-PCR. 18S was used as a house keeping gene. Data shown as mean  $\pm$  s.e.m and analysed using an ordinary two-way ANOVA with a Sidak post hoc test (n=6,  $p < 0.05$  \*,  $p < 0.01$  \*\*,  $p < 0.001$  \*\*\*,  $p < 0.0001$  \*\*\*\*).

## Discussion

Influenza infection results in up to half a million deaths every year, and renders millions of people seriously ill (WHO, 2009). Autopsies of patients who died during the 2009 “Swine Flu” pandemic showed evidence of immune dysregulation and lung damage (Mauad *et al.*, 2010). The mechanisms behind this dysregulation remain largely unknown. The current dogma is that pulmonary epithelial cells and alveolar macrophages are the primary targets of infection (Bender and Small Jr, 1992). However, recent evidence has suggested that the endothelium may play a larger role. Two separate studies have shown evidence of cell death in endothelial cells infected with influenza (Armstrong *et al.* 2012, Sumikoshi *et al.* 2008), and specifically targeting the endothelium has also been shown to decrease inflammation and improve survival (Teijaro *et al.*, 2011). However, none of these studies have directly shown influenza internalising into endothelial cells. Thus, the first aim of this study was to determine if influenza infection of endothelial cells *in vitro* and *in vivo* occurs *via* endocytosis. To confirm if endothelial cells were infected by influenza *in vivo*, immunohistochemistry was used on the lung of C57BL/6 mice, which were infected with X-31 for three days. There was evidence of co-localisation of influenza nucleoprotein and CD31, a protein found exclusively on endothelial cells. This was also confirmed *in vitro* using HMEC infected with X-31. In these cells, there was evidence of co-localisation between influenza nucleoprotein and early endosomes, as early as 30-minutes post infection. There was also evidence of nucleoprotein in areas of the cell other than early endosomes. This could potentially include late endosomes or the cytosol. This is consistent with previous studies that have shown influenza internalising into HeLa cells *via* endocytosis (Lakadamyali *et al.*, 2004), and with studies showing evidence for apoptosis in endothelial cells infected with influenza, as well as increases in viral titre (Sumikoshi *et al.*, 2008; Armstrong *et al.*, 2012). Both this study and existing literature support the hypothesis that influenza internalises into endothelial cells *via* endocytosis. However, the question remained: what were the molecular pathways involved in influenza-induced cytokine production in endothelial cells?

Nox2 deletion has been shown to reduce influenza-induced inflammation (Vlahos *et al.*, 2011). Nox2-dependent endosomal ROS production was shown to be critical for TNF $\alpha$  expression (Li *et al.*, 2006). Considering that influenza entry into endothelial cells is *via* endocytosis, endosomal Nox2 activity could be one of the pathways involved in influenza-induced inflammation. Thus, the second aim of this study was to determine if influenza infection resulted in an increase in endosomal ROS production.

Immunocytochemistry showed evidence of co-localisation between Nox2 and EEA1 in infected HMEC, confirming that Nox2 is present in the endosome. There was an increase in quantified OxyBURST fluorescence in WT MLEC infected with X-31 compared to the uninfected WT MLEC. This response was SOD-sensitive, confirming that the OxyBURST was detecting an increase in superoxide or its derivatives in these infected cells (Figure 4a, 4b). The increase in endosomal ROS in infected WT MLEC was abolished in Nox2<sup>-/-</sup> MLEC (Figure 4c, 4d), suggesting that influenza-induced endosomal ROS production was Nox2-dependent.

These results show that influenza A virus triggers a Nox2-dependent endosomal ROS response in endothelial cells. While TLR7 is more commonly associated with influenza-induced inflammation (Lund *et al.*, 2004; Wang *et al.*, 2008), TLRs 3, 7, 8 and 9 are all upregulated in infected patients (Lee *et al.*, 2013). TLR3<sup>-/-</sup> mice are protected from influenza-induced inflammation (Le Goffic *et al.*, 2007), and are all trafficked to endosomes from the endoplasmic reticulum (Blasius and Beutler, 2010). A physical association between TLR3 and Nox2 might be necessary for TLR3 activation (Yang *et al.*, 2013).

Thus, the third aim of this study was to determine if TLR3 or TLR7 activation resulted in a Nox2-dependent increase in endosomal ROS production in endothelial cells. Treatment with the TLR3 agonist poly I:C resulted in an increase in endosomal ROS production in WT MLEC compared to the untreated control, which was abolished in Nox2<sup>-/-</sup> MLEC (Figure 5a, 5b). In contrast, treatment with the TLR7 agonist did not result in an increase in endosomal ROS production in WT MLEC or Nox2<sup>-/-</sup>

MLEC (Figure 5c, 5d). Loos, et al. (2006) and Tissari, et al. (2005) both concluded that TLR7 is not expressed in endothelial cells using RT-PCR and western blots respectively. This suggests that any endothelial-derived endosomal ROS response caused by influenza infection would be triggered by TLR3 activation rather than TLR7. The effect of TLR3-induced ROS production on cytokine expression remains largely unstudied.

The fourth and final aim of this study was to determine if TLR3- or TLR7-induced cytokine production in endothelial cells was Nox2-dependent. A 6-hour treatment period with a TLR3 agonist resulted in an increase in expression of IL6, CXCL10, IFN $\beta$  and TNF $\alpha$  in WT MLEC. This increase was found to be Nox2-dependent for IL6, CXCL10 and TNF $\alpha$ , but not IFN $\beta$ . This difference could be due to differences in the downstream signalling pathways for these genes. TLR3-induced expression of IFN $\beta$  occurs through TRAF3, and subsequently IRF3. TLR3-induced expression of IL6, CXCL10 and TNF $\alpha$  occurs through TRAF6 and the activation of NF $\kappa$ B (Kawai and Akira, 2010). These results suggest that the IRF3 pathway is Nox2-independent, whereas the NF $\kappa$ B pathway is Nox2-dependent. TLR3-induced NF $\kappa$ B translocation to the nucleus in macrophages has been shown to be Nox2-dependent (Yang *et al.*, 2013), which is consistent with these findings. However, the same researchers also concluded that Nox2 was necessary for the translocation of IRF3 to the nucleus. This study found that changes in IFN $\beta$  expression occurred independently of Nox2. Considering the different roles that macrophages and endothelial cells play and the different levels of Nox2 expression, the differences in how Nox2 and TLR3 interact could be cell specific.

Interestingly, catalase pre-treatment resulted in an increase in TLR3-induced IL6, and TNF $\alpha$  expression, but not CXCL10 or IFN $\beta$ . Nox2 oxidase produces superoxide, which can then be converted into hydrogen peroxide by SOD. Hydrogen peroxide is then converted into water and oxygen by catalase. Catalase does not pass freely through lipid membranes and was thus acting from the endosome. This suggests a negative feedback loop in which endosomal superoxide production is necessary for TLR3-induced activation of NF $\kappa$ B, but endosomal hydrogen peroxide inhibits it. That

there was no further increase in TLR3-induced CXCL10 expression after catalase treatment could be explained by the already high increase in expression.

After a 6-hour treatment with a TLR7 agonist, there was an increase in IL6 and CXCL10 expression in MLEC that was not Nox2-dependent. While Loos, et al. (2006) and Tissari, et al. (2005) concluded that TLR7 is not expressed in the HUVEC cell line using RT-PCR and western blot, this modest increase in IL6 and CXCL10 expression after TLR7 activation suggests that it may be expressed at low levels in MLEC. Despite TLR7 activation not resulting in an increase in endosomal ROS production, and TLR7-induced cytokine production appearing to occur independently of Nox2, there was a trend for catalase pre-treatment increasing the TLR7-induced cytokine production for IL6, CXCL10, TNF $\alpha$  and IFN $\beta$ . Catalase appeared to stimulate an increase in cytokine expression regardless of treatment. This suggests hydrogen peroxide might have an inhibitory effect on constitutive cytokine expression in endothelial cells. There is a possibility the increase in IL6 and CXCL10 expression after treatment is due to non-specific effects of imiquimod treatment. Future experiments could account for this using TLR7 knockout MLEC or a more specific TLR7 agonist such as imidazoquinoline (Harrison, *et al.* 2007). It should also be noted that this was a cell-based assay and doesn't account for the variation you would see in *in vivo* studies. Utilising an endothelial cell-specific Nox2 knockout mouse would be the next step in experimentation.

Recently, the endothelium has been implicated in excessive inflammatory response associated with serious cases of influenza A virus infection. In summary, this study has demonstrated for the first time that influenza internalises into endothelial cells *via* endocytosis. Additionally, it showed that influenza A virus infects endothelial cells following intranasal delivery in a mouse model. This study also found that influenza infection resulted in a Nox2-dependent increase in endosomal ROS production in endothelial cells, likely mediated through TLR3. Finally, this study was also the first to demonstrate that TLR3-induced expression of IL6, CXCL10 and TNF $\alpha$  was Nox2-dependent, and that TLR3-induced IFN $\beta$  expression was Nox2-independent. Understanding these pathways could lead to

more potential therapies to treat influenza-induced inflammation. Tailoring these treatments to act within the endosome could be the key to improving the efficiency and decreasing off target effects.

## References

- Akaike, T, Noguchi, Y, Ijiri, S, Setoguchi, K, Suga, M, Zheng, YM, *et al.* (1996). Pathogenesis of influenza virus-induced pneumonia: involvement of both nitric oxide and oxygen radicals. *Proc. Natl. Acad. Sci. U. S. A.* **93**: 2448–2453.
- Armstrong, SM, Wang, C, Tigdi, J, Si, X, Dumpit, C, Charles, S, *et al.* (2012). Influenza infects lung microvascular endothelium leading to microvascular leak: role of apoptosis and claudin-5. *PLoS One* **7**: e47323.
- Bender, B, Small Jr, P (1992). Influenza: pathogenesis and host defense. *Semin. Respir. Infect.* **7**: 38–45.
- Blasius, AL, Beutler, B (2010). Intracellular Toll-like Receptors. *Immunity* **32**: 305-315.
- Domínguez-Cherit, G, Lapinsky, SE, Macias, AE, Pinto, R, Espinosa-Perez, L, la Torre, A de, *et al.* (2009). Critically ill patients with 2009 influenza A (H1N1) in Mexico. *JAMA* **302**: 1880–1887.
- Dostert, C, Pétrilli, V, Bruggen, R Van, Steele, C, Brooke, T (2008). Innate Immune Activation Through Nalp3 Inflammasome Sensing of Asbestos and Silica. *Science (80-. )*. **320**: 674–677.
- Harrison, LI, Astry, C, Kumar, S, Yunis, C (2007). Pharmacokinetics of 852A, an imidazoquinoline Toll-like receptor 7-specific agonist, following intravenous, subcutaneous, and oral administrations in humans. *J Clin Pharmacol.* **47** (8): 962-969.
- Kawai, T, Akira, S (2010). The role of pattern-recognition receptors in innate immunity: update on Toll-like receptors. *Nat. Immunol.* **11**: 373–384.
- Lakadamyali, M, Rust, M, Zhuang, X (2004). Endocytosis of influenza viruses. *Microbes Infect.* **6**: 929–936.
- Lee, N, Wong, CK, Hui, DSC, Lee, SKW, Wong, RYK, Ngai, KLK, *et al.* (2013). Role of human Toll-like receptors in naturally occurring influenza A infections. *Influenza Other Respi. Viruses* **7**: 666–

675.

Le Goffic, R, Pothlichet, J, Vitour, D, Meurs, E, Chignard, M, Mustapha, S-T (2007). Influenza A Virus Activates TLR3-dependent Inflammatory and RIG-1-Dependent Antiviral Response in Human Lung Epithelial Cells. *J. Immunol.* **178**: 3368–3372.

Li, Q, Harraz, MM, Zhou, W, Zhang, LN, Ding, W, Zhang, Y, *et al.* (2006). Nox2 and Rac1 Regulate H<sub>2</sub>O<sub>2</sub>-Dependent Recruitment of TRAF6 to Endosomal Interleukin-1 Receptor Complexes. *Mol. Cell. Biol.* **26**: 140–154.

Li, Q, Spencer, NY, Oakley, FD, Buettner, GR, Engelhardt, JF (2009). Endosomal Nox2 facilitates redox-dependent induction of NF-kappaB by TNF-alpha. *Antioxid. Redox Signal.* **11**: 1249–1263.

Loos, T, Dekeyzer, L, Struyf, S, Schutyser, E, Gijssbers, K, Gouwy, M, *et al.* (2006). TLR ligands and cytokines induce CXCR3 ligands in endothelial cells: Enhanced CXCL9 in autoimmune arthritis. *Lab. Investig.* **86**: 902–916.

Lund, JM, Alexopoulou, L, Sato, Karow, M, Adams, NC, Gale, NW, *et al.* (2004). Recognition of single-stranded RNA viruses by Toll-like receptor 7. *Proc Natl Acad Sci U S A* **101**: 5598–5603.

Luo, M (2012). Viral Molecular Machines. In *Advances in Experimental Medicine and Biology*, M.G. Rossmann, and V.B. Rao, eds. (Boston, MA: Springer US), pp 201–221.

Mauad, T, Hajjar, L a, Callegari, GD, Silva, LFF da, Schout, D, Galas, FRBG, *et al.* (2010). Lung pathology in fatal novel human influenza A (H1N1) infection. *Am. J. Respir. Crit. Care Med.* **181**: 72–79.

Oda, T, Akaike, T, Hamamoto, T, Suzuki, F, Hirano, T, Maeda, H (1989). Oxygen radicals in influenza-induced pathogenesis and treatment with pyran polymer-conjugated SOD. *Science* **244**: 974–976.

Pleschka, S (2008). RNA viruses and the mitogenic Raf/MEK/ERK signal transduction cascade. *Biol. Chem.* **389**: 1273–1282.

- Sumikoshi, M, Hashimoto, K, Kawasaki, Y, Sakuma, H, Suzutani, T, Suzuki, H, *et al.* (2008). Human Influenza Virus Infection and Apoptosis Induction in Human Vascular Endothelial Cells. *J. Med. Virol.* **80**: 1072–1078.
- Teijaro, JR, Walsh, KB, Cahalan, S, Fremgen, DM, Roberts, E, Scott, F, *et al.* (2011). Endothelial cells are central orchestrators of cytokine amplification during influenza virus infection. *Cell* **146**: 980–991.
- Tissari, J, Sirén, J, Meri, S, Julkunen, I, Matikainen S (2005). IFN- $\alpha$  enhances TLR3-mediated antiviral cytokine expression in human endothelial and epithelial cells by up-regulating TLR3 expression. *J Immunol.* **174**: 4289–4294.
- To, EE, Vlahos, R, Luong, R, Halls, ML, Reading, PC, King, PT, *et al.* (2017). Endosomal NOX2 oxidase exacerbates virus pathogenicity and is a target for antiviral therapy. *Nat. Commun.* **8**: 69.
- Vlahos, R, Stambas, J, Bozinovski, S, Broughton, BRS, Drummond, GR, Selemidis, S (2011). Inhibition of Nox2 oxidase activity ameliorates influenza A virus-induced lung inflammation. *PLoS Pathog.* **7**: e1001271.
- Wang, JP, Bowen, GN, Padden, C, Cerny, A, Finberg, RW, Newburger, PE, *et al.* (2008). Toll-like receptor-mediated activation of neutrophils by influenza A virus. *Blood* **112**: 2028–34.
- WHO (2009). Influenza Fact Sheet.
- Yang, C-S, Kim, J-J, Lee, SJ, Hwang, JH, Lee, C-H, Lee, M-S, *et al.* (2013). TLR3-triggered reactive oxygen species contribute to inflammatory responses by activating signal transducer and activator of transcription-1. *J. Immunol.* **190**: 6368–6377.
- Zhou, R, Yazdi, AS, Menu, P, Tschopp, J (2011). A role for mitochondria in NLRP3 inflammasome activation. *Nature* **469**: 221–225.

## **CHAPTER THREE:**

---

### **Determining the effect of toll-like receptor activation on vascular tone**

---

## Abstract

Hypotension is a sign of cardiopulmonary insufficiency in influenza A virus infection. However, the mechanisms by which this occurs remain unclear. TLR3 and TLR7 agonists, both of which are associated with influenza infection, also cause hypotension in patients. Thus, the aims of this study were to determine if TLR3 and TLR7 activation results in a change in vascular tone and to examine the mechanisms involved. Pig coronary artery ring segments were mounted in organ bath in Krebs physiological solution and pre-contracted to ~50% of the maximum contractile response with U46619. A concentration-response curve to TLR7 agonists imiquimod (3-300  $\mu$ M), gardiquimod (3-300  $\mu$ M) and resiquimod (3-300  $\mu$ M), and TLR3 agonist and poly I:C (1-30  $\mu$ g/ml) were performed in U46619 pre-contracted ring segments. To investigate the role of the endothelium, the endothelium was denuded in some segments. To examine signalling pathways involved, the ring segments were either left untreated or pre-treated with eNOS inhibitor, L-NAME (100  $\mu$ M), with  $K^+$  (25 mM), or with specific  $K^+$  channel inhibitors, apamin (300 nM), charybdotoxin (300 nM), paxilline (10  $\mu$ M), or BaCl<sub>2</sub> (100  $\mu$ M), before treatment with TLR agonists. To examine ROS signalling pathways involved, ring segments were pretreated with SOD (500u/ml), catalase (500u/ml), PEG-SOD (600u/ml), and PEG-catalase (500u/ml). TLR7 agonists resulted in a concentration-dependent relaxation of pig coronary artery. This response was endothelium-independent and potassium channel-dependent. Apamin pre-treatment significantly reduced TLR7-induced relaxation. Catalase pre-treatment significantly increased TLR7-induced relaxation. TLR3 resulted in partial relaxation of pig coronary artery of pig coronary artery that was entirely endothelial-dependent and was abolished after L-NAME treatment. PEG-SOD pre-treatment significantly increased TLR3-induced relaxation, and there was a trend in decreased TLR3-induced relaxation after pre-treatment with PEG-catalase. This study demonstrated distinct cellular and molecular pathways by which TLR3 and TLR7 cause vascular relaxation. Understanding these pathways could be the key to understanding cardiovascular complications that often arise following viral infection.

## Introduction

An underappreciated effect of influenza A virus infection is the exacerbation and increased susceptibility to cardiovascular complications. Influenza vaccination was shown to reduce the risk of hospitalisation due to stroke or cardiovascular disease (Nichols, et al. 2003) and to be protective against myocardial infarction (Smeeth, et al. 2004). Of the 300 000 Swine Flu deaths, approximately 83 000 of them were cardiovascular related (Dawood et al., 2012), and at least 10% of patients will present with cardiac symptoms (Rezkalla and Kloner, 2010).

Hypotension in influenza patients is a sign of cardiopulmonary insufficiency, which is characterised by heart failure and pulmonic regurgitation (WHO, 2010). This aspect of influenza infection is completely neglected in research. There has been no research of the role of cardiopulmonary insufficiency in infection or mechanisms involved. Chapter 2 examined the role of the endothelium in regulating inflammation in response to influenza infection. However, one of the major functions of the endothelium is to regulate vascular tone. Vascular tone is regulated by a number of different pathways, by a number of different cell types. The endothelium produces nitric oxide (NO) through endothelial nitric oxide synthase (eNOS) (reviewed by Knowles and Moncada, 1994). NO results in relaxation of vascular smooth muscle through the activation of soluble guanylate cyclase (reviewed by Mayer, 1994). In turn, guanylate cyclase results in an increase in cyclic guanosine monophosphate (cGMP) production, which causes relaxation of vascular smooth muscle by activating cGMP-dependent protein kinase that dephosphorylates the light myosin chain. The endothelium also produces a hyperpolarising factor called endothelium-derived hyperpolarizing factor (EDHF; Reviewed by Ozkor and Quyyumi, 2011) which causes relaxation of vascular smooth muscle through mechanisms that are still debated.

Direct activation of various potassium channels on vascular smooth muscle, can also cause relaxation (Reviewed by Ko, *et al.* 2008). There is a large number of identified potassium channels on the smooth muscle that have been implicated in smooth muscle relaxation. These include the large,

intermediate, and small conductance  $\text{Ca}^{2+}$ -activated  $\text{K}^+$  channels, which are calcium-activated channels categorised by the amount of charge passing across a cell membrane. Another important family of  $\text{K}^+$  channels, which regulate membrane potential of vascular smooth muscle are the inwardly rectifying potassium channels ( $\text{K}_{\text{ir}}$  channels).

Chapter 2 of this thesis and the studies by Tejiaro, *et al.* (2011) have examined the role of the endothelium in exacerbating influenza-induced inflammation, but they have not considered either the role of the endothelium or the ability of viral infection to modify vascular smooth muscle tone.

Several studies have shown that influenza infection resulted in oxidative stress and ROS production (Oda *et al.*, 1989; Vlahos, *et al.* 2011; To *et al.* 2017), including Chapter 2 of thesis, which showed TLR3 activation resulting in a Nox2-dependent increase in endosomal ROS production. ROS has been shown to play a very important role in regulating vascular tone. For example, hydrogen peroxide has been shown to cause endothelium-independent relaxation of the smooth muscle through activation of guanylate cyclase (Burke and Wolin, 1987).

As discussed in chapter 2, the toll-like receptors play an important role in influenza pathology. TLR3, TLR7, TLR8 and TLR9 are upregulated in influenza patients, and TLR3 and TLR7 are both involved in influenza-induced inflammation. While no studies to date have directly examined the effects of influenza on vascular tone, multiple studies have demonstrated that TLR activation influences vascular tone. Treatment with LPS, a component of bacteria, which activates TLR4, causes relaxation of rat aorta directly through activation of large conductance  $\text{Ca}^{2+}$ -activated  $\text{K}^+$  channels on the smooth muscle, as well as through an endothelium-dependent, nitric oxide pathway (Farias, *et al.* 2002).

Septic shock is defined as sepsis with severe hypotension and metabolic abnormalities (Singer, *et al.* 2016). TLR4 upregulation is associated with severe septic shock (Leon, *et al.* 2004).

Hypotension is a reported side effect of oral imiquimod treatment, suggesting that TLR7 activation may have direct effects on vascular tone (Aldara product sheet, 2014). While there have been, no studies looking at the effect of TLR7 on vascular tone *per se*, TLR7 activation has been shown to

cause airway relaxation. Isolated human airway smooth muscle strips relaxed when treated with imiquimod, and guinea pigs treated with intravenous imiquimod resulted in airway relaxation (Drake, et al. 2013). There is some debate on whether or not TLR7 is even expressed in vascular smooth muscle. Drake, et al. 2013, did not find TLR7 on airway smooth muscle. However, Kvarnhammar, et al. (2013) did find TLR7 expressed in human aortic smooth muscle cells. How TLR7 regulates vascular tone, and if it is endothelium-dependent or through directly targeting the smooth muscle, is unknown. Treatment with TLR3 agonists such as poly I:C and poly I:C conjugated with poly-L-lysine and carboxymethylcellulose have also been shown to result in hypotension in human trials (Krown, et al. 1985; Stevenson, et al. 1985), but there have been no studies exploring the mechanisms behind it.

While the cardiovascular effects of influenza can be devastating, it is surprising that there has been very little research examining the mechanisms involved. The effects of the endothelium on influenza-induced inflammation have been explored, but its role in regulating vascular tone in the context of infection is unknown. Some TLRs have been shown to cause vascular relaxation, however, for the viral sensors, TLR3 and TLR7 this has never been explored and the mechanisms behind this are unknown.

Thus, the aims of this study were to determine if TLR3 and TLR7 activation results in relaxation of vascular smooth muscle; determine if TLR3- and TLR7-dependent relaxation of vascular smooth muscle is endothelium-dependent, and if TLR-induced ROS production mediates relaxation of the vascular smooth muscle. Multiple TLR7 agonists were used to ensure that TLR7 activation was the cause of the vascular relaxation seen after imiquimod was added to the organ bath.

## Method

### *Protocol*

Pig hearts were obtained from the Australian Food Group abattoir (Laverton, Victoria, Australia) and transported back to the laboratory on ice. The right coronary artery was carefully dissected away from the surrounding pericardium. While kept in pre-warmed 37°C Krebs physiological salt solution (see Appendix 1), the artery was cut into small 4-5 mm ring sections. When required, the endothelium was removed by rubbing the inside of the artery with a small piece of plastic tubing.

The rings were then mounted in 10 ml organ baths in Krebs solution (37°C) and bubbled with carbogen (95% oxygen, 5% CO<sub>2</sub>). The tissues were then passively stretched to 5g and allowed to rest for 15 minutes. They were then re-tensioned to 5g and rested for another 15 minutes.

The maximum contraction of the tissue ( $K_{max}$ ) was obtained by exposing the coronary arteries to high potassium physiological salt solution (125mM K<sup>+</sup>; termed KPSS). Once the maximum tension was reached (after approximately 30-40 minutes), the KPSS solution was removed, the tissue was washed with Krebs and allowed to reach a baseline level of active force.

The tissues were pre-treated with either a K<sup>+</sup> solution (25 mM), L-NAME (100 µM), PEG-catalase (500u/ml), PEG-SOD (600u/ml), SOD (500u/ml), catalase (500u/ml), charybdotoxin (300 nM), apamin (300 nM), paxilline (10 µM), BaCl<sub>2</sub> (100 µM) or left untreated for 30 minutes. The PEG conjugated SOD and catalase can pass through plasma membranes, whereas the unconjugated SOD and catalase either have their effects extracellularly or are taken into endosomes with the TLR agonists.

After treatment with the antagonist, the tissue was contracted to approximately 50% of the  $K_{max}$  by titrating the concentration of U46619. The tissues pre-treated with K<sup>+</sup> were not contracted further with U46619, as they developed a contraction ~50% of the  $K_{max}$ .

Once a stable level of active force was obtained, the tissue was then treated with either the TLR7 agonists imiquimod (3-300 µM), resiquimod (3-300 µM) or gardiquimod (3-300 µM), or TLR3 agonist poly I:C (1-30 µg/ml) in cumulative concentrations. At the termination of the TLR concentration

response curve, the endothelium integrity was examined by washing the tissue with Krebs three times, followed by a 15-minute rest period. The tissues were then re- contracted to 50% of the  $K_{max}$  with U46619, and then exposed to a single concentration of the endothelium-dependent vasodilator, substance P (1  $\mu$ M).

#### *Analysis*

All values are given as mean  $\pm$  S.E.M. Data were analysed with a standard two-way ANOVA with a Holm-Sidak *post hoc* test.

#### *Drugs and Solution*

<b>Chemicals</b>	<b>Manufacture</b>	<b>Storage</b>
L-NAME	Sigma	-20 <sup>o</sup> C in DMSO
Substance P	Sigma	-20 <sup>o</sup> C in endotoxin free water
Charybdotoxin	Sigma	-20 <sup>o</sup> C in endotoxin free water
Apamin	Sigma	-20 <sup>o</sup> C in endotoxin free water
PEG-catalase	Sigma	-20 <sup>o</sup> C in endotoxin free water
PEG-SOD	Sigma	-20 <sup>o</sup> C in endotoxin free water
Catalase	Sigma	-20 <sup>o</sup> C in endotoxin free water
SOD	Sigma	-20 <sup>o</sup> C in endotoxin free water
Imiquimod	Invivogen	-20 <sup>o</sup> C in endotoxin free water
Poly I:C	Invivogen	-20 <sup>o</sup> C in endotoxin free water
Resiquimod	Invivogen	-20 <sup>o</sup> C in endotoxin free water
Gardiquimod	Invivogen	-20 <sup>o</sup> C in endotoxin free water
BaCl <sub>2</sub>	Sigma	Made up fresh in Krebs solution

## Results

### *Involvement of the endothelium in TLR-induced relaxation.*

Increasing concentrations of TLR7 agonists imiquimod (3-300 $\mu$ M) and resiquimod (3-300 $\mu$ M) resulted in complete, near 100% relaxation of pre-contracted pig coronary artery (Figure 1a; Figure 2).

Increasing concentrations of TLR7 agonist gardiquimod (3-300 $\mu$ M) also resulted in relaxation of pre-contracted pig coronary artery, but the effects were less potent than resiquimod ( $p=0.006$ ; Figure 2).

Removal of the endothelium had no effect on imiquimod-induced relaxation ( $p=0.85$ ) (Figure 1a; Figure 2). However, removal of the endothelium abolished relaxation in response to substance P

Increasing concentrations of TLR3 agonist poly I:C resulted in approximately 40-60% relaxation of pre-contracted pig coronary artery. In contrast to TLR7, removal of the endothelium abolished poly I:C-induced relaxation of pre-contracted pig coronary artery ( $p=0.002$ ) (Figure 3a) in a similar manner to the response to SP.

### *Involvement of K-channels in TLR7-induced relaxation.*

Pre-treating pig coronary artery with  $K^+$  (25mM), which is a means to inhibit non-selectively, K-channel activation and subsequent relaxation of the vascular smooth muscle, resulted in a rightward shift of the concentration-response curve ( $p=0.004$ ). Pre-treatment with  $K^+$  in combination with the eNOS inhibitor L-NAME (100 $\mu$ M) also resulted in a rightward shift of the concentration-response curve ( $p=0.0007$ ). Pre-treating pig coronary artery with L-NAME alone had no effect on imiquimod-induced relaxation ( $p=0.99$ ) (Figure 1b).

Pre-treatment with the small conductance calcium-activated potassium channel inhibitor, apamin (100nM) did not result in a significant decrease of imiquimod -induced relaxation overall ( $p=0.07$ ), but there was a significant difference at the 30 $\mu$ M concentration (Figure 4a). Pre-treatment with the intermediate and large conductance calcium-activated potassium channel inhibitor, charybdotoxin (100nM), and with large conductance calcium-activated potassium channel inhibitor, paxilline

(10 $\mu$ M) had no effect on imiquimod-induced relaxation (Figure 4a, Figure 4b) ( $p=0.44$ ,  $p=0.32$ , respectively). Pre-treatment with BaCl<sub>2</sub> (100 $\mu$ M), which specifically inhibits inwardly rectifying potassium channels, did not affect imiquimod-induced relaxation (Figure 4c).

*Involvement of eNOS in TLR3-induced relaxation.*

Pre-treatment with L-NAME, or K<sup>+</sup> in addition to L-NAME, abolished poly I:C-induced relaxation of pre-contracted pig coronary artery ( $p=0.03$ ,  $p=0.01$ , respectively). Pretreating pig coronary artery with K<sup>+</sup> alone had no effect on poly I:C-induced relaxation ( $p=0.92$ ) (Figure 3b).

*Hydrogen peroxide has an inhibitory effect on TLR7-induced relaxation.*

Pre-treatment with catalase (500u/ml) significantly increased imiquimod-induced relaxation of pre-contracted pig coronary artery ( $p=0.04$ ) (Figure 5a). Pre-treatment with PEG-catalase (500u/ml) had no effect on imiquimod-induced relaxation ( $p=0.99$ ) (Figure 5b). Pre-treatment with neither SOD nor PEG-SOD (600u/ml) affected the imiquimod-induced relaxation ( $p=0.81$ ,  $p=0.98$ , respectively; Figure 6).

*PEG-SOD treatment sensitises pig coronary artery to TLR3-induced relaxation.*

Pre-treatment with catalase (600u/ml) had no effect on poly I:C-induced relaxation ( $p=0.95$ ; Figure 7a). There was a trend in decreased on poly I:C-induced relaxation in pig coronary artery pretreated with PEG-catalase (600u/ml) but it was not significant ( $p=0.51$ ; Figure 7b). Pre-treatment with SOD did not modify the poly I:C-induced relaxation of pre-contracted pig coronary artery ( $p=0.90$ ) (Figure 8a). Pre-treatment with PEG-SOD did not increase poly I:C-induced relaxation of pre-contracted pig coronary artery overall ( $p=0.33$ ), but there was a significant difference at the 3  $\mu$ g/ml poly I:C ( $p=0.04$ ) (Figure 8b).

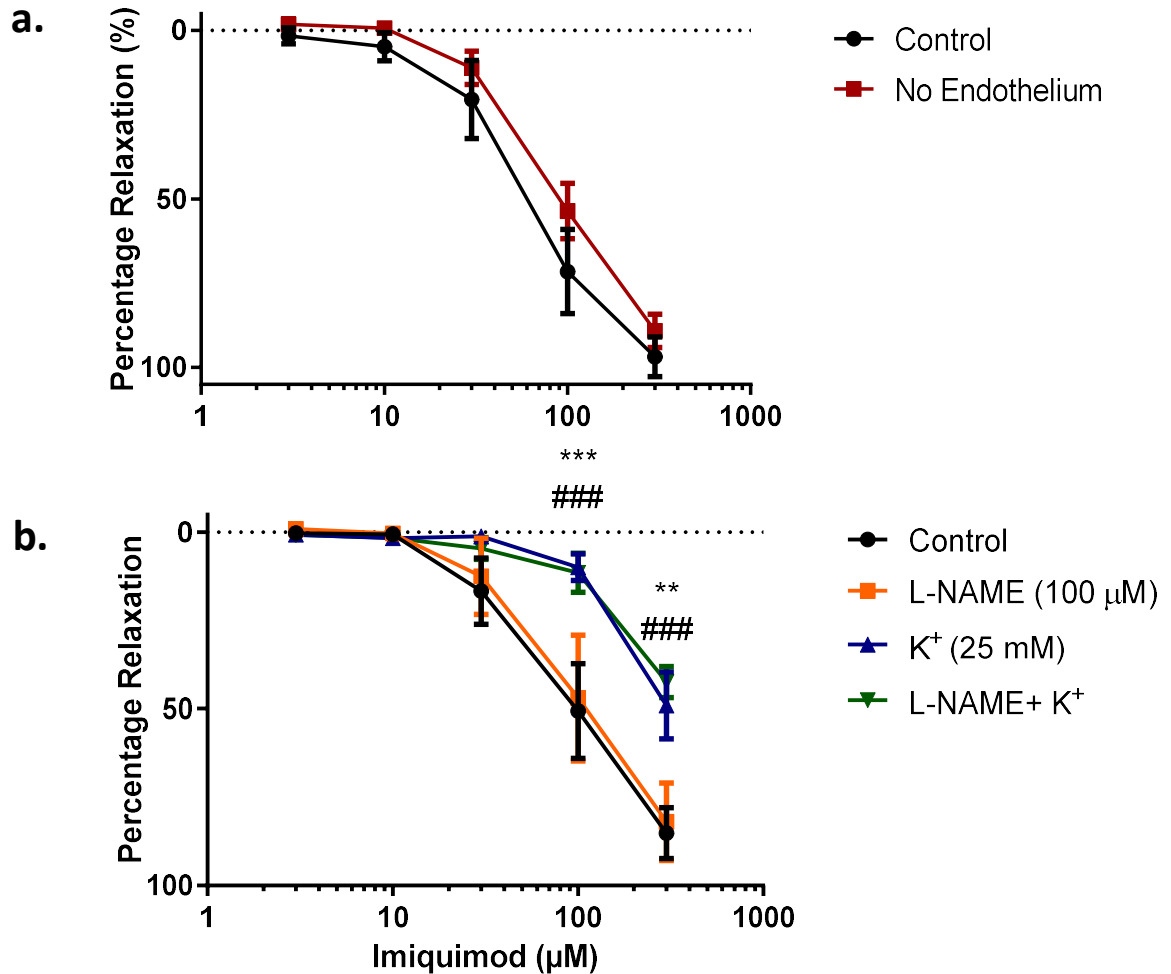


**Figure 1. TLR7 activation results in relaxation of pig coronary artery independently of the endothelium, but *via* a potassium channel-dependent pathway.**

Pig coronary artery ring segments were pre-contracted to approximately 50% of the  $K_{max}$  with thromboxane  $A_2$  receptor agonist U46619 and then treated with increasing concentrations of imiquimod (3-300 $\mu$ M). **a.** To determine if the response was endothelium-dependent, the endothelium was removed with gentle rubbing of the luminal side of the blood vessel. **b.** To determine if  $K^+$  channels were involved in TLR7-mediated relaxation, the pig coronary artery was pre-treated with  $K^+$  (25mM). To determine if NO-mediated TLR-induced smooth muscle relaxation, pig coronary artery was pre-treated with L-NAME (100 $\mu$ M). (\* Control compared to L-NAME, # Control compared to  $K^+$  treated group). Data shown as mean $\pm$ s.e.m and analysed using an ordinary two-way ANOVA with a Holm-Sidak *post hoc* test (n=5,  $p < 0.05$  \*,  $p < 0.01$  \*\*,  $p < 0.001$  \*\*\*,  $p < 0.0001$  \*\*\*\*).

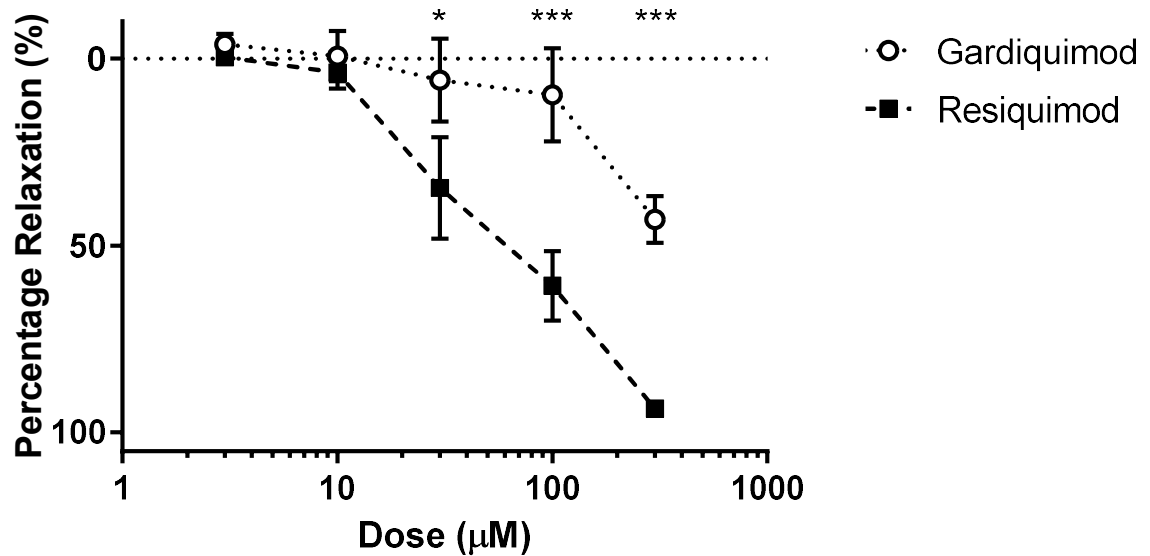


**Figure 2. Treatment with TLR7 agonists gardiquimod and resiquimod cause relaxation of smooth muscle in pig coronary artery.** Pig coronary artery ring segments were pre-contracted to approximately 50% of the  $K_{max}$  with thromboxane  $A_2$  receptor agonist U46619 and then treated with increasing concentrations of either resiquimod (3-300µM) or gardiquimod (3-300µM). Data shown as mean  $\pm$  s.e.m and analysed using an ordinary two-way ANOVA with a Holm-Sidak post hoc test (n=5,  $p < 0.05$  \*,  $p < 0.01$  \*\*,  $p < 0.001$  \*\*\*,  $p < 0.0001$  \*\*\*\*).

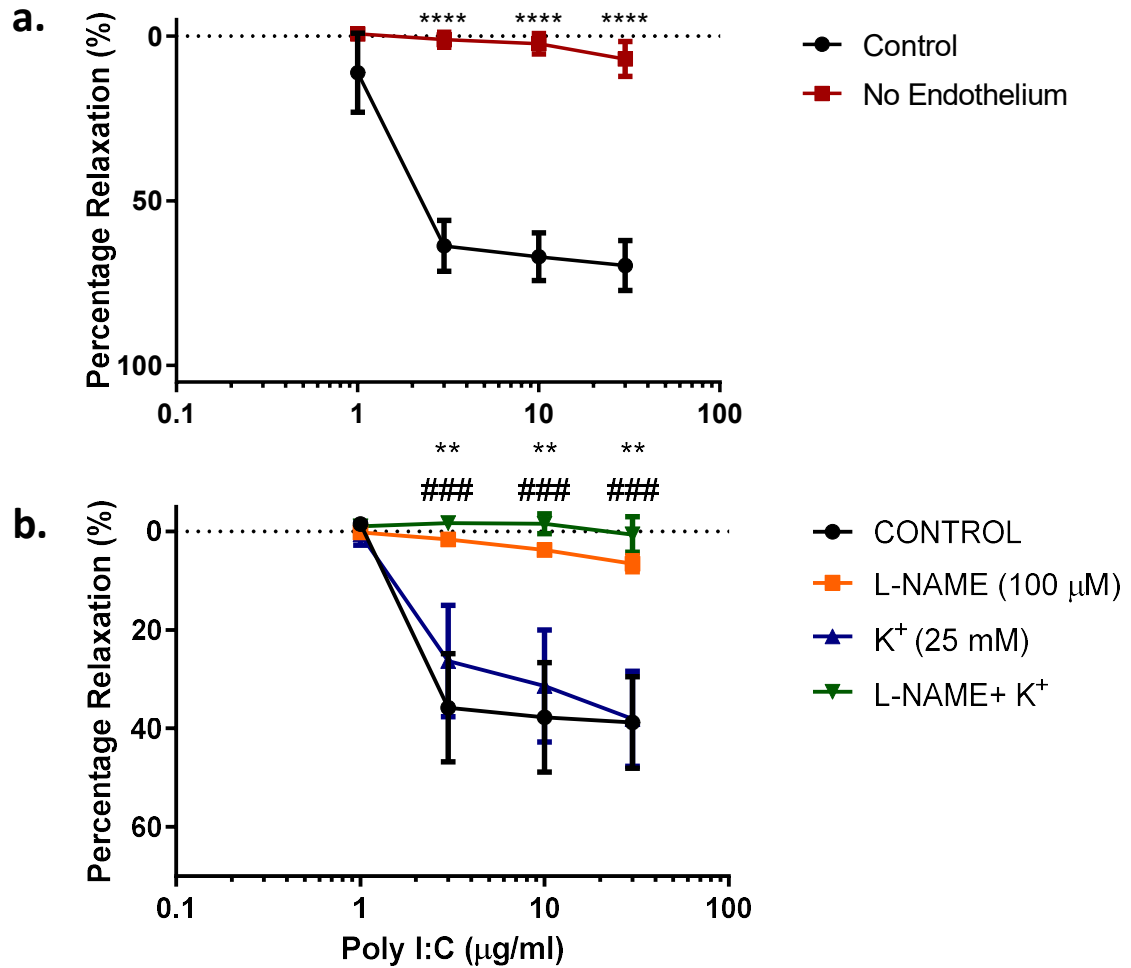


**Figure 3. TLR3 activation results in endothelium-dependent relaxation of smooth muscle in pig coronary artery through an eNOS, nitric oxide-dependent pathway.**

Pig coronary artery ring segments were pre-contracted to approximately 50% of the  $K_{max}$  with thromboxane  $A_2$  receptor agonist U46619 and then treated with increasing concentrations of poly I:C (1-30  $\mu\text{g/ml}$ ). **a.** To determine if the response is endothelium-dependent, the endothelium was removed with gentle rubbing. **b.** To determine if  $K^+$  channels were involved in TLR3-mediated relaxation, the pig coronary artery was pre-treated with  $K^+$  (25mM). To determine if nitric oxide mediated TLR3-induced smooth muscle relaxation, pig coronary artery was pre-treated with L-NAME (100 $\mu\text{M}$ ). (\* Control compared to L-NAME, # Control compared to the  $K^+$  treated group). Data shown as mean  $\pm$  s.e.m and analysed using an ordinary two-way ANOVA with a Holm-Sidak *post hoc* test (n=4,  $p < 0.05$  \*,  $p < 0.01$  \*\*,  $p < 0.001$  \*\*\*,  $p < 0.0001$  \*\*\*\*).

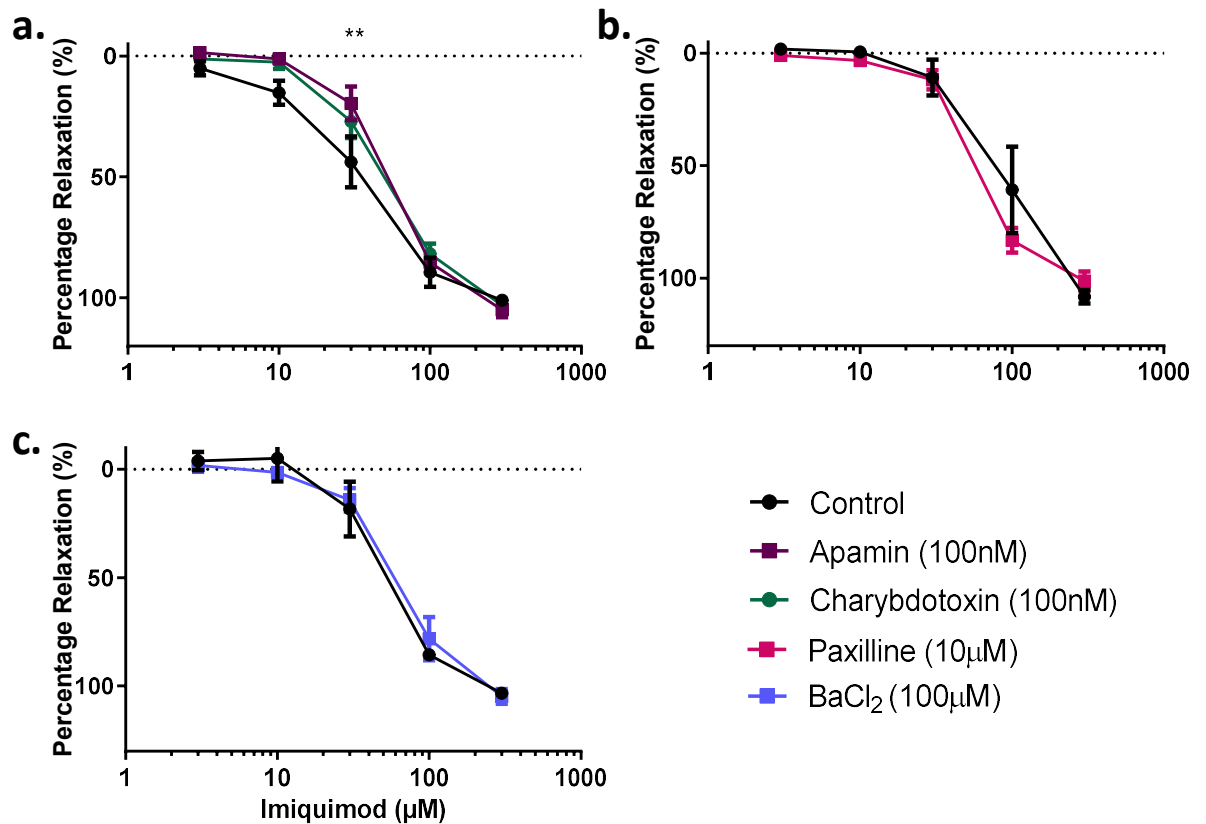


**Figure 4. TLR7-induced smooth muscle relaxation occurs partly through apamin-sensitive potassium channels.**

Pig coronary artery ring segments were pre-contracted to approximately 50% of the  $K_{max}$  with thromboxane  $A_2$  receptor agonist U46619 and then treated with increasing concentrations of imiquimod (3-300μM). To determine which potassium channels are involved in TLR7-induced relaxation, pig coronary was pre-treated with multiple specific potassium channel blockers. **a.** Small conductance calcium activated potassium channels (SK channels) were inhibited with apamin (100nM). Large and intermediate conductance calcium activated potassium channels were inhibited with charybdotoxin (100nM). **b.** Large conductance calcium activated potassium channels were inhibited with paxilline (10μM). **c.** Inwardly rectifying potassium channels were inhibited with  $BaCl_2$  (100μM). Data shown as mean  $\pm$  s.e.m and analysed using an ordinary two-way ANOVA with a Holm-Sidak *post hoc* test ( $n=3$ ,  $p<0.05$  \*,  $p<0.01$  \*\*,  $p<0.001$  \*\*\*,  $p<0.0001$ \*\*\*\*).

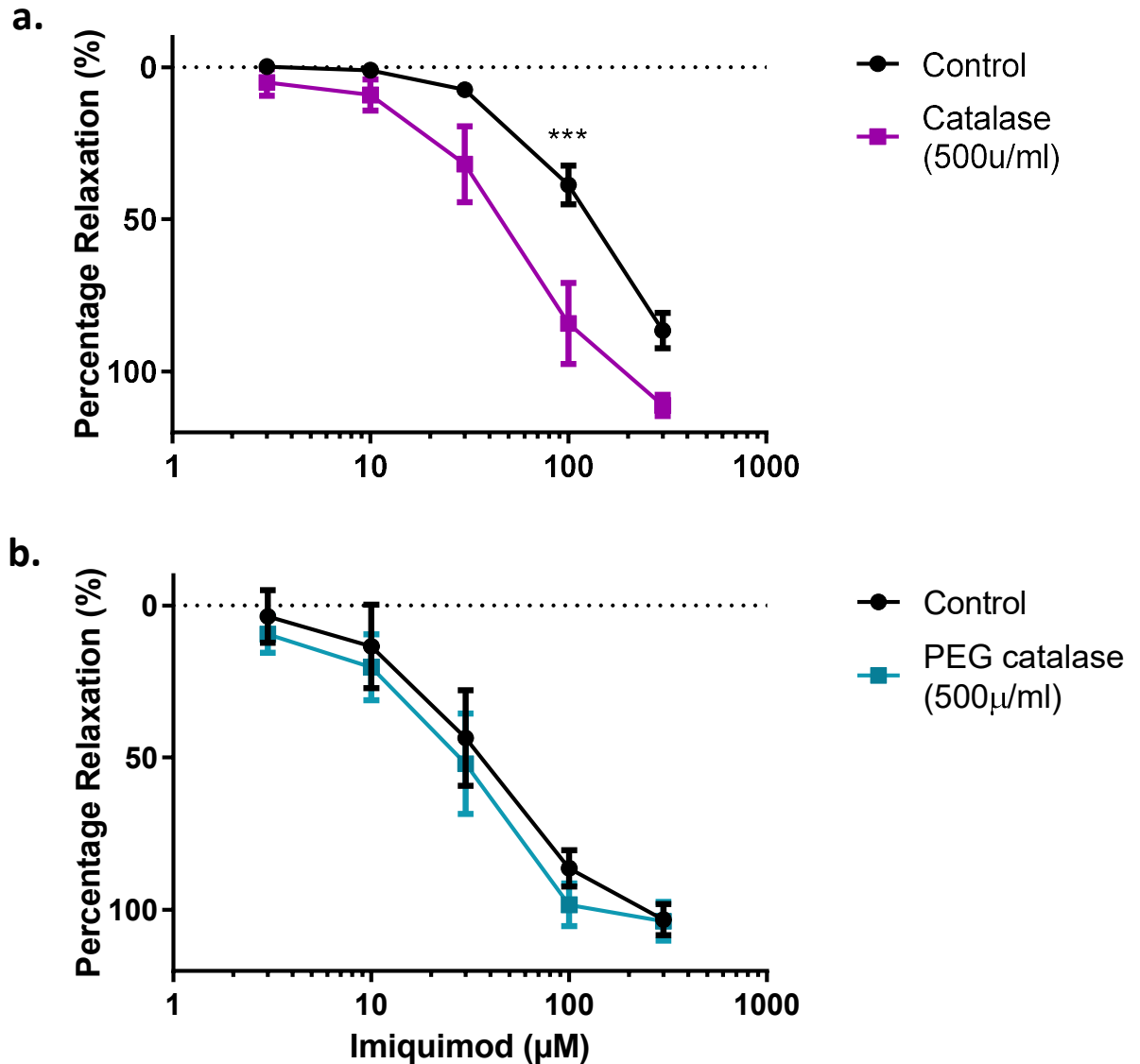


**Figure 5. Evidence that catalase treatment increases TLR7-induced relaxation in pig coronary artery.**

Pig coronary artery ring segments were pre-contracted to approximately 50% of the  $K_{max}$  with thromboxane  $A_2$  receptor agonist U46619 and then treated with increasing concentrations of imiquimod (3-300 $\mu$ M). To determine if TLR7-mediated relaxation is influenced by hydrogen peroxide production, pig coronary artery ring segments were pre-treated with catalase, both **a.** unjugated catalase (500u/ml) and, **b.** PEG conjugated catalase (500u/ml). Data shown as mean  $\pm$  s.e.m and analysed using an ordinary two-way ANOVA with a Holm-Sidak post hoc test (n=5,  $p < 0.05$  \*,  $p < 0.01$  \*\*,  $p < 0.001$  \*\*\*,  $p < 0.0001$  \*\*\*\*).

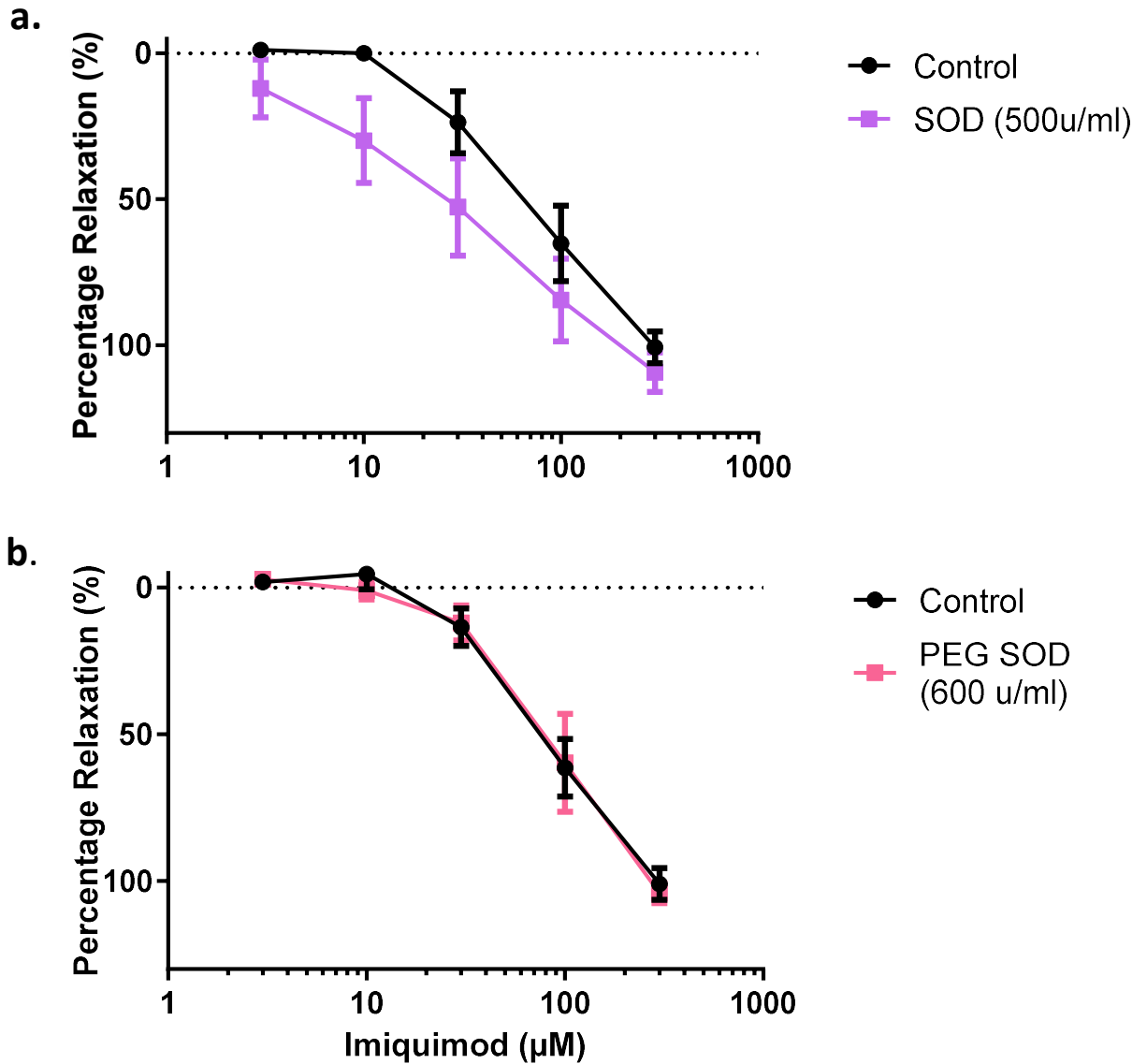


**Figure 6. Evidence that superoxide dismutase treatment has little effect on TLR7-induced relaxation in pig coronary artery.**

Pig coronary artery ring segments were pre-contracted to approximately 50% of the  $K_{max}$  with thromboxane  $A_2$  receptor agonist U46619 and then treated with increasing concentrations of imiquimod (3-300µM). To determine if TLR7-mediated relaxation is due to TLR7-induced superoxide production, pig coronary artery was pre-treated with SOD, both **a.** unjugated (500u/ml) and, **b.** PEG conjugated SOD (600u/ml). Data shown as mean±s.e.m and analysed using an ordinary two-way ANOVA with a Holm-Sidak post hoc test (n=5, p<0.05 \*, p<0.01 \*\*, p<0.001 \*\*\*, p<0.0001 \*\*\*\*).

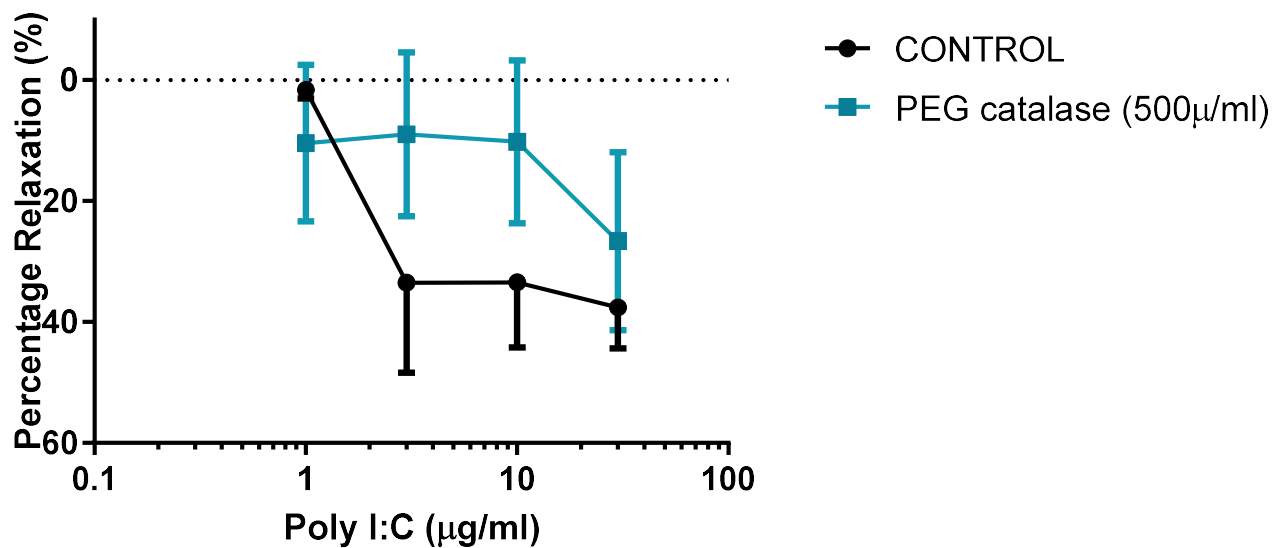
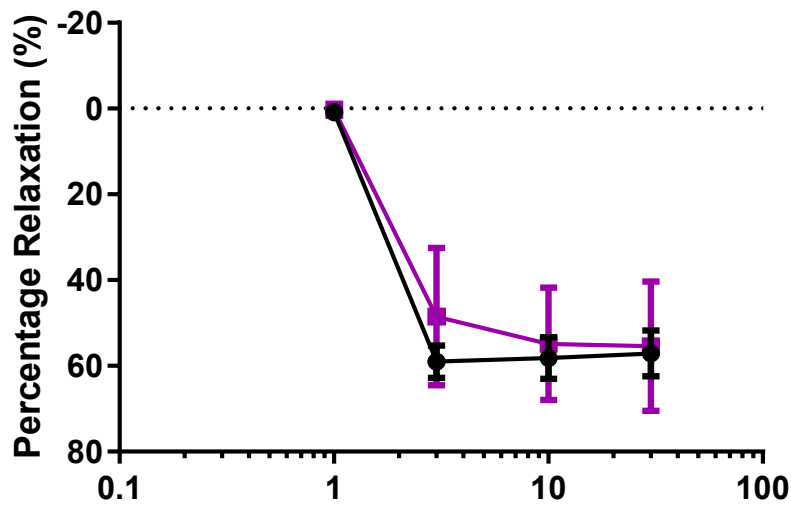


**Figure 7. Evidence that PEG-catalase treatment inhibits TLR3-induced relaxation of pig coronary artery.**

Pig coronary artery ring segments were pre-contracted to approximately 50% of the  $K_{max}$  with thromboxane  $A_2$  receptor agonist U46619 and then treated with increasing concentrations of poly I:C (1-30 µg/ml). To determine if TLR3-mediated relaxation is due to TLR3-induced hydrogen peroxide production, pig coronary artery was pre-treated with SOD, both **a.** unconjugated (500u/ml) and, **b.** PEG conjugated catalase (500u/ml). Data shown as mean±s.e.m and analysed using an ordinary two-way ANOVA with a Holm-Sidak post hoc test (n=4-5, p<0.05 \*, p<0.01 \*\*, p<0.001 \*\*\*, p<0.0001 \*\*\*\*).

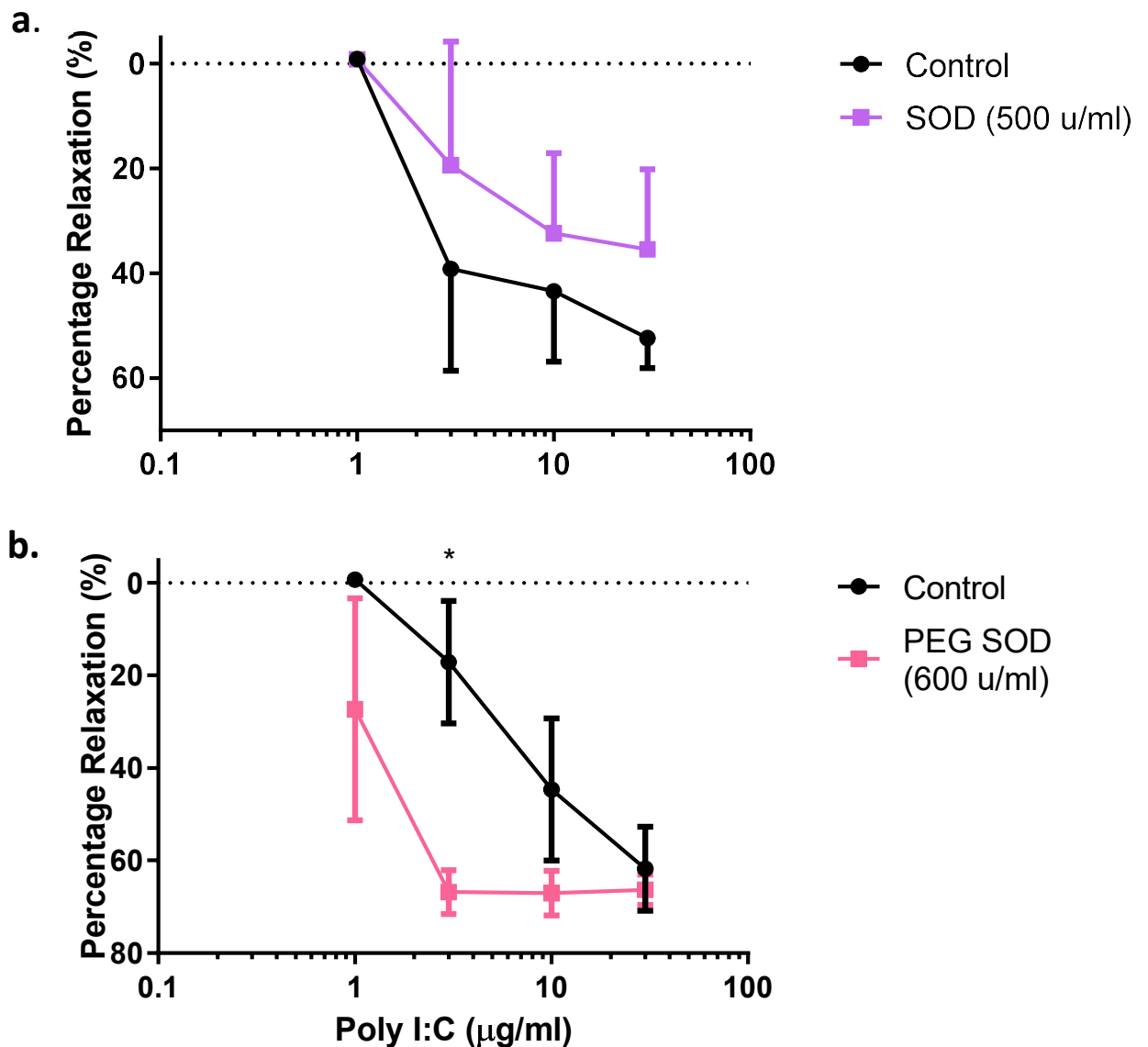


**Figure 8. Evidence that superoxide dismutase increases TLR3-induced relaxation in pig coronary artery.**

Pig coronary artery ring segments were pre-contracted to approximately 50% of the  $K_{max}$  with thromboxane  $A_2$  receptor agonist U46619 and then treated with increasing concentrations of poly I:C (1-30 µg/ml). To determine if TLR3-mediated relaxation is due to TLR3-induced superoxide production, pig coronary artery segments were pre-treated with SOD, both **a.** unjugated (500u/ml) and, **b.** PEG conjugated SOD (500u/ml). Data shown as mean±s.e.m and analysed using an ordinary two-way ANOVA with a Holm-Sidak post hoc test (n=3, p<0.05 \*, p<0.01 \*\*, p<0.001 \*\*\*, p<0.0001 \*\*\*\*).

## Discussion

This study examined the previously unexplored role of the toll-like receptors in regulating vascular tone. This is the first study to demonstrate that TLR3 and TLR7 agonists cause relaxation of the vasculature and to examine the distinct pathways involved.

The TLR7 agonist imiquimod caused a concentration-dependent and maximum relaxation of pre-contracted pig coronary artery. This would explain how imiquimod treatment resulted in hypotension in some patients (Aldara product sheet, 2014). While this is the first demonstration of TLR7-induced relaxation of vascular smooth muscle, previous studies have shown that imiquimod treatment resulted in relaxation of pre-contracted human *airway* smooth muscle (Drake, *et al.* 2013).

Other TLR7 agonists, gardiquimod and resiquimod, also caused concentration-dependent relaxation of contracted pig coronary artery, however, gardiquimod was significantly less potent and a maximum was not reached. This is despite gardiquimod treatment having more antitumor activity than imiquimod in a mouse model of melanoma (Ma, *et al.* 2010). Why gardiquimod treatment results in a less vascular relaxation than imiquimod or resiquimod remains unclear.

In the current study, denuding the endothelium had no effect on TLR7-induced relaxation of pig coronary smooth muscle, even though this abolished the substance P dependent response. This is consistent with chapter 2 which showed that treating endothelial cells with imiquimod had a minimal effect, both in terms of cytokine expression and endothelial ROS production. However, while both the study by Drake *et al.* and their previous study in guinea pigs (Kaufman, *et al.* 2010) concluded that imiquimod-induced relaxation of airway smooth muscle was through nitric oxide production, the findings of the present chapter showed that inhibiting eNOS with L-NAME had no effect on imiquimod-induced relaxation of pig coronary artery. Additionally, Drake *et al.* found that TLR7 is not expressed on airway smooth muscle. This is contested by Kvarnhammar *et al.* (2013), who did find TLR7 expressed in human airway smooth muscle cells.

In the current study, pre-treatment with 25 mM K<sup>+</sup> inhibited the TLR7-induced relaxation of pig coronary smooth muscle. The addition of potassium to the organ bath depolarises the smooth muscle and inhibits potassium channel-dependent relaxation. This suggests involvement of the potassium channels on the smooth muscle in TLR7 mediated relaxation. The reasons for the discrepancy between our finding and Drake *et al.* could be that this study is using pig coronary artery rather than an airway smooth muscle preparation. While non-specifically targeting potassium channels with a high potassium solution suppressed TLR7-induced relaxation of pig coronary smooth muscle, specifically inhibiting either large conductance calcium activated, intermediate conductance calcium-activated or inwardly rectifying potassium channels had no effect on relaxation. Inhibiting small conductance calcium-activated potassium channels (also known as SK<sub>Ca</sub> channels) had a small inhibitory effect on TLR7-induced relaxation, suggesting that TLR7 might activate these potassium channels to cause partial relaxation of the smooth muscle. The signalling mechanisms from TLR7 activation to SK<sub>Ca</sub> channel activation are unknown.

Hydrogen peroxide has been shown to increase expression of calmodulin, which is required for SK<sub>Ca</sub> channel activation by calcium (Reviewed by Aldeman, 2016), in the Korean ginseng plant (Parvin *et al.* 2012). However, this study showed that catalase pre-treatment made pig coronary artery more sensitive to imiquimod-induced relaxation, suggesting that an alternate TLR7 regulated pathway may be involved. The effect of catalase on TLR7-induced relaxation was consistent with both the findings in chapter 2, which showed that imiquimod-induced cytokine production increased in endothelial cells pretreated with catalase, and with To, *et al.* (2017), who found a negative feedback loop in which hydrogen peroxide produced by Nox2 as a result of TLR7 activation deactivated TLR7 by oxidation of a specific cysteine residue. Interesting, while pre-treatment with catalase increased TLR7-induced relaxation of coronary smooth muscle, treatment with PEG-catalase had no effect. Unconjugated catalase cannot pass through plasma membrane, which suggests that the catalase is being taken into the smooth muscle cells via endocytosis with the imiquimod.

TLR3 agonist exposure also resulted in relaxation of pre-contracted pig coronary artery but, unlike TLR7, it only resulted in partial relaxation (~40-60%). Also, in contrast to TLR7, this TLR3-mediated relaxation of the smooth muscle is endothelium-dependent and occurs *via* activation of eNOS, and not by potassium channel activation. Chapter 2 showed TLR3 activation resulting in a Nox2-dependent increase in endosomal superoxide production. As discussed previously, hydrogen peroxide is a derivative of superoxide. Previous studies have shown that hydrogen peroxide induces eNOS expression through Ca<sup>2+</sup>/calmodulin-dependent protein kinase and janus kinase 2 (Cai *et al.*, 2001). Hydrogen peroxide has also been shown to result in eNOS activation (Thomas, *et al.* 2002). Treating rabbit aorta with hydrogen peroxide resulted in L-NAME-sensitive relaxation. The same study also found that hydrogen peroxide activates phosphoinositide 3-kinase, which in turn activates AKT, or protein kinase B, which phosphorylates eNOS and increases its activity. This is consistent with our finding which showed that TLR3-mediated relaxation was L-NAME sensitive. It is also consistent with our findings that TLR3-induced relaxation increased in pig coronary that was pre-treated with PEG-SOD, which would increase the amount of hydrogen peroxide, and the trend for decreased relaxation in pig coronary artery that was pre-treated with PEG-catalase. A similar mechanism could be involved with LPS-induced hypotension and septic shock. TLR4 directly activates Nox4 oxidase, a source of hydrogen peroxide (Park, *et al.* 2004).

In summary, the toll-like receptors play an important role in influenza-induced inflammation, but there have been no studies examining the effect of toll-like receptors, in particular TLR3 and TLR7 on vascular tone. This study has unravelled distinct signalling pathways by which TLR3 and TLR7 relax smooth muscle in the coronary artery (Figure 9). Future studies should further examine the mechanisms by which TLR7 activation results in SK<sub>Ca</sub> channel activation; the effect of TLR agonists on vascular tone in an *in vivo* model, and if these pathways play a role in viral pathology, particular in influenza-induced cardiovascular dysfunction.

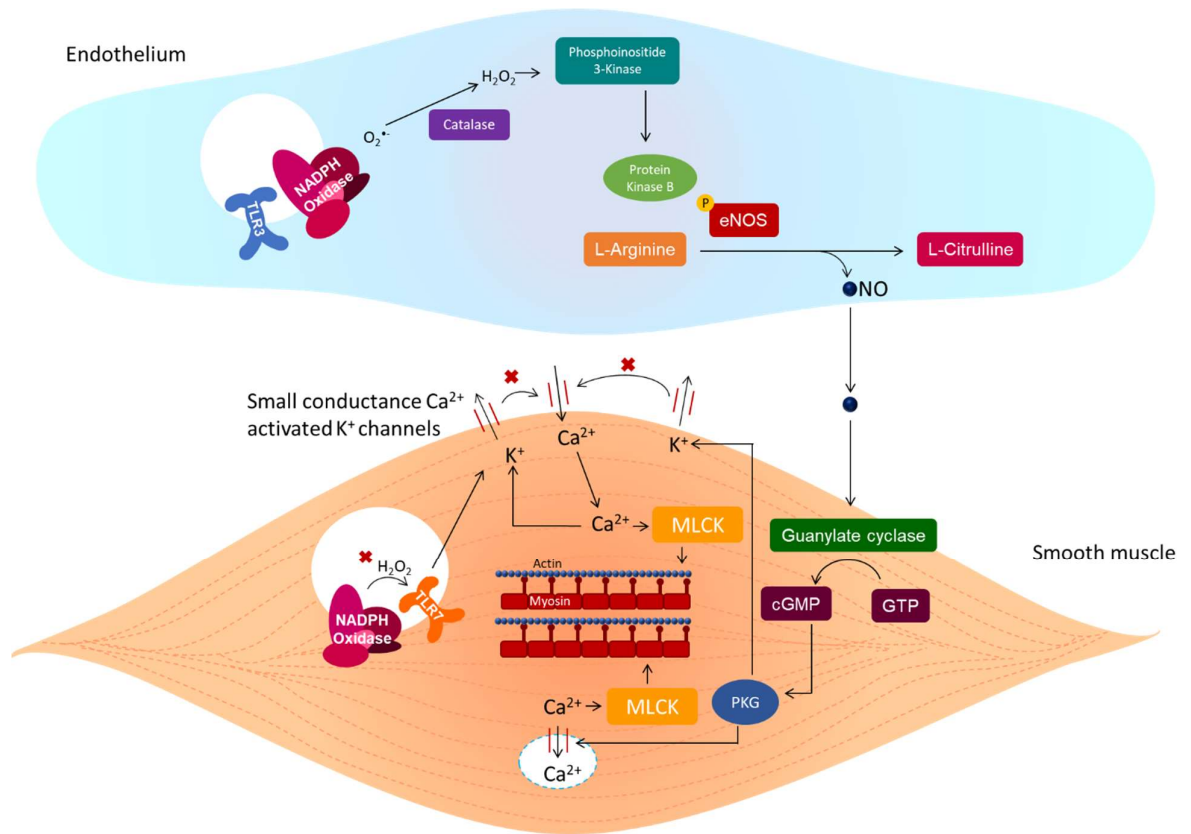


**Figure 9. Proposed mechanisms by which TLR3 and TLR7 cause smooth muscle relaxation.** TLR7 activation on the smooth muscle causes relaxation through activation of small conductance  $\text{Ca}^{2+}$  activated  $\text{K}^+$  channels. As seen by To, *et al.* (2017) hydrogen peroxide inhibited TLR7 activation. Endothelial TLR3 resulted in relaxation through eNOS activation. Study two showed that TLR3 activation resulted in Nox2-derived endosomal superoxide production. TLR3 activation of eNOS was hydrogen peroxide dependent. A potential mechanism for this to occur through is phosphoinositide 3-kinase (Thomas *et al.*, 2002).

## References

- Adelman, JP (2016). SK channels and calmodulin. *Channels* **10**: 1–6.
- Aldara product sheet (2014) iNova Pharmaceuticals
- Arnold, WP, Mittal, CK, Katsuki, S, Murad, F (1977). Nitric oxide activates guanylate cyclase and increases guanosine 3':5'-cyclic monophosphate levels in various tissue preparations. *Proc. Natl. Acad. Sci.* **74**: 3203–3207.
- Cai, H, Davis, ME, Drummond, GR, Harrison, DG (2001). Induction of Endothelial NO Synthase by Hydrogen Peroxide via a Ca<sup>2+</sup>/Calmodulin-Dependent Protein Kinase II/Janus Kinase 2-Dependent Pathway. *Arterioscler. Thromb. Vasc. Biol.* **21**: 1571–1576.
- Carvajal, J, Germain, M, Huidobro-Toro, JP, Weiner, CP (2000). Molecular mechanism of cGMP-mediated smooth muscle relaxation. *J. Cell. Physiol.* **184**: 409–420.
- Dawood, FS, Iuliano, a D, Reed, C, Meltzer, MI, Shay, DK, Cheng, P-Y, *et al.* (2012). Estimated global mortality associated with the first 12 months of 2009 pandemic influenza A H1N1 virus circulation: a modelling study. *Lancet Infect. Dis.* **12**: 687–695.
- Drake, MG, Scott, GD, Proskocil, BJ, Fryer, AD, Jacoby, DB, Kaufman, EH (2013). Toll-like receptor 7 rapidly relaxes human airways. *Am. J. Respir. Crit. Care Med.* **188**: 664–672.
- Farias, NC, Borelli-Montigny, GL, Fauaz, G, Feres, T, Borges, ACR, Paiva, TB (2002). Different mechanism of LPS-induced vasodilation in resistance and conductance arteries from SHR and normotensive rats. *Br. J. Pharmacol.* **137**: 213–220.
- Kaufman, EH, Fryer, AD, Jacoby, DB (2011). Toll-like receptor 7 agonists are potent and rapid bronchodilators in guinea pigs. *J. Allergy Clin. Immunol.* **127**: 462–469.
- Ko, E a, Han, J, Jung, ID, Park, WS (2008). Physiological roles of K<sup>+</sup> channels in vascular smooth muscle cells. *J. Smooth Muscle Res.* **44**: 65–81.

- Krown, SE, Kerr, D, Stewart, WE, Field, AK, Oettgen, HF (1985). Phase I trials of poly(I,C) complexes in advanced cancer. *J. Biol. Response Mod.* **4**: 640–649.
- Kvarnhammar, AM, Tengroth, L, Adner, M, Cardell, LO (2013). Innate Immune Receptors in Human Airway Smooth Muscle Cells: Activation by TLR1/2, TLR3, TLR4, TLR7 and NOD1 Agonists. *PLoS One* **8**: 1–10.
- Ma, F, Zhang, J, Zhang, J, Zhang, C (2010). The TLR7 agonists imiquimod and gardiquimod improve DC-based immunotherapy for melanoma in mice. *Cell. Mol. Immunol.* **7**: 381–388.
- Mayer, B (1994). Regulation of Nitric Oxide Synthase and Soluble Guanylyl Cyclase. *Cell Biochemistry and Function.* **12**: 167-177
- Nichol, KL, Nordin James, Mullooly, J, Lask Richard, Fillbrandt, K (2003). Influenza Vaccination and Reduction in Hospitalization for Cardiac Disease. *N Engl J Med* **348**: 1322–1332.
- Knowles, RG Moncada, S (1994) Nitric oxide synthases in mammals. *Biochem. J.* **298**: 249-258
- Oda, T, Akaike, T, Hamamoto, T, Suzuki, F, Hirano, T, Maeda, H (1989). Oxygen radicals in influenza-induced pathogenesis and treatment with pyran polymer-conjugated SOD. *Science* **244**: 974–976.
- Opal, SM, Laterre, P-F, Francois, B, LaRosa, SP, Angus, DC, Mira, J-P, *et al.* (2013). Effect of Eritoran, an Antagonist of MD2-TLR4, on Mortality in Patients With Severe SepsisThe ACCESS Randomized TrialEritoran for the Treatment of Severe Sepsis. *Jama* **309**: 1154–1162.
- Opal, SM, Scannon, PJ, Vincent, J, White, M, Carroll, SF, Palardy, JE, *et al.* (1999). Relationship between Plasma Levels of Lipopolysaccharide (LPS) and LPS-Binding Protein in Patients with Severe Sepsis and Septic Shock. *J. Infect. Dis.* **180**: 1584–1589.
- Ozkor, MA, Quyyumi, and AA (2011). Endothelium-Derived Hyperpolarizing Factor and Vascular Function. *Cardiol. Researcg Pract.* **2011**: 156146.

- Park, HS, Jung, HY, Park, EY, Kim, J, Lee, WJ (2004). Cutting Edge: Direct Interaction of TLR4 with NADPH Oxidase 4 Isozyme Is Essential for Oxygen Species and Activation of NF- $\kappa$ B. *J. Immunol.* **173**: 3589–3593.
- Parvin, S, Lee, OR, Sathiyaraj, G, Khorolragchaa, A, Kim, YJ, Sri Renuka Devi, B, *et al.* (2012). Interrelationship between calmodulin (CaM) and H<sub>2</sub>O<sub>2</sub> in abscisic acid-induced antioxidant defense in the seedlings of *Panax ginseng*. *Mol. Biol. Rep.* **39**: 7327–7338.
- Rezkalla, SH, Kloner, R a (2010). Influenza-related viral myocarditis. *WMJ* **109**: 209–213.
- Singer, M, Deutschman, CS, Seymour, CW, Shankar-Hari, M, Annane, D, Bauer, M, *et al.* (2016). The third international consensus definitions for sepsis and septic shock. *Jama* **315**: 801–810.
- Smeeth, L, Ph, D, Thomas, SL, Ph, D, Hall, AJ, Ph, D, *et al.* (2004). Risk of myocardial infarction and stroke after acute infection or vaccination. *N. Engl. J. Med.* **351**: 2611–2618.
- Stevenson, HC, Abrams, PG, Schoenberger, CS, Smalley, RB, Herberman, RB, Foon, KA (1985). A phase I evaluation of poly(I,C)-LC in cancer patients. *J. Biol. Response Mod.* **4**: 650–655.
- Teijaro, JR, Walsh, KB, Cahalan, S, Fremgen, DM, Roberts, E, Scott, F, *et al.* (2011). Endothelial cells are central orchestrators of cytokine amplification during influenza virus infection. *Cell* **146**: 980–991.
- Thiemermann, C, Vane, J (1990). Inhibition of nitric oxide synthesis reduces the hypotension induced by bacterial lipopolysaccharides in the rat in vivo. *Eur. J. Pharmacol.* **182**: 591–595.
- Thomas, S, Chen, K, Keaney, J (2002). Hydrogen peroxide activates endothelial nitric-oxide synthase through coordinated phosphorylation and dephosphorylation via a phosphoinositide 3-kinase-dependent signaling pathway. *J. Biol. Chem.* **277**: 6017–6024.
- To, EE, Vlahos, R, Luong, R, Halls, ML, Reading, PC, King, PT, *et al.* (2017). Endosomal NOX2 oxidase exacerbates virus pathogenicity and is a target for antiviral therapy. *Nat. Commun.* **8**: 69.

Vlahos, R, Stambas, J, Bozinovski, S, Broughton, BRS, Drummond, GR, Selemidis, S (2011). Inhibition of Nox2 oxidase activity ameliorates influenza A virus-induced lung inflammation. *PLoS Pathog.* **7**: e1001271.

WHO (2010). WHO guidelines for pharmacological management of pandemic (H1N1) 2009 influenza and other influenza viruses

Wolin, MS, Burke, TM (1987). Hydrogen peroxide elicits activation of bovine pulmonary arterial soluble guanylate cyclase by a mechanism associated with its metabolism by catalase. *Biochem. Biophys. Res. Commun.* **143**: 20–25.

## **CHAPTER FOUR:**

---

**Endothelial Nox4 oxidase negatively regulates airway neutrophil infiltration and alleviates influenza virus pathology**

---

## Abstract

Recent studies have implicated the endothelial cell in influenza A virus-induced inflammation. Nox4 is highly expressed in the endothelium and, while it has been shown to have a protective role in cardiovascular disease, its role in influenza infection is unknown. Thus, the purpose of this study was to examine the role of endothelial Nox4 in influenza pathology. WT and endothelial Nox4 overexpressing mice were infected with X31 ( $10^4$  PFU) or given PBS intranasally. Body weight was measured daily. Mice were culled 3 or 7 days post infection. BALF cell count and differential cell staining was used to examine airway inflammation. Superoxide production in the BALF cells was measured with an L-012 enhanced chemiluminescence assay. Lungs were extracted and weighed. Lung expression of Nox4, and inflammatory cytokines and chemokines were measured with QPCR. Lung Nox4 expression in WT mice was significantly decreased following influenza infection at both day 3 ( $p < 0.05$ ) and day 7 ( $p = 0.04$ ). Influenza infected Nox4 TG mice lost less weight than WT mice 3 days post infection ( $p = 0.0002$ ). Viral titre was decreased in infected Nox4 TG mice compared to the infected WT mice, 3 ( $p = 0.0002$ ) and 7 days post infection ( $p = 0.007$ ). Unlike the infected WT mice, there was no significant increase in lung alveolitis, peribronchiolar inflammation and inflammation in infected Nox4 TG mice at day 3. Airway inflammation was significantly less in infected Nox4 TG mice compared to the WT mice, 3 days post infection ( $p = 0.01$ ). Neutrophil infiltration in particular was significantly less in the infected Nox4 TG mice compared to the WT mice 3 days post infection ( $p = 0.02$ ), and a strong trend 7 days post infection ( $p = 0.06$ ). The oxidative burst from the BALF cells extracted from infected Nox4TG mice was significantly less than the WT mice, both at 3 ( $p < 0.0001$ ) and 7 days ( $p < 0.0001$ ) post-infection. Expression of CXCL10 ( $p = 0.002$ ), CCL3 ( $p = 0.02$ ), and CXCL2 ( $p = 0.02$ ) in the lung tissue was significantly lower in Nox4 TG mice compared to the WT mice 3 days post infection. IFN $\beta$  expression was decreased in infected Nox4 TG mice compared to the WT, 7 days post infection ( $p < 0.05$ ). In conclusion, endothelial Nox4 has a protective effect against influenza morbidity and is potential target for treating influenza-induced inflammation.

## Introduction

Severe cases of influenza are characterised by an excessive and detrimental inflammatory response, lung damage (Mauad *et al.*, 2010), and cardiovascular complications (Dawood *et al.*, 2012). While most of the literature implicates epithelial cells, macrophages and other inflammatory cells in influenza-induced inflammation and lung damage, recent studies have examined the role of the endothelial cell. For example, Armstrong *et al.*, (2012) found that in response to influenza infection, endothelial cells showed signs of apoptosis and increased permeability of the endothelial monolayer, which could account for the pulmonary oedema often seen in seriously ill patients. Teijaro *et al.*, (2011) found that specifically targeting endothelial cells using the anti-inflammatory , sphingosine-1-phosphate analogue AAL-R ameliorated the influenza-induced cytokine storm. In Chapter 2, we demonstrated that influenza infection of endothelial cells resulted in a Nox2-dependent elevation in endosomal ROS production, and a Nox2-dependent increase in NF- $\kappa$ B-induced cytokines.

While Chapter 2 primarily focussed on endothelial Nox2, the Nox4 isoform is expressed in at least 100-fold higher amounts than Nox2 (Van Buul *et al.*, 2005) in endothelial cells and importantly it has a different mode of activation and pattern of physiological effects. Unlike Nox2, which requires the assembly of multiple subunits for activation, Nox4 is constitutively active once it forms a heterodimer with p22phox and is thought to be regulated primarily through expression (Von Löhneysen *et al.*, 2008). Nox4 oxidase also differs from the other NADPH oxidases in that, due to its extended E-loop, it directly produces hydrogen peroxide rather than superoxide.

These differences in structure, function and location become important when considering the role of Nox2 and Nox4 in the vasculature. Nox4 and Nox2 have been shown to activate distinct kinase pathways in response to stimulation by agonists in HEK293 cells (Anilkumar *et al.*, 2008). While Nox2 has been found to exacerbate oxidative stress, inflammation and infarct volume in mouse models of stroke (Walder *et al.*, 1997; de Silva *et al.*, 2011; Chen *et al.*, 2012), Nox4 was found to be protective (Schröder *et al.*, 2012). Nox4 accounted for approximately 75% of the hydrogen peroxide formed in

the vasculature and promoted angiogenesis. Nox4 also limited angiotensin-induced dysfunction, promoted nitric oxide production, and the production of heme oxygenase (HO1) (Fredenburgh *et al.*, 2007). HO1 is produced in response to oxidative stress and has been shown to have a protective, antioxidant effects against lung disease (Raval and Lee, 2010). Nox4 has also been shown to have protective anti-inflammatory effects against atherosclerosis and is down regulated in patients with atherosclerosis and diabetes, and in mouse models of atherosclerosis (Gray *et al.*, 2016). Interestingly, overexpressing Nox4 specifically in endothelial cells, resulted in enhanced vasodilation and reduced systolic blood pressure (Ray *et al.*, 2011).

While there have been several studies examining the role of Nox4 in inflammatory pathways in the setting of cardiovascular diseases, there have been very few examining the role of Nox4 in influenza pathology or any other lung diseases. Nox4 has been shown to have a detrimental effect in a mouse model of lung fibrosis (Carnesecci *et al.*, 2011). Deletion of Nox4 in mice resulted in less severe lung fibrosis following bleomycin, as well as, reduced epithelial cell death and inflammation compared with the WT mice.

While Nox4 has been shown to generally possess protective effects on the vasculature, in the context of infection, Nox4 appears to have a detrimental effect. In the context of bacterial infection, the bacterial product LPS, drives pulmonary oedema in a Nox4-dependent manner (Grinnell *et al.*, 2012). Acute lung injury and the more severe acute respiratory distress syndrome were symptoms characteristic of the patients who died during the Swine Flu pandemic (Domínguez-Cherit *et al.*, 2009; Mauad *et al.*, 2010). Grinnell *et al.* found that in a LPS-induced model of sepsis, the attenuation of PTP1B activity by NOX4-dependent oxidation was found to be protective against pulmonary oedema. While this was a model of bacterial infection that only examined one pathway regulated by Nox4, it may suggest that the protective vascular effects of Nox4 may not extend to influenza infection.

To the best of our knowledge, there has been only one study examining the role of Nox4 specifically in influenza. Human mucoepidermoid pulmonary carcinoma (NCI-H292) cells infected with the highly pathogenic influenza strain A/Puerto Rico/8/34 H1N1 PR8, had increased Nox4 expression (Amatore *et al.*, 2015). Treatment with NADPH oxidase inhibitor diphenyleneiodonium (DPI) and knocking down Nox4 with siRNA prevented viral replication in these cells. Basal expression of Nox4 expression is low in epithelial cells (Kolářová *et al.*, 2010). An *in vivo* model examining Nox4 in the endothelium, where it is highly expressed, may be more clinically relevant.

There have been no studies examining the effect of endothelial Nox4 on influenza pathology in a mouse model. Thus, the aim of this chapter was to establish if Nox4 expressed in endothelium influenced the airways and lung inflammation, and morbidity to influenza A virus infection *in vivo*. To study endothelial Nox4, we made use of our novel endothelial Nox4 overexpressing mouse, which possesses a 2-3 fold increase in Nox4 expression in endothelium (Ray *et al.*, 2011).

## Methods

### *Animals*

The experiments described in this study were approved by the Animal Experimentation Ethics Committee of Monash University and conducted in compliance with the guidelines of the National Health and Medical Research Council (NHMRC) of Australia on animal experimentation. The mice used were males and aged matched (10-15 weeks) and were given unlimited water and standard mouse chow. The wild type C57BL6J mice were obtained from Monash Animal Services (Monash University, Melbourne), and the endothelial Nox4 overexpressing mice were obtained from our collaborator, Professor Ajay Shah from King's College London, United Kingdom. The Nox4 overexpressing mice were achieved using a tie2 promoter/enhancer construct containing the entire Nox4 cDNA, microinjected into fertilised oocytes of CBA/C57BL6 mice. The mice were then backcrossed for over 10 generations into a C57BL6J background (Ray, *et al.* 2011).

### *Virus*

The strain of influenza A virus used was Hong Kong X-31 (H3N2), a low pathogenic, mouse-adapted strain supplied by A/Prof John Stambas (School of Medicine, Deakin University, CSIRO) and Professor Patrick Reading (Peter Doherty Institute, The University of Melbourne). The virus was stored at concentration of  $7 \times 10^8$  PFU/ml, at  $-80^\circ\text{C}$ . At the time of infection, the virus was diluted to  $2 \times 10^5$  PFU/ml and kept on ice.

### *Infection, cull and bronchoalveolar lavage*

Mice were weighed and then anaesthetised with isoflurane. They were then infected with Hong Kong X31 ( $10^4$  PFU) diluted in 50 $\mu$ l PBS or given 50 $\mu$ l PBS, intranasally. Mice were monitored and weighed daily. They were then culled on either day 3 or day 7 with an overdose of ketamine-xylazine (100 mg/kg) via intraperitoneal injection. To extract BALF from the culled mice, the tip of a 23-gauge needle was severed and the blunt tip was then covered with plastic tubing. The skin covering the

throat was then removed, the tissue in front of the trachea was removed, and a small incision was made in the trachea. The modified needle was slowly inserted into the incision to avoid further punctures and clamped in place with a bulldog clip. Using a 1 ml syringe kept in line with the trachea, 400µl of cold, sterile PBS was injected into the lungs and the torso was massaged. The BALF was then removed from the lungs with the syringe and kept on ice. This process was repeated 3 times with 300µl of PBS. Approximately 1ml of BALF was removed from each mouse. The lungs were then removed and weighed. The large left lobe was fixed in 10% formalin and the rest was frozen with liquid nitrogen for RNA extraction.

#### *Lung Sections*

The left lung lobe of each mouse was washed in PBS and fixed in 10% formalin overnight. The lung was then processed in paraffin wax and cut into 3-4 µm longitudinal sections. These sections were stained with hematoxylin and eosin (H&E) by the Monash Histology Platform (Monash University, Clayton, Australia).

#### *BALF cell counting and differentials.*

10µl of the BALF was mixed in 10µl trypan blue. 10µl of the mixture was then counted with a Countess Cell Counter. The amount of BALF was usually 1ml. If less BALF was taken it was assumed that the concentration of cells in the BALF that was unable to be removed was the same. 50 000 cells were made up in 200µl PBS and were put on slides using a Cytospin centrifuge. The slides were allowed to dry, fixed in 100% propanol, and allowed to dry again overnight. Slides were then stained with Rapid 1 dye for 4 minutes while agitating constantly, and then rinsed thoroughly with water. Slides were then stained with Rapid 2 dye for 4 minutes while agitating constantly, and then rinsed with water again. Slides were then submerged in one, 70% ethanol, two, absolute ethanol, three, xylene for 5 minutes, and xylene again for another 5 minutes. Finally, the slides were mounted in DPX mounting medium and cover slipped.

### *Chemiluminescence*

50 000 cells from the BAL fluid from each animal were seeded in a Thermo Fisher 96-well plate, clear bottom white polystyrene plate in Dulbecco's Modified Eagle's Medium (DMEM) (10% FBS) in triplicate. A blank triplicate containing only DMEM was included. When adhered, the cells were washed with Krebs-HEPES (warmed to 37°C). 200µl of the assay solution (Krebs-HEPES (37°C) containing L-012 (10<sup>-4</sup> M) and PDB (10<sup>-6</sup> M)) were added to each well in light-sensitive conditions. Luminescence (relative light units RFU/sec) was measured using a Hidex multi-detection platform. The temperature was set at 37°C, luminescence in each well was measured for one second over 60 cycles.

### *Real-Time PCR*

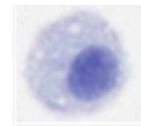
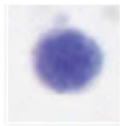
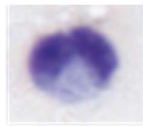
The right lobe of the lung was put into a tube containing 500µl of a Buffer RLT mixture containing 1% β-mercaptoethanol, minced with scissors, and then homogenised while on ice. The sample was then centrifuged in a Eppendorf 5424 (8.4 cm radius) at 14 000 rpm for 5 minutes. The supernatant was removed and combined with an equal amount of 70% RNase free ethanol, transferred to a spin column and spun at 10 000 rpm to 15 seconds. 700µl of Buffer RW1 was added to the spin column which was spun at 10 000 rpm to 15 seconds. DNase was mixed with Buffer RDD at a ratio of 1:7. 80µl of this mixture was added to the spin column and left at room temperature for 15 minutes. 500µl of Buffer RPE was added to the spin column which was spun at 10 000 rpm to 15 seconds. Another 500µl of Buffer RPE was added to the spin column which was spun at 10 000 rpm to 2 minutes. The spin column was run at 14 000 rpm for 1 minute with a new collection tube to remove residual flow through. The column was placed in an Eppendorf tube, 30µl of RNase free water was left to sit in the spin column for one minute and spun for 10 000 rpm for another minute to elute the RNA.

The extracted RNA was measured using a NanoDrop 1000 spectrophotometer and converted to cDNA using high capacity cDNA reverse transcriptase kit. The mRNA expression of IL-6, CXCL10, IFN-

$\beta$ , TNF- $\alpha$ , IL-1 $\beta$ , and Nox4, was quantified using a TaqMan<sup>®</sup> gene expression assay. 100 ng of cDNA was loaded into each well, and 10 ng of cDNA was loaded into each well for the 18S housekeeping. The plate was run for 2 minutes at 50<sup>°</sup>C, 1 hour at 95<sup>°</sup>C, and alternating between 95<sup>°</sup>C for 15 seconds and 60<sup>°</sup>C for a minute for 40 cycles.

#### *Statistical Analysis*

Lung weight and cell counts were analysed using a one-way ANOVA with a Sidak *post hoc* test. Using light microscopy, the lung sections and the fixed BALF slides were scanned and uploaded to the Aperio microscope scanner (Leica biosystems, Nussloch, Germany) by the Monash Histology Platform. The images were viewed using Aperio Imagescope software. The differentials and scoring of the lung sections were performed in a blinded manner. 100 cells from five random fields in each group were categorised as macrophages, eosinophils, neutrophils and lymphocytes, and a percentage of each cell type was calculated.



Eosinophil   Lymphocyte   Neutrophil   Macrophage

**Figure 1.** Examples of each cell type examined in the differential counting.

To estimate the number of cells, the percentage of live cell count was determined. The data were then analysed with one-way ANOVA with a Sidak *post hoc* test. Two researchers examined five random fields of the H & E stained lung sections and graded the alveolitis, peribronchiolar inflammation and inflammatory cell infiltration on a scale of 0-5, with 0 being negligible and 5 being severe, and the data were then analysed with one-way ANOVA with a Sidak *post hoc* test. For the gene expression assays, fold change in expression was calculated by finding the  $\Delta$ -threshold cycle by subtracting the CT from the 18S CT for each treatment group, finding the  $\Delta\Delta$ -CT by subtracting the average  $\Delta$ -CT of uninfected wildtype mice from the  $\Delta$ -CT for each treatment group, and then calculating  $2^{-(\Delta\Delta-CT)}$ . The fold change in cytokine expression was then analysed using a one-way ANOVA with a Sidak *post hoc* test. The viral titre was calculated similarly except the Nox4 TG viral titre was normalised to the Nox4 TG uninfected group. A ROUT outlier test (Q=0.1%) was also used on the viral titre data. The viral titre and the fold-change in Nox4 expression and viral titre were analysed with an ordinary Students unpaired t-test. The chemiluminescence and body weight data were analysed using a two-way ANOVA with a Sidak *post hoc* test.

### Drugs and Solutions

Chemicals	Manufacture	Storage temperature
RNeasy minikit	Qiagen	-20°C
DNase and Buffer RDD	Qiagen	-20°C
High capacity cDNA reverse transcriptase kit	Applied Biosystems	-20°C
TaqMan® assay solution	Life Technologies	4°C
18S housekeeping	Applied Biosystems	-20°C
Nox4, IL6, CXCL10, IFNβ, TNFα and IL1β PCR primers	Applied Biosystems	-20°C
Trypan blue	Invitrogen	Room temperature
Rapid 1	Amber Scientific	Room temperature
Rapid 2	Amber Scientific	Room temperature
DPX mounting medium	Ajax Finechem	Room temperature
Dulbecco's Modified Eagle's Medium	Sigma	4°C
L-012 (dissolved in DMSO)	Wako Chemical	-20°C
Phorbol dibutyrate (PDB)	Sigma	-20°C
β-mercaptoethanol	Sigma	4°C

## Results

### *Lung Nox4 Expression*

There was a significantly ( $p < 0.05$ ) higher Nox4 expression in the lung tissue of X31-infected WT mice 3 days post infection compared to the uninfected WT mice (Figure 2a). There was also a significantly ( $p = 0.04$ ) lower Nox4 expression of X31-infected WT mice 7 days post infection compared to the uninfected WT mice (Figure 2b).

### *Viral Titre*

There was a significantly lower viral titre in Nox4 TG mice compared to the WT mice, both 3 ( $p = 0.0002$ ) and 7 days ( $p = 0.007$ ) post infection (Figure 3).

### *Weight Loss*

There was no significant change in weight in uninfected WT or the Nox4 TG mice over the course of 7 days. There was significant weight loss in X31-infected WT mice compared to the uninfected WT mice from day 2 onwards ( $p < 0.0001$ ). There was a significantly less weight loss in infected Nox4 transgenic mice compared to the infected WT mice at day 2 ( $p = 0.002$ ) and day 3 ( $p = 0.0002$ ) post infection, but not at day 4 ( $p = 0.66$ ), day 5 ( $p = 0.99$ ), day 6 ( $p = 0.77$ ), or day 7 ( $p = 0.46$ , Figure 4).

### *Lung Weight*

The lungs of X31-infected WT mice weighed significantly more than the uninfected WT mice, 3 ( $p = 0.0003$ ) and 7 ( $p = 0.002$ ) days post infection. The lungs of X-31 infected Nox4 TG mice did not weigh significantly more than the uninfected Nox4 TG mice three days post infection ( $p = 0.31$ , Figure 5a). The lungs of infected Nox4 TG mice weighted significantly more than the uninfected Nox4 TG mice 7 days post infection ( $p = 0.0002$ ) and the no change in lung weight between the X31-infected WT and Nox4 TG mice 7 days post infection ( $p = 0.95$ , Figure 5b).

### *Lung Inflammation*

Alveolitis ( $p=0.01$ ), peribronchiolar inflammation ( $p=0.0004$ ) and inflammatory cells ( $p=0.002$ ) was rated significantly higher in the lungs of WT mice infected for 3 days than the uninfected mice.

Alveolitis ( $p=0.65$ ), peribronchiolar inflammation ( $p=0.11$ ) and inflammatory cells ( $p=0.19$ ) in the lungs of infected Nox4 TG mice after three day was not rated significantly higher than the uninfected Nox4 TG mice. Peribronchiolar inflammation was rated significantly lower in infected Nox4 TG mice compared to the infected WT mice ( $p=0.02$ , Figure 6).

Seven days post infection there was a significant increase in alveolitis ( $p=0.0003$ ), peribronchiolar inflammation ( $p<0.0001$ ) and inflammatory cells ( $p<0.0001$ ) in the lungs of both WT mice and Nox4 TG ( $p=0.0003$ ,  $p<0.0001$ , and  $p<0.0001$ , respectively). There was a strong trend in decreased peribronchiolar inflammation in infected Nox4 TG mice compared to infected WT mice ( $p=0.06$ , Figure 7).

### *Airway Inflammation and cell differentials*

There was a significant increase in BALF cell count ( $\sim 1.8 \times 10^6$  cells,  $p<0.0001$ ) in X31-infected WT mice 3 days post infection compared to uninfected WT mice ( $\sim 2.1 \times 10^5$  cells). To a larger degree, there was also a significant increase in BALF cell count ( $\sim 3.1 \times 10^6$  cells,  $p<0.0001$ ) in X31-infected WT mice 7 days post infection compared to uninfected WT mice ( $\sim 3.0 \times 10^5$  cells).

There was a significant decrease in BALF cell infiltration in X31-infected Nox4 TG mice 3 days post infection ( $\sim 1.2 \times 10^6$  cells,  $p=0.01$ ), but not 7 days post infection ( $\sim 2.4 \times 10^6$  cells,  $p=0.48$ ) compared to the infected WT mice (Figure 8).

Specific cell types were also examined. There was a significant increase in eosinophil ( $p=0.02$ , Figure 9a), lymphocyte ( $p=0.001$ , Figure 10a), neutrophil ( $p<0.0001$ , Figure 11a), and macrophage infiltration ( $p=0.003$ , Figure 12a), in WT mice infected with X31 3 days post infection. Similarly, there was a significant increase in eosinophil ( $p<0.0001$ , Figure 9b), and neutrophil ( $p=0.0008$ , Figure 11b),

and macrophage infiltration ( $p=0.006$ , Figure 12b) but, surprisingly, no difference in lymphocyte infiltration ( $p=0.50$ , Figure 10b) in WT mice infected with X31 7 days post infection. There was a significant decrease in neutrophil infiltration in infected Nox4 TG mice 3 days post infection ( $p=0.02$ ) and a strong trend in decreased neutrophil infiltration 7 days post infection ( $p=0.06$ ) compared to the WT mice. There was no alteration in eosinophil infiltration in infected Nox4 TG ( $p=0.78$ ) 3 days post infection, but there was a significant decrease 7 days post infection ( $p=0.03$ ) compared to the WT mice. There was no significant difference between Nox4TG and WT mice in lymphocyte or macrophage infiltration 3 days post infection ( $p=0.36$ ,  $p=0.99$ , respectively) or 7 days post infection ( $p=0.63$ ,  $p=0.99$ , respectively).

#### *Superoxide production*

There was a significant ( $p<0.0001$ ) increase in superoxide production by BALF inflammatory cells as measured by L-012 chemiluminescence in X31-infected WT mice compared to uninfected mice 3 and 7 days post infection. There was also a significant ( $p<0.0001$ ) increase in superoxide detected by L-012 chemiluminescence in infected Nox4 transgenic than uninfected transgenic mice 3 and 7 days post infection. There was a significant decrease in detected superoxide in infected Nox4 transgenic mice compared with infected WT mice ( $p<0.0001$ ; Figure 13).

#### *Lung Cytokine Expression*

There was a significant increase in IL-6 ( $p<0.0001$ ), CXCL10 ( $p=0.0007$ ), IFN- $\beta$  ( $p=0.02$ ), TNF- $\alpha$  ( $p=0.0003$ ), IL-1 $\beta$  ( $p=0.02$ ), CXCL2 ( $p=0.006$ ) and CCL3 ( $p=0.01$ ) expression in the lungs of X31-infected WT mice 3 days post infection compared to the uninfected WT mice, but not in IL17a expression ( $p=0.18$ ) (Figure 14). There was a significant increase in CXCL10 expression in the lungs of X31-infected WT mice 7 days post infection ( $p=0.03$ ), a trend in increased cytokine expression in IL-6 ( $p=0.11$ ), IFN- $\beta$  ( $p=0.14$ ), TNF- $\alpha$  ( $p=0.10$ ), CXCL2 ( $p=0.56$ ), IL17a ( $p=0.33$ ), and CCL3 ( $p=0.06$ ), but no significant difference in IL-1 $\beta$  ( $p=0.95$ ) compared to the uninfected WT mice (Figure 15).

There was no significant difference in expression of IL-6 ( $p=0.56$ ), IFN- $\beta$  ( $p=0.99$ ), TNF- $\alpha$  ( $p=0.35$ ), IL-1 $\beta$  ( $p=0.99$ ), and IL17a ( $p=0.57$ ) between X31-infected Nox4 transgenic mice and WT mice three days post infection, but there was a significant decrease in CXCL10 ( $p=0.002$ ), CXCL2 ( $p=0.02$ ) and CCL3 ( $p=0.02$ ) expression. There was no difference in IL-6 ( $p=0.24$ ), CXCL10 ( $p=0.71$ ), TNF- $\alpha$  ( $p=0.87$ ), IL-1 $\beta$  ( $p=0.95$ ), IL17a ( $p=0.96$ ), CXCL2 ( $p=0.96$ ), or CCL3 ( $p=0.33$ ) expression between infected Nox4 TG and WT mice 7 days post infection. However, there was a significant decrease in IFN- $\beta$  expression in infected Nox4 transgenic mice compared to infected WT mice seven days post infection ( $p<0.05$ ).

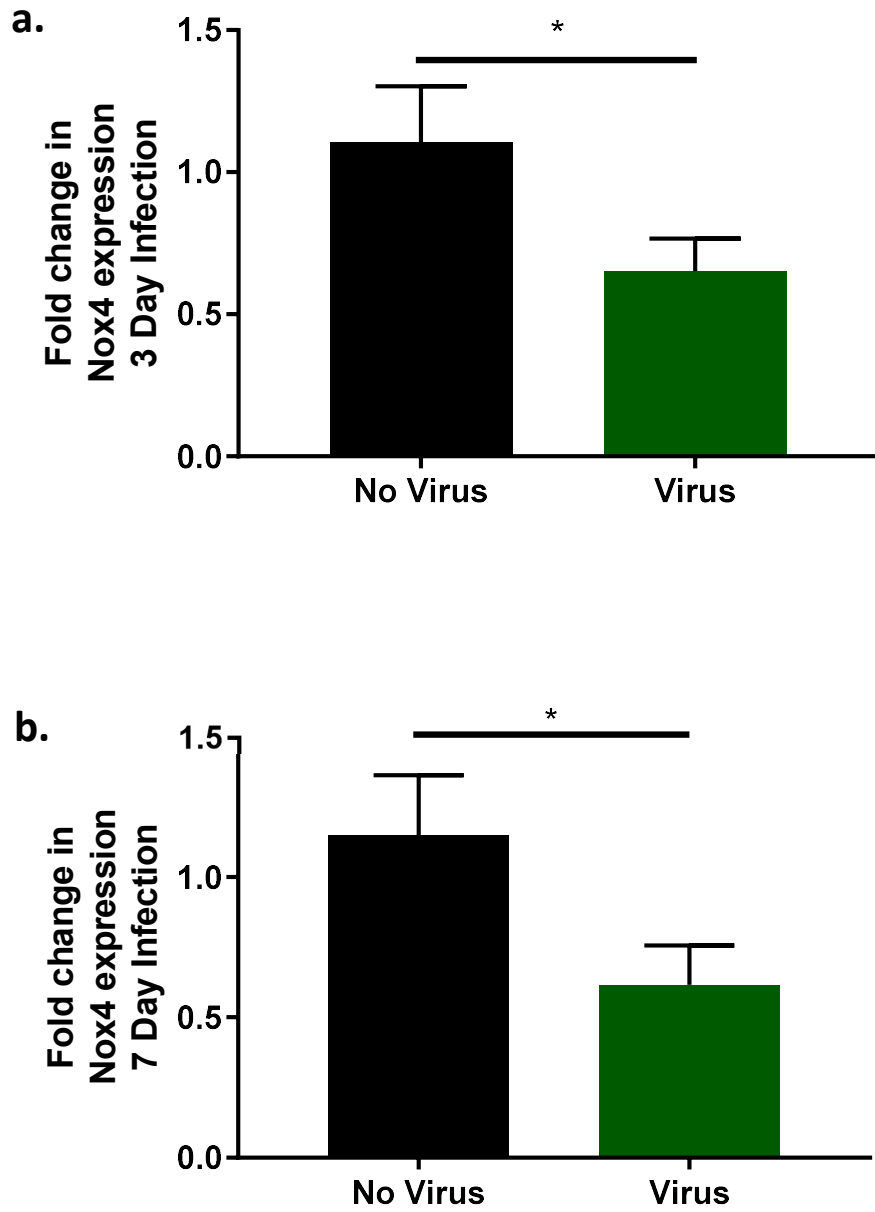


**Figure 2. Lung Nox4 expression was decreased in mice infected with influenza A virus.**

WT mice were infected with X31 ( $10^4$  PFU). Lung Nox4 mRNA expression was measured **a.** 3 days and for **b.** 7 days post infection with RT-PCR. 18S was used as a housekeeping gene. Data shown as mean $\pm$ s.e.m and analysed using an unpaired t-test (n=6-15, p<0.05 \*, p<0.01 \*\*, p<0.001 \*\*\*, p<0.0001 \*\*\*\*).

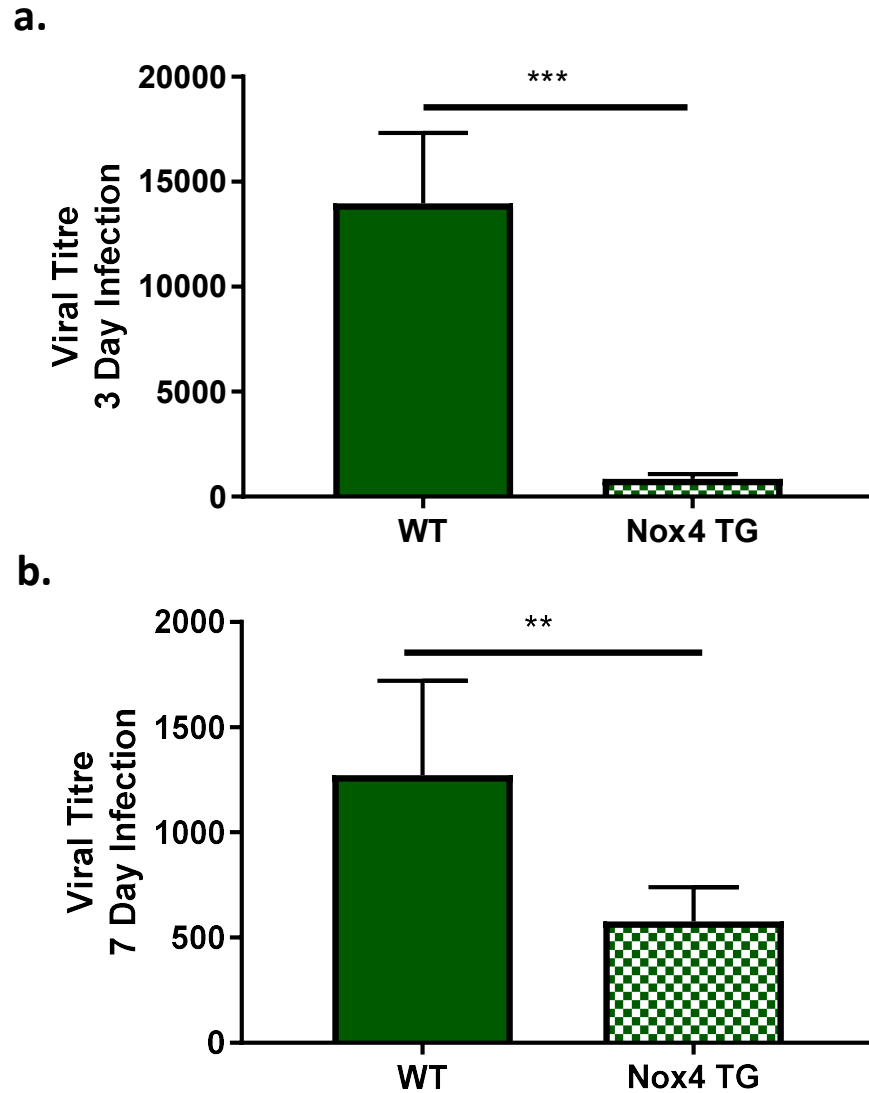


**Figure 3. Decreased in viral titre in endothelial Nox4 overexpressing mice infected with influenza A virus 3 and 7 days post infection compared to the infected WT mice.**

WT and Nox4 transgenic mice were infected with X31 ( $10^4$  PFU). Lung viral mRNA for influenza nucleoprotein were measured **a.** 3 and **b.** 7 days post infection. 18S was used as a housekeeping gene. Data shown as mean $\pm$ s.e.m and analysed using an unpaired t-test (n=6-15, p<0.05 \*, p<0.01 \*\*, p<0.001 \*\*\*, p<0.0001 \*\*\*\*).

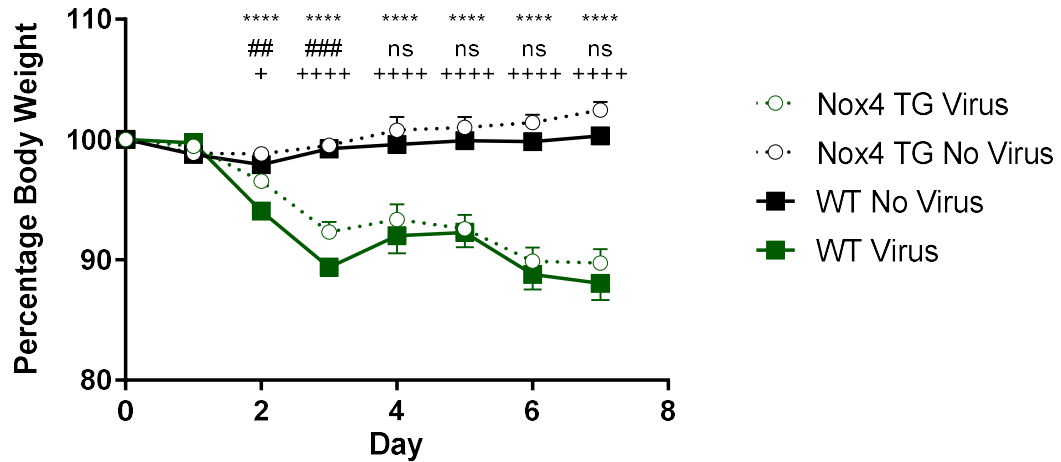


**Figure 4. Endothelial Nox4 overexpressing mice infected with influenza A virus lost less weight 3 days after infection compared to the infected WT mice.**

Body weight of X31-infected ( $10^4$  PFU) WT and Nox4 transgenic mice as a percentage of the pre-infection body weight. Data shown as mean $\pm$ s.e.m and analysed using an ordinary two-way ANOVA with a Sidak *post hoc* test (\* WT No Virus compared to WT Virus, # WT Virus compared to Nox4 TG Virus, + and for Nox4 TG No Virus compared to Nox4 TG Virus) (n=8-15) (p<0.05).

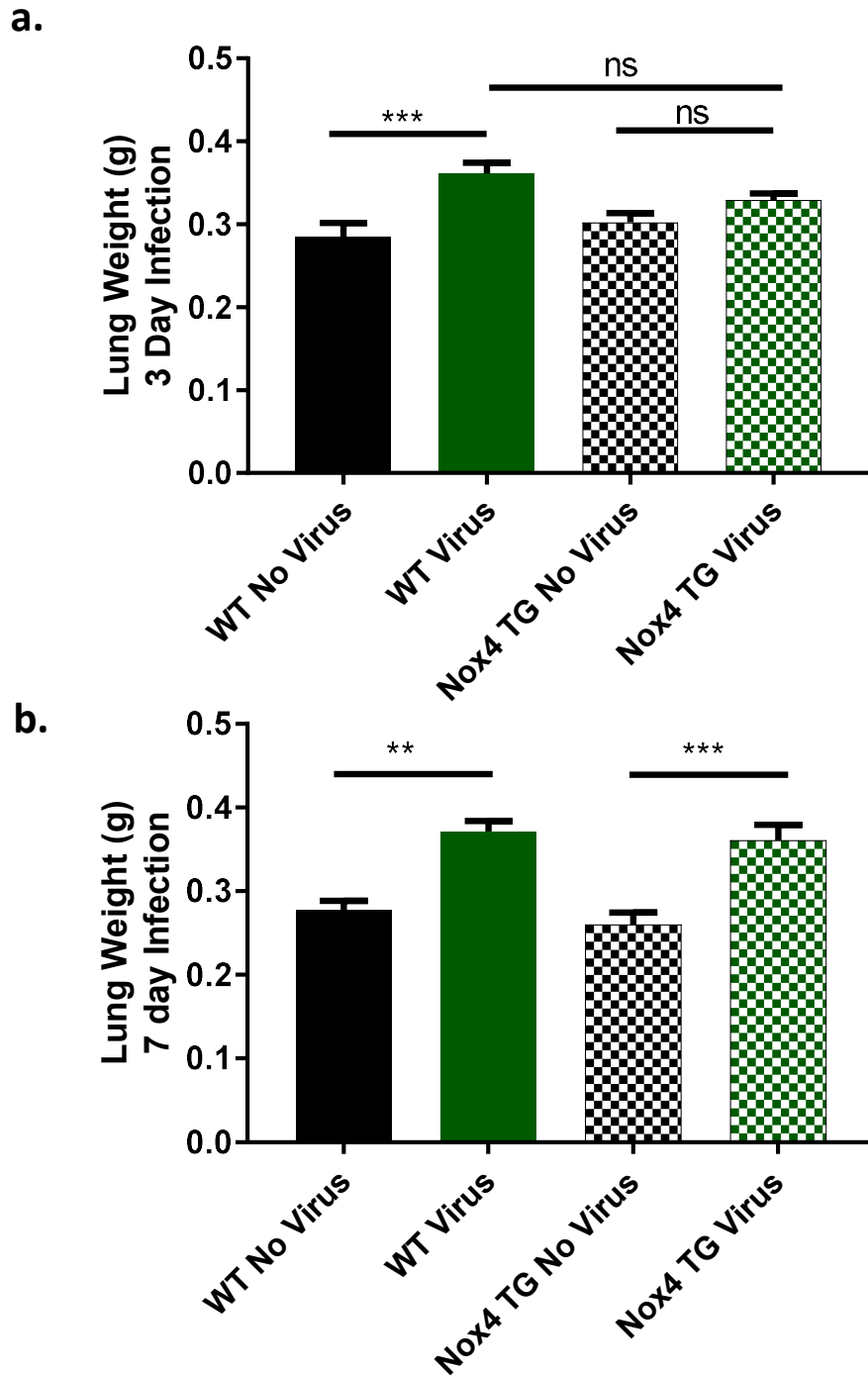


**Figure 5. Endothelial Nox4 overexpressing mice infected with influenza A virus had a decreased lung weight compared to infected wild type mice, 3 days post infection.**

Lung weight (g) of WT and Nox4 transgenic mice **a.** 3 and **b.** 7 days post infection with X31 ( $10^4$  PFU). Data shown as mean $\pm$ s.e.m and analysed using an ordinary one-way ANOVA with a Sidak *post hoc* test (n=7-15) (p<0.05).

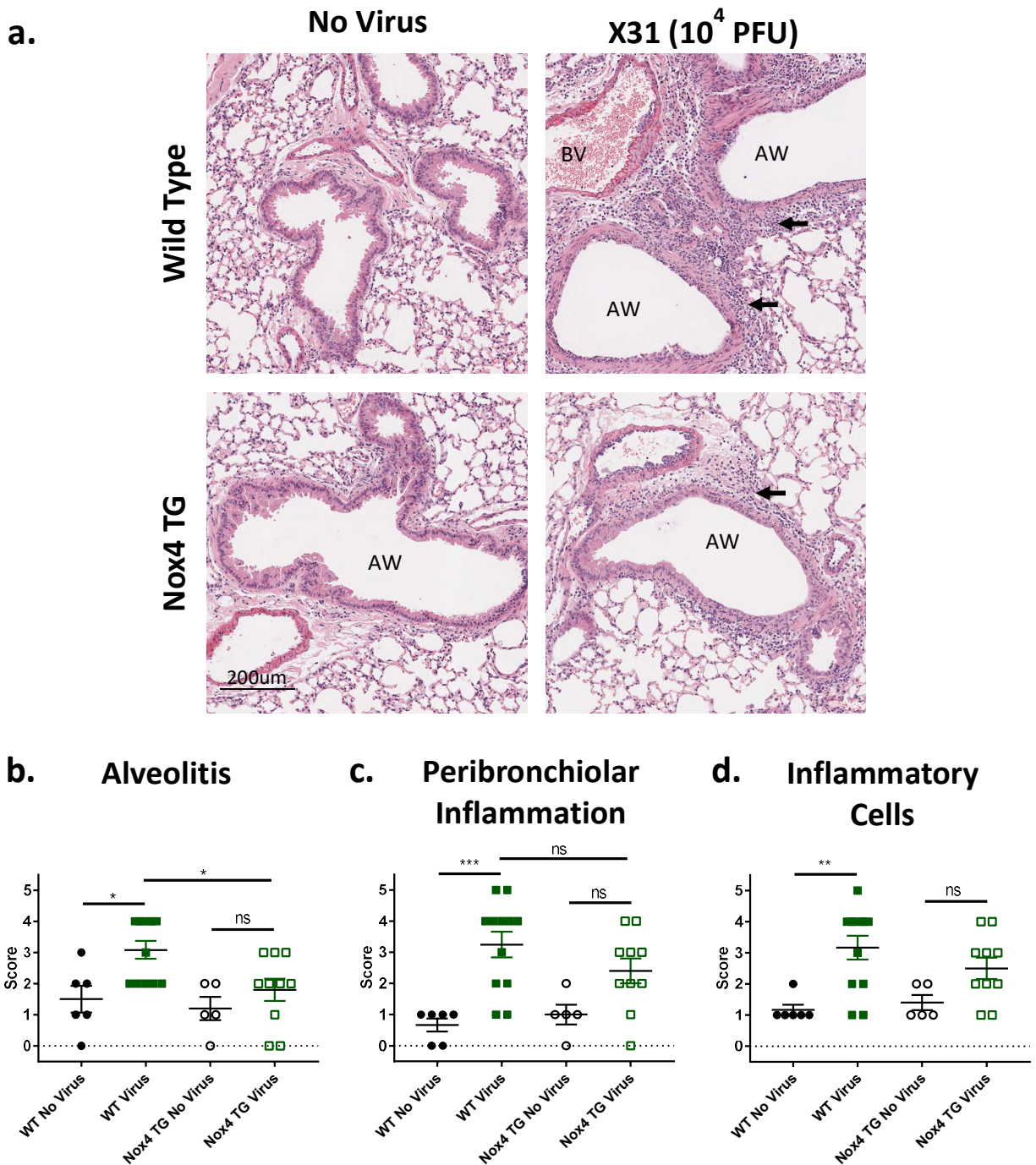


**Figure 6. The lungs of influenza-infected Nox4 transgenic mice had less alveolitis, peribronchiolar inflammation and inflammatory cells than influenza infected WT mice, three days post infection.**

A. Hematoxylin and eosin stained paraffin sections of lungs of WT and Nox4 TG mice three days post infection with X31 ( $10^4$  PFU) or treatment with PBS. B. Alveolitis, C. peribronchiolar inflammation and D. inflammatory cell infiltration were graded on a 0-5 scale. Data shown as mean $\pm$ s.e.m and analysed using an ordinary one-way ANOVA with a Sidak post hoc test (n=6-12) (p<0.05). Airway labelled AL, blood vessel labelled BV. The black arrows are showing examples of peribronchiolar inflammation.

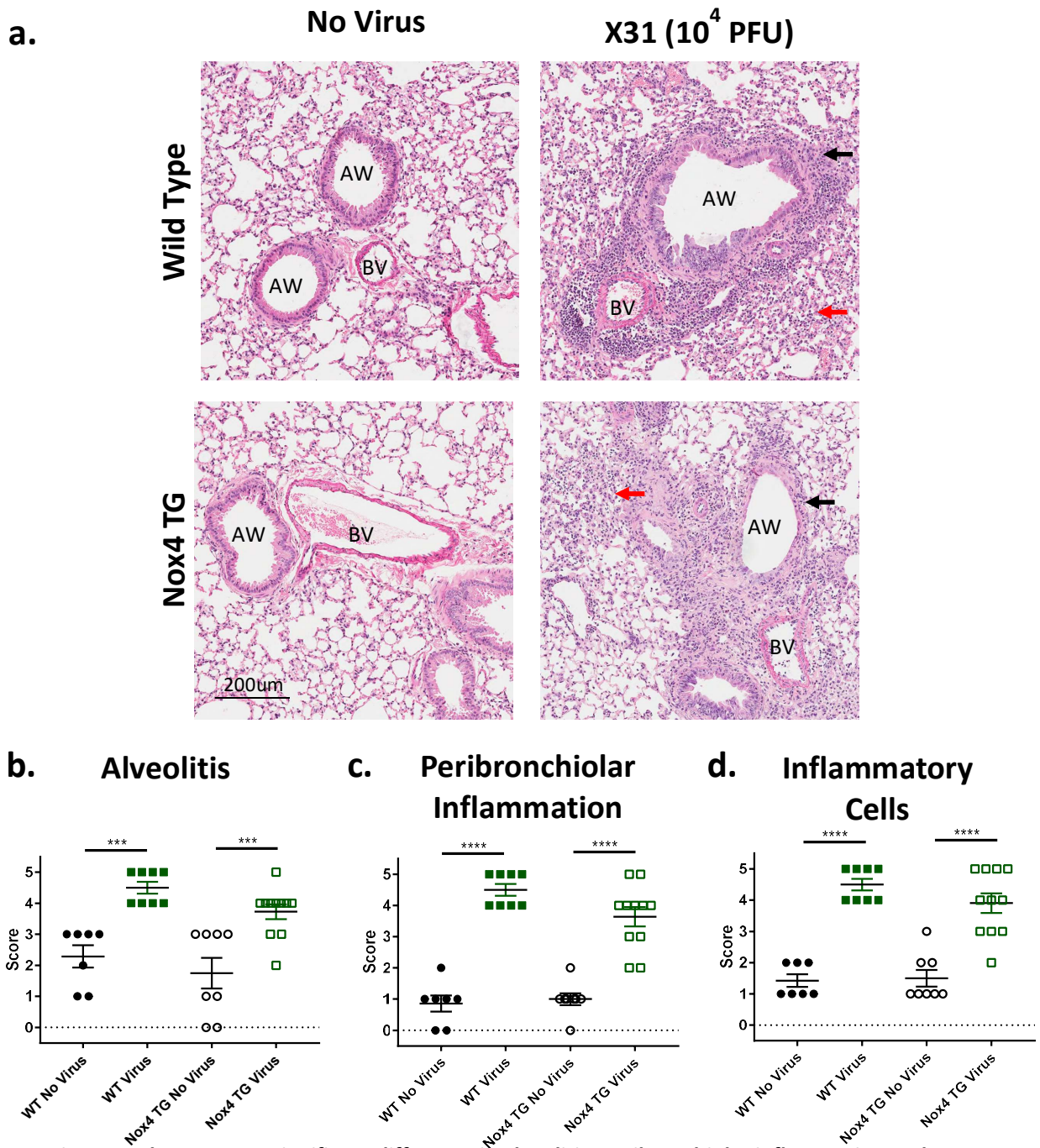


**Figure 7.** There was no significant difference in alveolitis, peribronchiolar inflammation and inflammatory cells in the lungs of influenza-infected Nox4 TG mice compared to infected WT mice seven days post infection.

**A.** Hematoxylin and eosin stained paraffin sections of lungs of WT and Nox4 TG mice three days post infection with X31 (10<sup>4</sup> PFU) or treatment with PBS. **B.** Alveolitis, **C.** Peribronchiolar inflammation and **D.** inflammatory cell infiltration were graded on a 0-5 scale. Data shown as mean±s.e.m and analysed using an ordinary one-way ANOVA with a Sidak *post hoc* test (n=6-12) (p<0.05). Airway labelled AL, blood vessel labelled BV. The black arrows are showing examples of 137 peribronchiolar inflammation. The red arrows are showing examples of alveolitis.

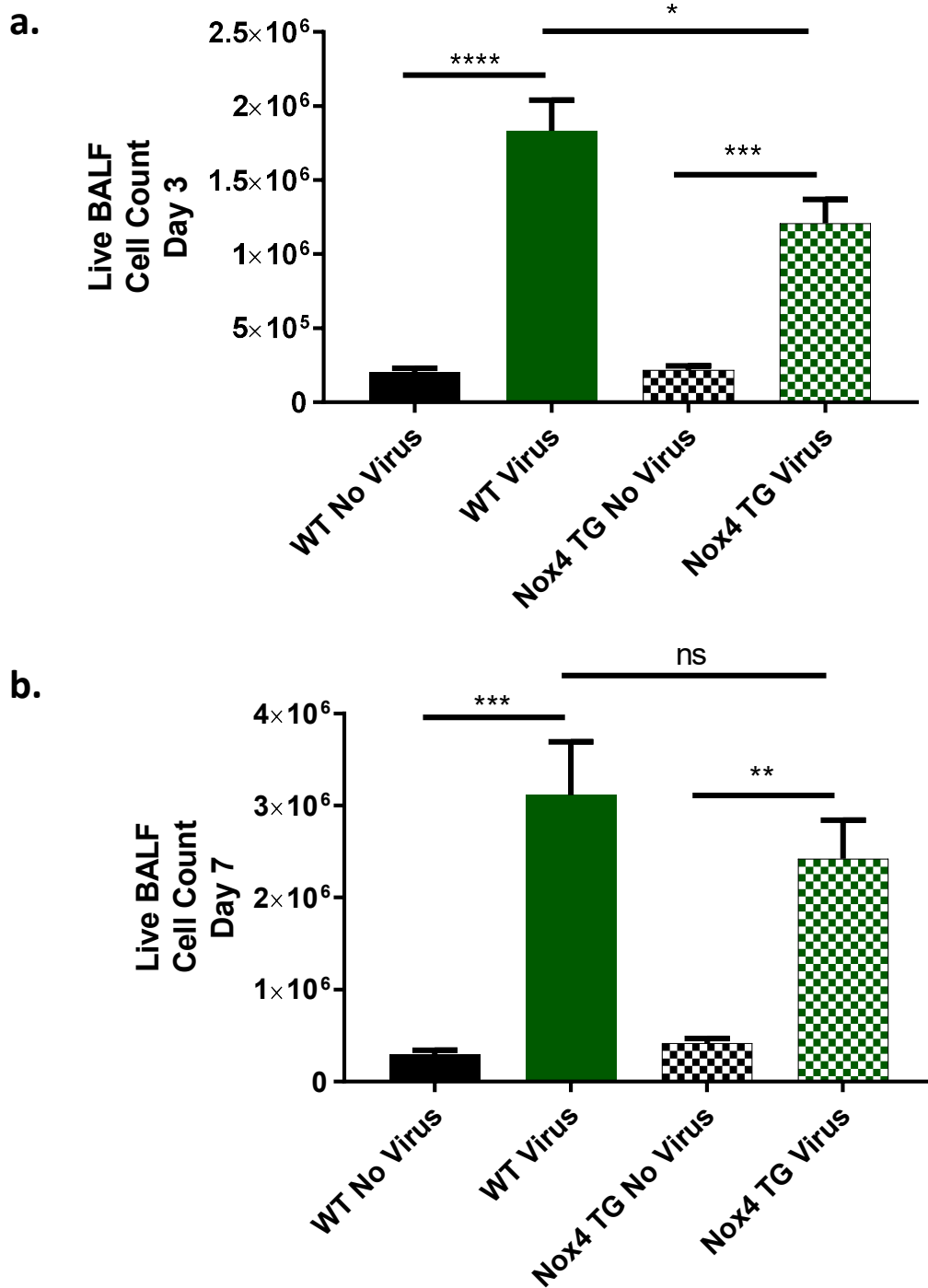


**Figure 8.** Endothelial Nox4 overexpressing mice infected with influenza A virus had a decrease in airway inflammation compared to infected wild type mice.

WT and Nox4 transgenic mice were infected with X31 ( $10^4$  PFU). BALF fluid was extracted **a.** 3 and **b.** 7 days post infection and live cells were counted. Data shown as mean $\pm$ s.e.m and analysed using an ordinary one-way ANOVA with a Sidak *post hoc* test. (n=8-15) (p<0.05)

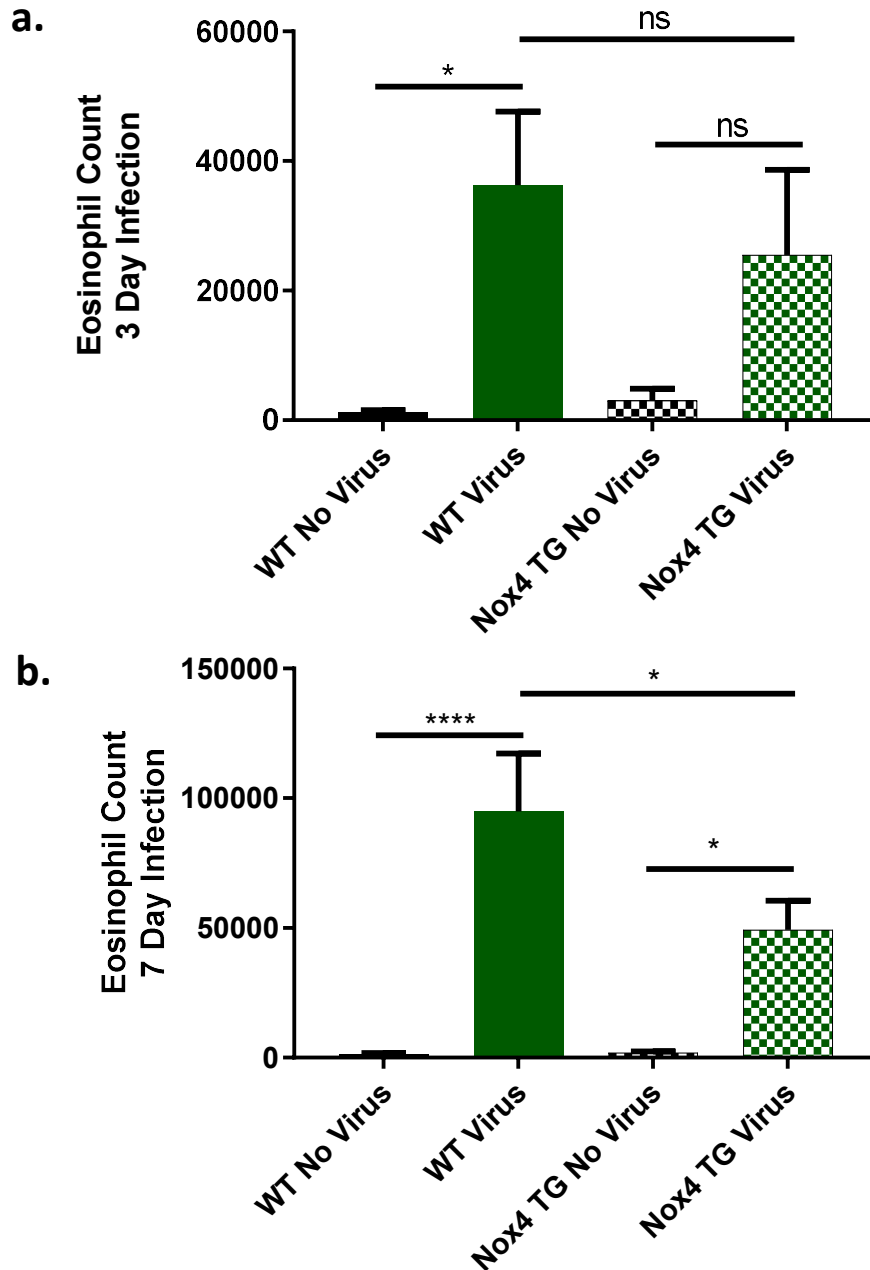


**Figure 9. Influenza A virus infected endothelial Nox4 overexpressing mice had decreased eosinophil infiltration compared to the infected wild type mice.**

BALF cells from X31-infected ( $10^4$  PFU) WT and Nox4 transgenic mice were fixed and stained with RAPID 1 and 2. The percentage of alveolar eosinophil infiltration in 500 cells were counted and total eosinophil infiltration was calculated from the BALF live cell count **a.** 3 and **b.** 7 days post infection. Data shown as mean $\pm$ s.e.m and analysed using an ordinary one-way ANOVA with a Sidak *post hoc* test (n=5-11) ( $p < 0.05$ ).

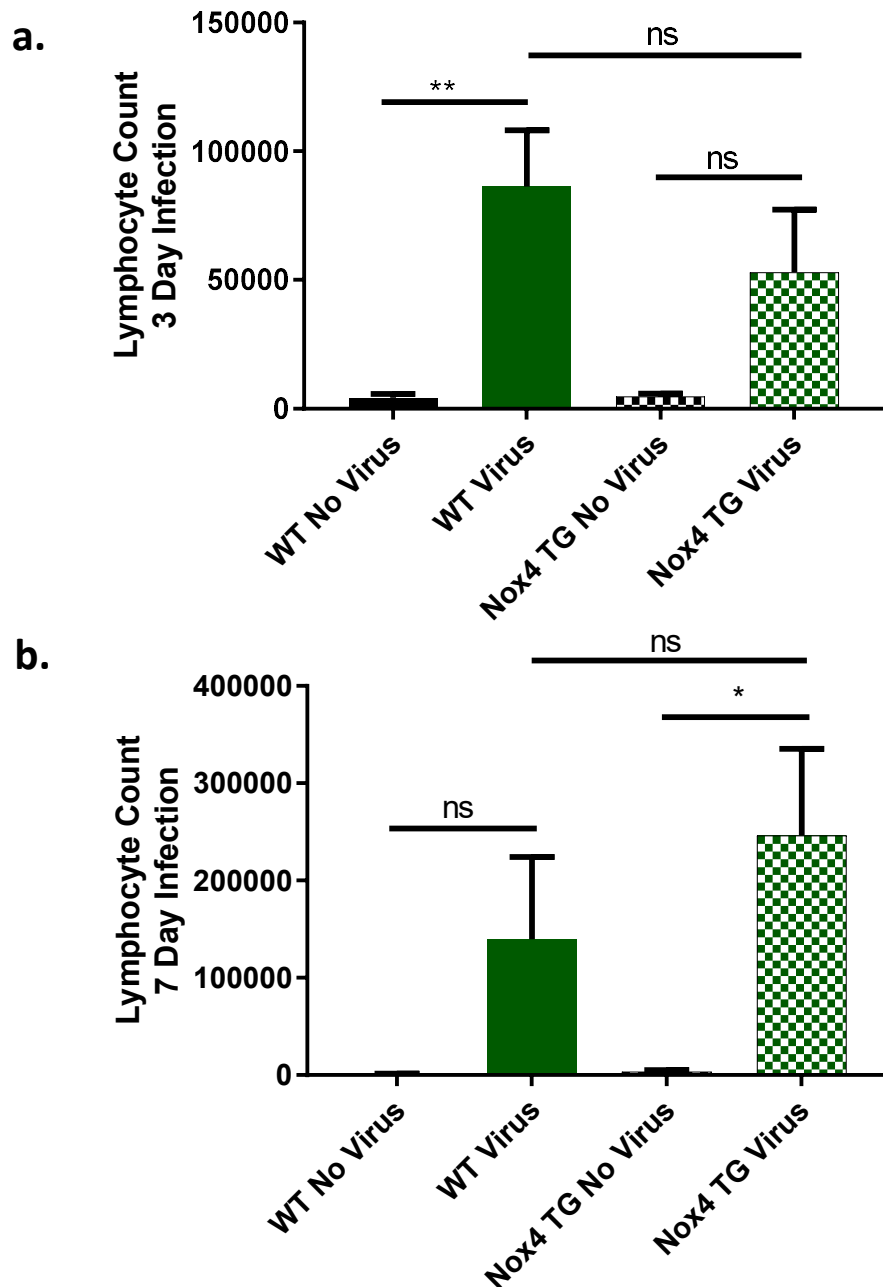


**Figure 10. Influenza A virus infected endothelial Nox4 overexpressing mice had no difference in lymphocyte infiltration compared to the infected wild type mice.**

BALF cells from X31-infected ( $10^4$  PFU) WT and Nox4 transgenic mice were fixed and stained with RAPID 1 and 2. The percentage of alveolar lymphocyte infiltration in 500 cells were counted and total lymphocyte infiltration was calculated from the BALF live cell count **a.** 3 and **b.** 7 days post infection. Data shown as mean $\pm$ s.e.m and analysed using an ordinary one-way ANOVA with a Sidak *post hoc* test (n=5-11) ( $p < 0.05$ ).

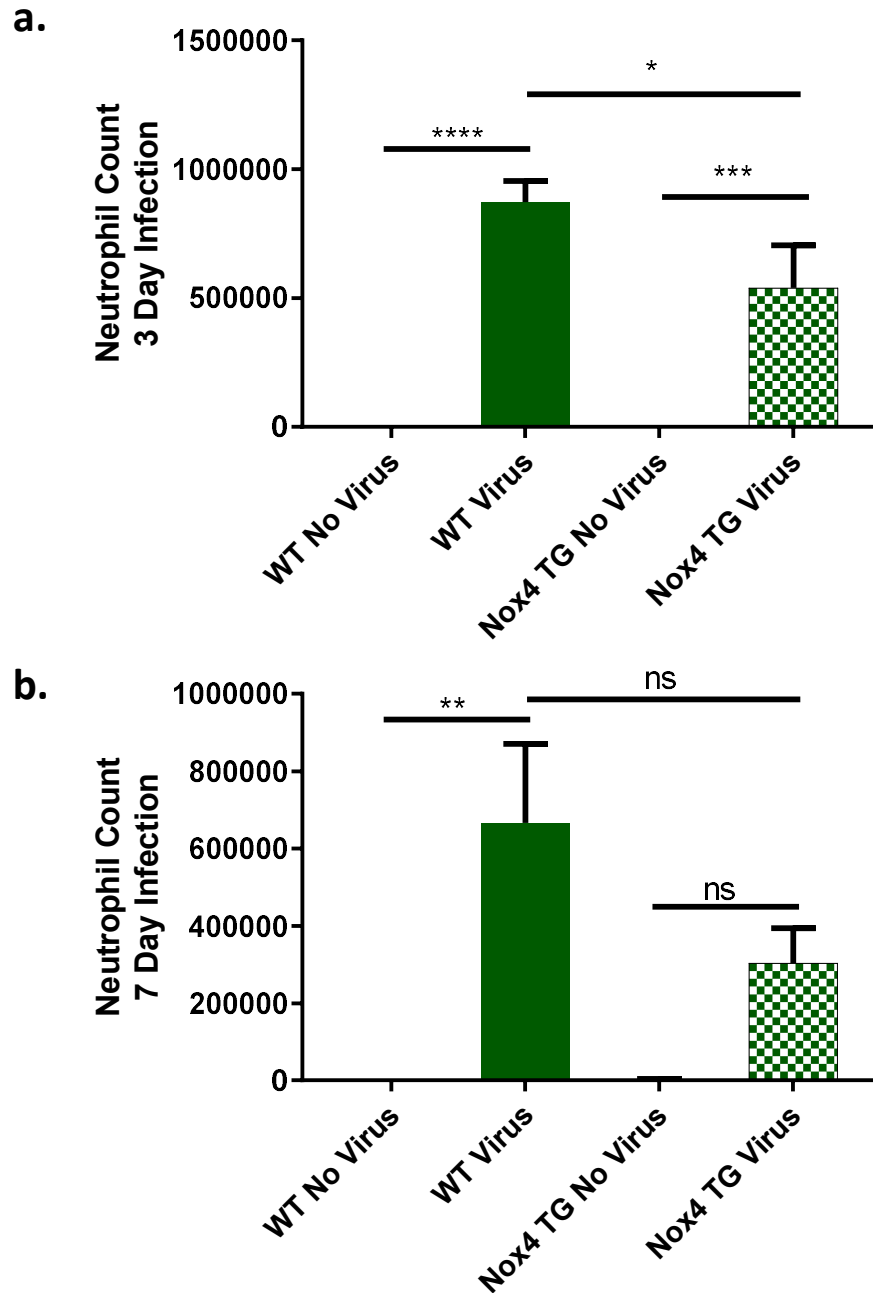


**Figure 11. Influenza A virus infected endothelial Nox4 overexpressing mice had decreased neutrophil infiltration compared to the infected wild type mice.**

BALF cells from X31-infected ( $10^4$  PFU) WT and Nox4 transgenic mice were fixed and stained with RAPID 1 and 2. The percentage of alveolar neutrophil infiltration in 500 cells were counted and total neutrophil infiltration was calculated from the BALF live cell count **a.** 3 and **b.** 7 days post infection. Data shown as mean $\pm$ s.e.m and analysed using an ordinary one-way ANOVA with a Sidak *post hoc* test (n=5-11) ( $p < 0.05$ ).

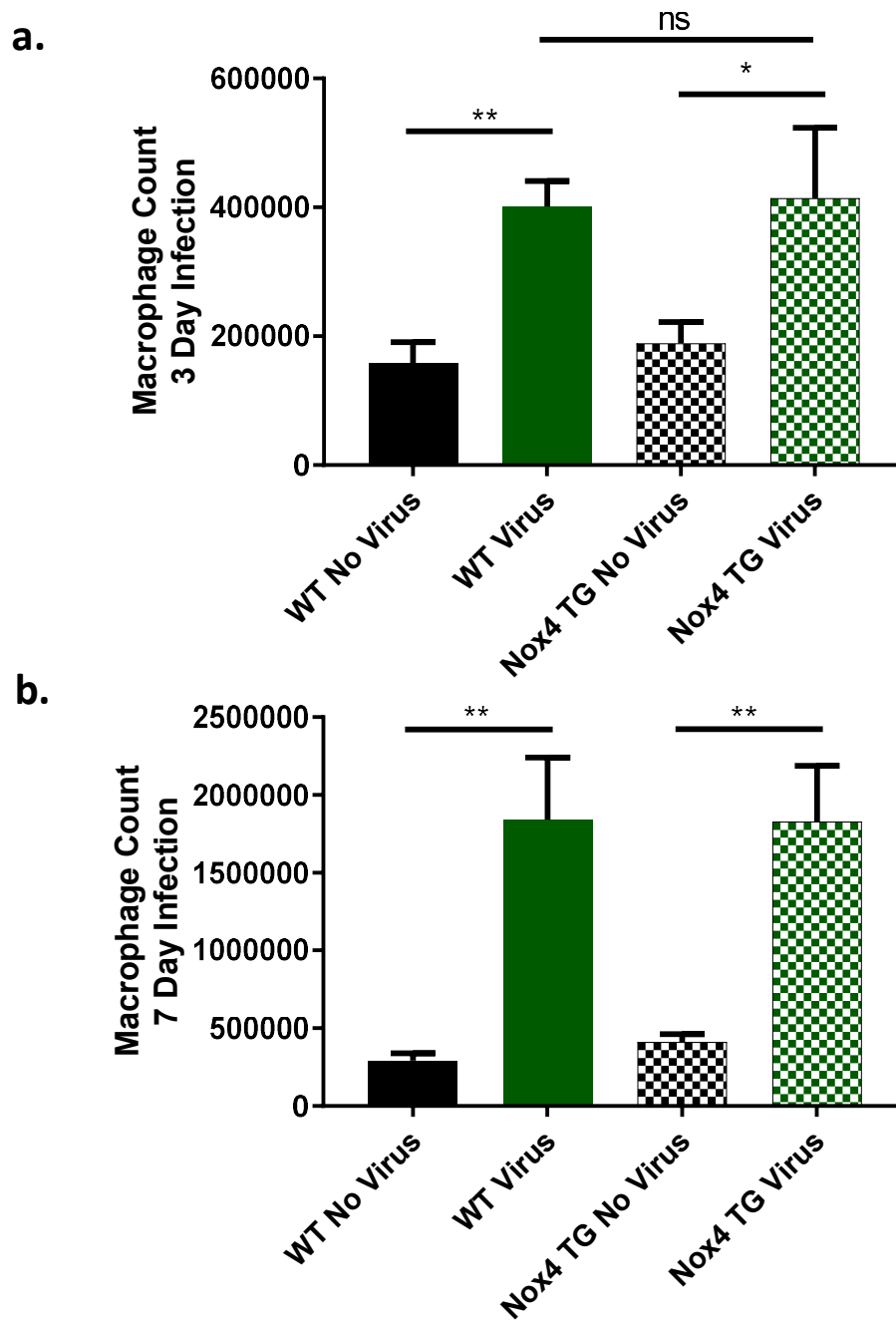


**Figure 12.** Influenza A virus infected endothelial Nox4 overexpressing mice had no difference in macrophage infiltration compared to the infected wild type mice.

BALF cells from X31-infected ( $10^4$  PFU) WT and Nox4 transgenic mice were fixed and stained with RAPID 1 and 2. The percentage of alveolar macrophage infiltration in 500 cells were counted and total macrophage infiltration was calculated from the BALF live cell count **a.** 3 and **b.** 7 days post infection. Data shown as mean $\pm$ s.e.m and analysed using an ordinary one-way ANOVA with a Sidak *post hoc* test (n=5-11). ( $p < 0.05$ )

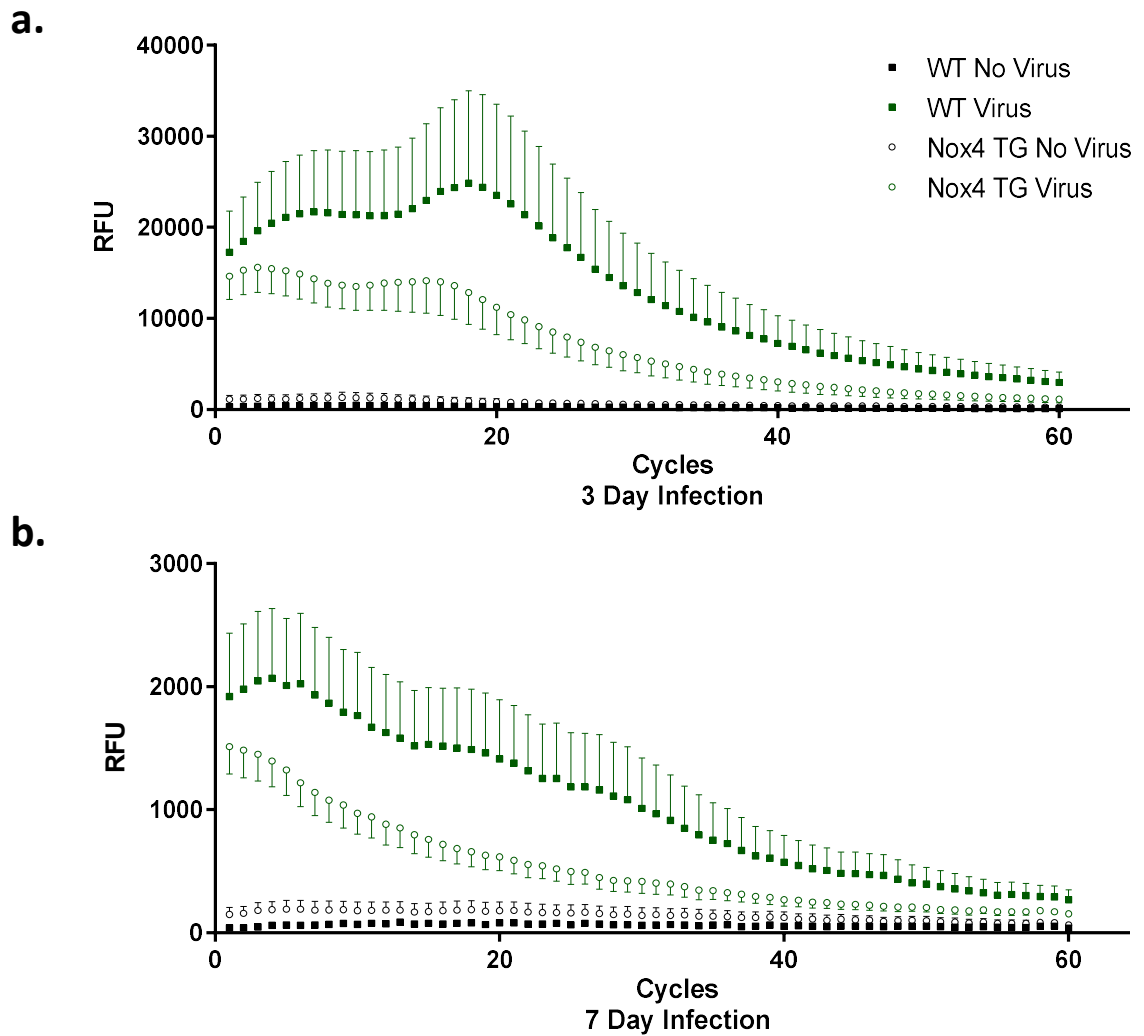


**Figure 13. Evidence that endothelial Nox4 overexpression results in a decrease in BALF cell superoxide production measured with L-012 after 3 and 7 days influenza A virus infection.**

50 000 BALF cells extracted from X31-infected ( $10^4$  PFU) WT and Nox4 transgenic mice **a.** 3 and **b.** 7 days post infection with X31 were seeded in triplicated into a 96 well plate. Extracellular superoxide production in these cells were measured with an L-012 enhanced chemiluminescence assay. Data shown as mean $\pm$ s.e.m and analysed using an ordinary two-way ANOVA with a Sidak *post hoc* test. (n=7-15) (p<0.05).

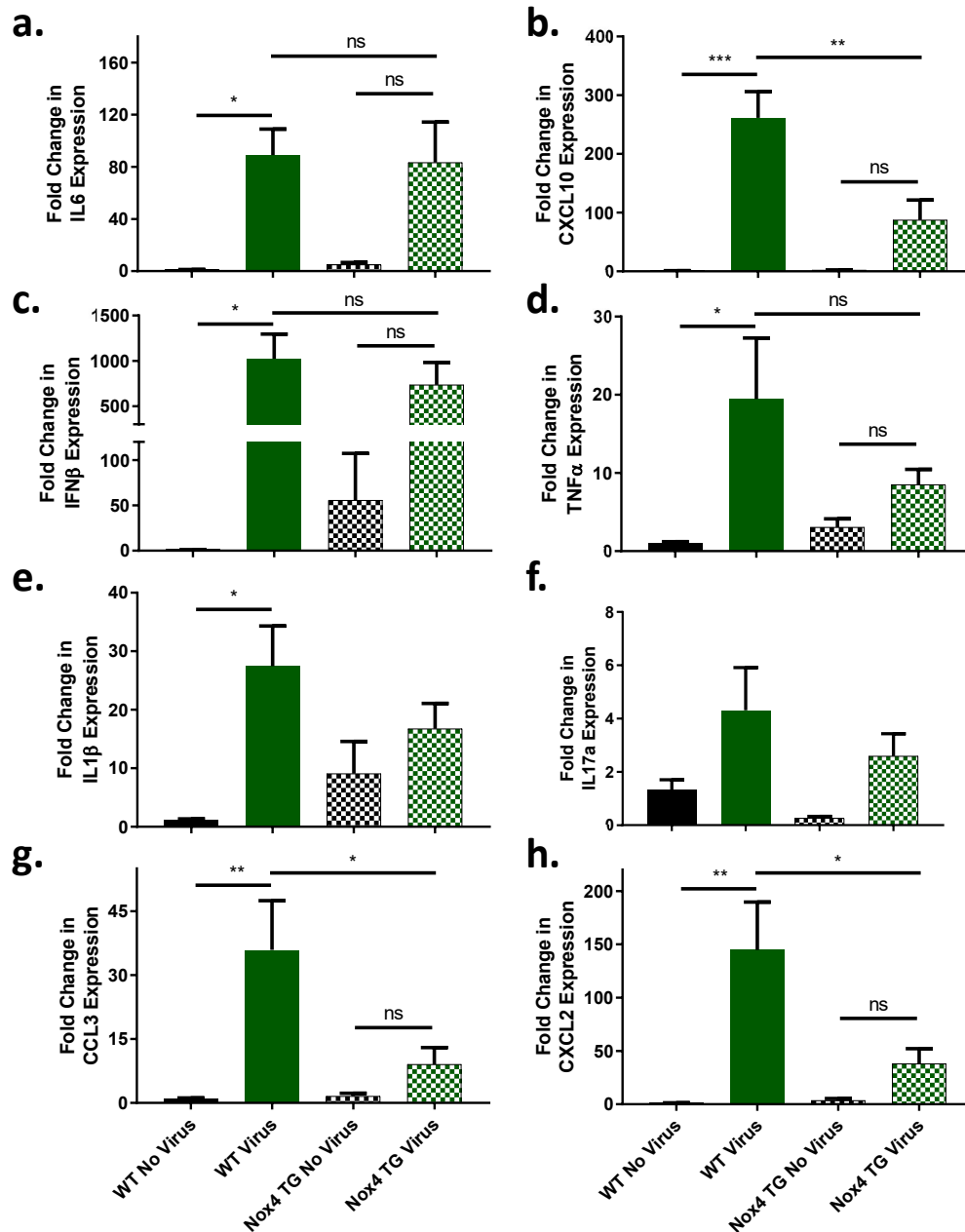


**Figure 14.** There was a significant decrease in CXCL10, CCL3 and CXCL2 expression in Nox4 overexpressing mice infected with influenza A virus 3 days post infection.

WT and Nox4 TG mice were infected with X31 ( $10^4$  PFU) for 3 days. Lung RNA expression of **a.** IL6, **b.** CXCL10, **c.** IFN $\beta$ , **d.** TNF $\alpha$ , **e.** IL1 $\beta$ , **f.** IL17a, **g.** CCL3, and **h.** CXCL2 were measured with RT-PCR. 18S was used as a housekeeping gene. Data shown as mean $\pm$ s.e.m and analysed using an ordinary one-way ANOVA with a Sidak *post hoc* test (n=8-15) ( $p < 0.05$ ).

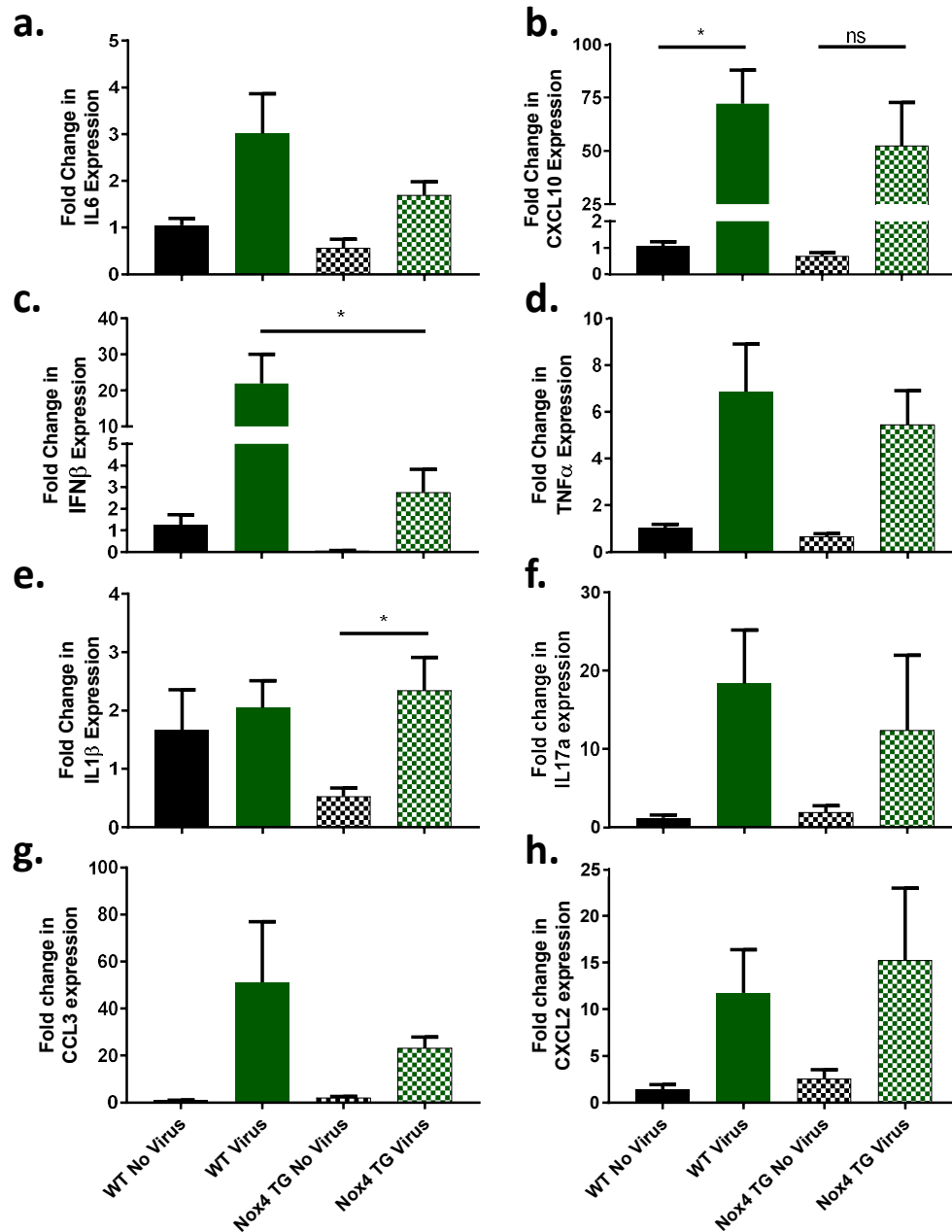


**Figure 15. Endothelial Nox4 overexpressing mice infected with influenza A virus for 7 days had a decrease in IFNβ expression compared to infected wild type mice.**

WT and Nox4 TG mice were infected with X31 ( $10^4$  PFU) for 7 days. Lung RNA expression of **a.** IL6, **b.** CXCL10, **c.** IFNβ, **d.** TNFα, **e.** IL1β, **f.** IL17a, **g.** CCL3, and **h.** CXCL2 were measured with RT-PCR. 18S was used as a housekeeping gene. Data shown as mean±s.e.m and analysed using an ordinary one-way ANOVA with a Sidak *post hoc* test (n=3-11) (p<0.05).

## Discussion

While a majority of the literature focuses on epithelial and inflammatory cells, recent studies have examined the role of the endothelium in influenza-induced inflammation (Teijaro *et al.*, 2011).

Chapter 2 examined intracellular pathways by which endothelial Nox2 regulates influenza-induced cytokine expression. While Nox2 has been shown to exacerbate influenza-induced inflammation (Vlahos *et al.*, 2011) and mediates inflammatory signalling in influenza-infected macrophages (To *et al.*, 2017), Nox4 is highly expressed in the endothelium (Van Buul *et al.*, 2005) and has been shown to mediate distinct pathways to Nox2 (Anilkumar *et al.*, 2008). This study sought to examine the role of endothelial Nox4 in influenza pathology using the Nox4 overexpressing mice developed by our collaborator Professor Ajay Shah. These transgenic mice expressed Nox4 at 2-3 fold higher levels than that of WT mice and they produce 2-3 times the amount of hydrogen peroxide (Schröder *et al.*, 2012).

This study found that lung Nox4 expression was significantly decreased in WT mice infected with influenza strain X31 compared to uninfected controls, both at three and seven days post infection. In contrast, Amatore *et al.*, (2015) found that both primary and secondary epithelial cells infected with the highly pathogenic PR8 influenza strain *in vitro* had increased Nox4 expression and increased Nox4 protein detected by western blot. Another important point to consider is that the anti-Nox4 antibody used by Amatore *et al.*, (2015) is found to be ineffective and is no longer available from Santa Cruz, calling their findings into question (Altenhöer, *et al.* 2012). The current study examined lung Nox4 expression regardless of cell type in an *in vivo* model, over multiple days and with a different strain of virus. The specific effects of influenza infection on Nox4 expression in cells other than the epithelium is largely unknown. It should be noted that basal Nox4 expression in epithelial cells is low, particularly when compared to Nox2 and Nox1 (Kolářová *et al.*, 2010). Given the low basal expression of Nox4 in the epithelial cells, the role of Nox4 in the endothelium may be more clinically relevant. Influenza infection has been shown to result in Nox2 upregulation (Kash *et al.*, 2004). Silencing Nox2 in lung endothelial cells has led to increased Nox4 expression and vice versa (Pendyala *et al.*, 2009). A

similar mechanism could be responsible for the decrease in Nox4. For instance, nitric oxide has been shown to cause down regulation of Nox2 in human endothelial cells (Duerrschmidt *et al.*, 2006). Chapter 3, in addition to Thomas *et al.* (2002), demonstrated that hydrogen peroxide drives eNOS production in endothelial cells. Since these Nox4 TG mice are producing ~2-3 times more hydrogen peroxide than WT mice, this could mean an increase in nitric oxide production and, subsequently, Nox2 downregulation.

The main focus of the study by Amatore, et al (2015) was viral replication. They found that Nox4 was essential for viral replication in epithelial cells. In contrast, our study found that that viral titre was decreased in the lungs of Nox4 TG mice compared to the infected WT mice, both 3 and 7 days post infections. As stated previously, this study used X31 rather than the more pathogenic PR8 influenza strain, specifically upregulated endothelial Nox4 in an *in vivo* model rather than an *in vitro* model examining epithelial cells.

Weight loss was one of the indicators of morbidity assessed in this study. While all mice lost weight when infected with X31, infected Nox4 TG mice lost less weight than infected WT mice up to three days post infection, but not from 4 days onwards. This suggests that endothelial Nox4 has protective effects in the earlier stages of influenza infection. There were similar findings with the other markers of morbidity. Lung weight was used as an indicator of pulmonary oedema and inflammation. Mice infected with influenza had increased lung weight, the lung weight of infected Nox4 TG mice was decreased at day 3.

There are some contradictions between the current literature and our findings. Nox4 has been shown to oxidise PTP1B (Chen *et al.*, 2008). Oxidation of PTP1B was found to exacerbate LPS-induced pulmonary oedema (Grinnell *et al.*, 2012). Should the same pathways be involved in influenza-induced pulmonary oedema, endothelial Nox4 overexpression should have exacerbated influenza-induced morbidity in the current model. However, the study by Grinnell *et al.*, is examining a bacterial

model of oedema and only one particular pathway that Nox4 regulates. In addition, the current study is only examining the effect of endothelial Nox4.

This study also examined the oxidative burst in lung inflammatory cells. There was an increase in extracellular superoxide production from the BALF cells of infected mice, but it was significantly less in the Nox4 TG mice. Nox4 has been shown to drive the production of the antioxidant heme oxygenase (HO1) (Schröder *et al.*, 2012), which has been shown to have protective effects in a mouse model of lung injury (Fredenburgh *et al.*, 2007). This could account for the decrease in oxidative burst and the reduced lung weight in infected Nox4 TG mice. Another factor that could explain the differences in ROS production are the types of inflammatory cell in the BALF. BALF obtained from uninfected mice, primarily contained macrophages, whereas the BALF infected mice had a higher percentage of neutrophils. Compared to the infected WT mice, BALF from the infected Nox4 TG mice had a decreased percentage of neutrophils. This decrease in neutrophil infiltration could explain the decreased oxidative burst.

A hallmark of serious cases of influenza infection is an excessive and detrimental inflammatory response (Mauad *et al.*, 2010; Domínguez-Cherit *et al.*, 2009). This study found an increase in airway inflammatory cell infiltration, alveolitis, peribronchiolar inflammation and overall lung inflammation in influenza-infected mice in WT mice both 3 and 7 days post infection. However, there was no increase in airway inflammatory cell infiltration, alveolitis and peribronchiolar inflammation and overall inflammation in the lungs of infected Nox4 TG mice, 3 days post infection. This decrease in inflammation correlates with the decrease in weight loss, lung weight and viral titre in infected Nox4 TG mice at day three.

Influenza infected Nox4 TG mice had decreased expression of CXCL10, CCL3 and CXCL2 three days post infection, and in IFN $\beta$  seven days post infection. The activation of CXCR3 by CXCL10 triggers influenza-induced neutrophil infiltration, and the deletion of CXCL10 and CXCR3 results in increased survival (Ichikawa *et al.*, 2013). The decrease in CXCL10 expression in the influenza-infected Nox4 TG

mice compared to infected WT mice is consistent with both the decrease in neutrophil infiltration and the decrease in lung weight seen in infected Nox4 TG mice. CXCL10 also contributes to the oxidative burst from neutrophils extracted from an acid-triggered acute lung injury (Ichikawa, *et al.* 2013). This is consistent with the L-012 data in this study, which showed a decreased oxidative burst in infected Nox4 TG mice compared to the infected WT mice. CCL3 and CXCL2 have also been shown to be involved in the recruitment of neutrophils in models of bacterial infection (Zeng *et al.*, 2003; De Filippo *et al.*, 2013), and are both upregulated in influenza infection (Wareing *et al.*, 2004). The downregulation of CCL3 in infected Nox4 TG explains the decrease in neutrophil infiltration. CCL3, and CXCL10 are all known to trigger the infiltration of macrophages in influenza infection (Zeng, *et al.* 2003; Ichikawa, *et al.* 2013) yet, despite the decrease in these chemokines, there was no change in the number of macrophages in the infected Nox4 TG. Either these are redundant pathways, or a compensatory mechanism is involved.

In summary, Nox4 has been shown to be protective against inflammatory and ischemic stress. This study has shown for the first time that endothelial Nox4 also ameliorates the symptoms of influenza infection, including oxidative stress, eosinophil and neutrophil infiltration, lung damage, and cytokine expression. This study further highlights the role of the endothelium in influenza pathology and the opposing roles of Nox isoforms in this context. Specifically increasing endothelial Nox4 activity could be a means of reducing influenza-induced inflammation and oxidative stress and improve patient outcomes.

## References

- Altenhöfer, S, Kleikers, PWM, Radermacher, KA, Scheurer, P, Hermans, JJR, Schiffers, P, *et al.* (2012). The NOX toolbox: Validating the role of NADPH oxidases in physiology and disease. *Cell. Mol. Life Sci.* **69**: 2327–2343.
- Amatore, D, Sgarbanti, R, Aquilano, K, Baldelli, S, Limongi, D, Civitelli, L, *et al.* (2015). Influenza virus replication in lung epithelial cells depends on redox-sensitive pathways activated by NOX4-derived ROS. *Cell. Microbiol.* **17**: 131–145.
- Anilkumar, N, Weber, R, Zhang, M, Brewer, A, Shah, AM (2008). NOX4 and NOX2 NADPH oxidases mediate distinct cellular redox signaling responses to agonist stimulation. *Arterioscler. Thromb. Vasc. Biol.* **28**: 1347–1354.
- Armstrong, SM, Wang, C, Tigdi, J, Si, X, Dumpit, C, Charles, S, *et al.* (2012). Influenza infects lung microvascular endothelium leading to microvascular leak: role of apoptosis and claudin-5. *PLoS One* **7**: e47323.
- Carneseccchi, S, Deffert, C, Donati, Y, Basset, O, Hinz, B, Preynat-Seauve, O, *et al.* (2011). A Key Role for NOX4 in Epithelial Cell Death During Development of Lung Fibrosis. *Antioxid. Redox Signal.* **15**: 607–619.
- Chen, H, Kim, GS, Okami, N, Narasimham, P, Chan, PH (2012). NADPH oxidase is involved in post-ischemic brain inflammation. *Neurobiol. Dis.* **42**: 341–348.
- Chen, K, Kirber, MT, Xiao, H, Yang, Y, Keaney, JF (2008). Regulation of ROS signal transduction by NADPH oxidase 4 localization. *J. Cell Biol.* **181**: 1129–1139.
- Dawood, FS, Iuliano, a D, Reed, C, Meltzer, MI, Shay, DK, Cheng, P-Y, *et al.* (2012). Estimated global mortality associated with the first 12 months of 2009 pandemic influenza A H1N1 virus circulation: a modelling study. *Lancet Infect. Dis.* **12**: 687–695.
- De Silva, TM, Brait, VH, Drummond, GR, Sobey, CG, Miller, AA (2011). Nox2 oxidase activity accounts

for the oxidative stress and vasomotor dysfunction in mouse cerebral arteries following ischemic stroke. *PLoS One* **6**: e28393

Domínguez-Cherit, G, Lapinsky, SE, Macias, AE, Pinto, R, Espinosa-Perez, L, la Torre, A de, *et al.*

(2009). Critically ill patients with 2009 influenza A (H1N1) in Mexico. *JAMA* **302**: 1880–1887.

Duerschmidt, N, Stielow, C, Muller, G, Pagano, PJ, Morawietz, H (2006). NO-mediated regulation of

NAD(P)H oxidase by laminar shear stress in human endothelial cells. *J. Physiol.* **576**: 557–567.

Filippo, K De, Dudeck, A, Hasenberg, M, Nye, E, Rooijen, N Van, Hartmann, K, *et al.* (2013). Mast cell

and macrophage chemokines CXCL1 / CXCL2 control the early stage of neutrophil

recruitment during tissue inflammation. *Blood* **121**: 4930–4937.

Fredenburgh, LE, Perrella, MA, Mitsialis, SA (2007). The role of heme oxygenase-1 in pulmonary

disease. *Am. J. Respir. Cell Mol. Biol.* **36**: 158–165.

Gray, SP, Marco, E Di, Kennedy, K, Chew, P, Okabe, J, El-Osta, A, *et al.* (2016). Reactive Oxygen

Species Can Provide Atheroprotection via NOX4-Dependent Inhibition of Inflammation and

Vascular Remodeling. *Arterioscler. Thromb. Vasc. Biol.* **36**: 295–307.

Grinnell, KL, Chichger, H, Braza, J, Duong, H, Harrington, EO (2012). Protection against LPS-induced

pulmonary edema through the attenuation of protein tyrosine phosphatase-1B oxidation.

*Am. J. Respir. Cell Mol. Biol.* **46**: 623–632.

Ichikawa, A, Kuba, K, Morita, M, Chida, S, Tezuka, H, Hara, H, *et al.* (2013). CXCL10-CXCR3 enhances

the development of neutrophil-mediated fulminant lung injury of viral and nonviral origin.

*Am. J. Respir. Crit. Care Med.* **187**: 65–77.

Kash, JC, Basler, CF, García-Sastre, A, Carter, V, Billharz, R, Swayne, DE, *et al.* (2004). Global host

immune response: pathogenesis and transcriptional profiling of type A influenza viruses

expressing the hemagglutinin and neuraminidase genes from the 1918 pandemic virus. *J.*

*Virology* **78**: 9499–9511.

- Kolářová, H, Binó, L, Pejchalová, K, Kubala, L (2010). The expression of NADPH oxidases and production of reactive oxygen species by human lung adenocarcinoma epithelial cell line A549. *Folia Biol. (Praha)*. **56**: 211–217.
- Löhneysen, K Von, Noack, D, Jesaitis, AJ, Dinauer, MC, Knaus, UG (2008). Mutational analysis reveals distinct features of the Nox4-p22 phox complex. *J. Biol. Chem.* **283**: 35273–35282. Mauad, T, Hajjar, L a, Callegari, GD, Silva, LFF da, Schout, D, Galas, FRBG, *et al.* (2010). Lung pathology in fatal novel human influenza A (H1N1) infection. *Am. J. Respir. Crit. Care Med.* **181**: 72–79.
- Pendyala, S, Gorshkova, IA, Usatyuk, P V., He, D, Pennathur, A, Lambeth, JD, *et al.* (2009). Role of Nox4 and Nox2 in Hyperoxia-Induced Reactive Oxygen Species Generation and Migration of Human Lung Endothelial Cells. *Antioxid. Redox Signal.* **11**: 747–764.
- Ray, R, Murdoch, CE, Wang, M, Santos, CX, Zhang, M, Alom-Ruiz, S, *et al.* (2011). Endothelial Nox4 NADPH oxidase enhances vasodilatation and reduces blood pressure in vivo. *Arterioscler. Thromb. Vasc. Biol.* **31**: 1368–1376.
- Schröder, K, Zhang, M, Benkhoff, S, Mieth, A, Pliquett, R, Kosowski, J, *et al.* (2012a). Nox4 is a protective reactive oxygen species generating vascular NADPH oxidase. *Circ. Res.* **110**: 1217–1225.
- Schröder, K, Zhang, M, Benkhoff, S, Mieth, A, Pliquett, R, Kosowski, J, *et al.* (2012b). Nox4 is a protective reactive oxygen species generating vascular NADPH oxidase. *Circ. Res.* **110**: 1217–1225.
- Teijaro, JR, Walsh, KB, Cahalan, S, Fremgen, DM, Roberts, E, Scott, F, *et al.* (2011). Endothelial cells are central orchestrators of cytokine amplification during influenza virus infection. *Cell* **146**: 980–991.
- Thomas, S, Chen, K, Keane, J (2002). Hydrogen peroxide activates endothelial nitric-oxide synthase through coordinated phosphorylation and dephosphorylation via a phosphoinositide 3-

kinase-dependent signaling pathway. *J. Biol. Chem.* **277**: 6017–6024.

To, EE, Vlahos, R, Luong, R, Halls, ML, Reading, PC, King, PT, *et al.* (2017). Endosomal NOX2 oxidase exacerbates virus pathogenicity and is a target for antiviral therapy. *Nat. Commun.* **8**: 69.

Van Buul, J, Fernandez-Borja, M, Anthony, E, Hordijk, P (2005). Expression and localization of NOX2 and NOX4 in primary human endothelial cells. *Antioxidants Redox Signal.* **7**: 308–317.

Vlahos, R, Stambas, J, Bozinovski, S, Broughton, BRS, Drummond, GR, Selemidis, S (2011). Inhibition of Nox2 oxidase activity ameliorates influenza A virus-induced lung inflammation. *PLoS Pathog.* **7**: e1001271.

Walder, CE, Green, SP, Darbonne, WC, Mathias, J, Rae, J, Dinauer, MC, *et al.* (1997). Ischemic stroke injury is reduced in mice lacking a functional NADPH oxidase. *Stroke* **28**: 2252–2258.

Wareing, MD, Lyon, AB, Lu, B, Gerard, C, Sarawar, SR (2004). Chemokine expression during the development and resolution of a pulmonary leukocyte response to influenza A virus infection in mice. *J. Leukoc. Biol.* **76**: 886–895.

Zeng, X, Moore, TA, Newstead, MW, Hernandez-Alcoceba, R, Tsai, WC, Theodore, J. (2003). Intrapulmonary expression of macrophage inflammatory protein 1  $\alpha$  ( CCL3 ) induces neutrophil and NK cell accumulation and stimulates innate immunity in murine bacterial pneumonia. *Infection and Immunity.* **71**: 1306–1315.

## **CHAPTER FIVE:**

---

### **General Discussion**

---

### **Summary of Major Findings**

Oxidative stress, inflammation and lung damage are the hallmarks of influenza infection. A majority of the current literature focuses on macrophages and epithelial cells, the primary targets of influenza. However, recent evidence suggests that the endothelium may play a large role in influenza pathology. This thesis explores the role of the endothelium in influenza infection. In particular, it examines the role of endothelial ROS signalling in influenza infection (Figure 1).

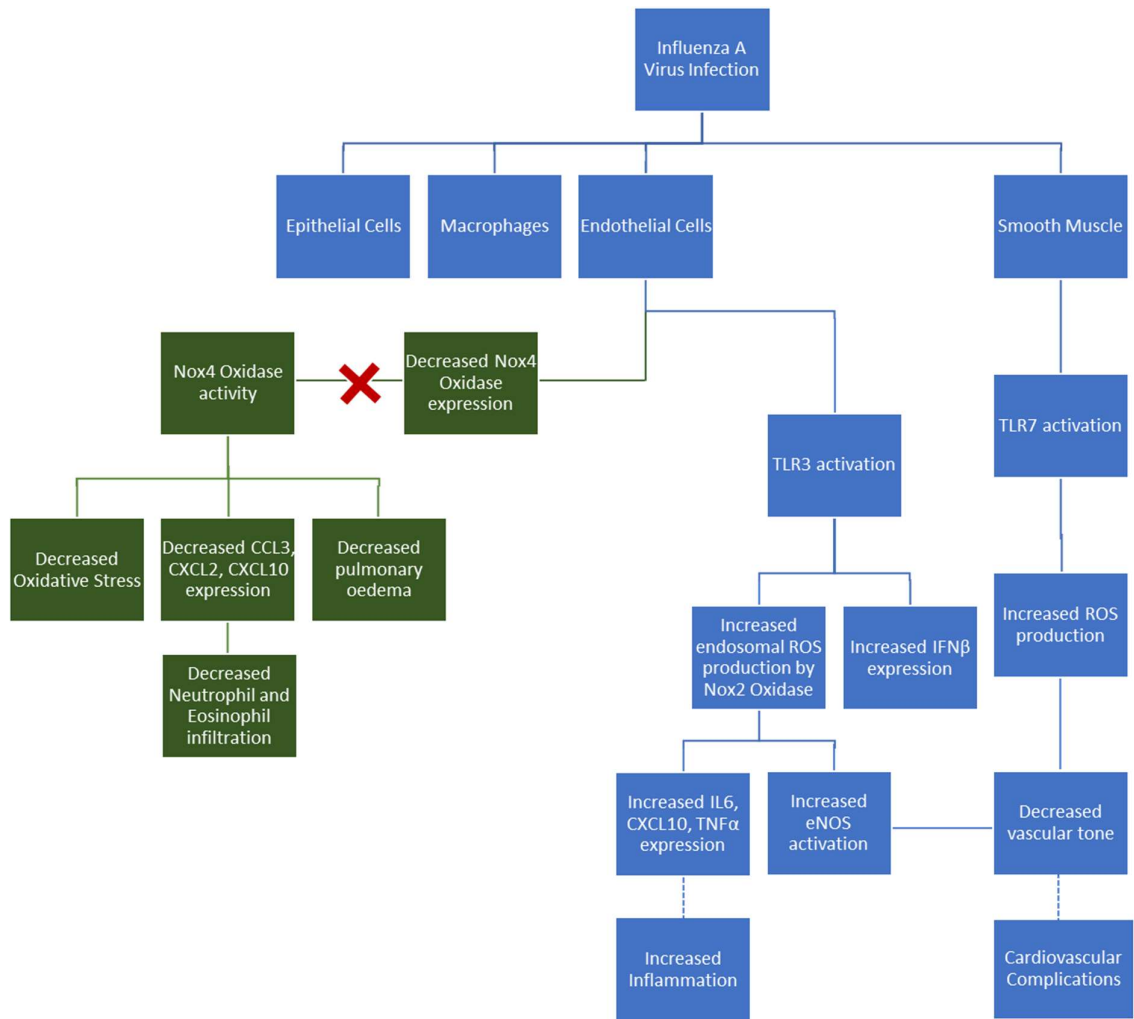


**Figure 1.** Proposed mechanisms by which the endothelium contributes to influenza pathology.

Influenza infection and TLR3-activation result in an increase in Nox2-dependent endosomal ROS production. TLR3 activation also causes an increase in inflammatory cytokine production both dependently and independently of Nox2. TLR3 activation decreases vascular tone through eNOS, and TLR7 activation decreases vascular tone through activation of potassium channels on the smooth muscle. Influenza infection results in a decrease in lung Nox4 expression. Nox4 decreases influenza-induced oxidative stress, CCL3, CXCL2 and CXCL10 expression, neutrophil and eosinophil infiltration and pulmonary oedema.

## Chapter 2: Influenza infection induces Nox2-dependent endosomal ROS production

Using fluorescence microscopy, this study demonstrated that influenza internalises into endothelial cells *in vivo*. Influenza has been shown to internalise into both HeLa cells and macrophages *via* endocytosis. This study showed influenza nucleoprotein colocalising with early endosomes in endothelial cells infected with X31.

While the endothelium has been associated with influenza-induced inflammation, the mechanisms behind this increase are unclear. Nox2 has been shown to exacerbate symptoms in mice infected with influenza strains X31 and PR8 (Vlahos *et al.*, 2011). Nox2<sup>-/-</sup> mice had decreased alveolar inflammation, viral titre, and oxidative stress. Influenza A virus infection has also been shown to result in a Nox2-dependent increase in endosomal ROS production in macrophages (To *et al.*, 2017). Similarly, this study also found a Nox2-dependent increase in endosomal ROS production in endothelial cells. While To, *et al.* found that TLR7 was required for influenza-induced endosomal ROS production in macrophages, in this study TLR7-activation by imiquimod did not result in an increase in endosomal ROS production in endothelial cells. However, TLR3 activation by poly I:C resulted in a Nox2-dependent increase in endosomal ROS production.

Endosomal ROS production has been shown to have a role in inflammatory signalling. Endosomal Nox2 signalling has been shown to be necessary for TNF $\alpha$  expression by NF- $\kappa$ B in MCF-7 cells, a human breast cancer cell line (Li *et al.*, 2009). While there has been no such association shown with TLR7, TLR3 and Nox2 have been shown to form a physical association that is necessary for NF- $\kappa$ B, IRF3, and STAT1-mediated innate activation in macrophages (Yang *et al.*, 2013). In this study, poly I:C treatment in MLEC resulted in a Nox2-dependent increase in IL6, CXCL10 and TNF $\alpha$  expression, which are all triggered by the NF- $\kappa$ B pathway. Unlike the study by Yang, *et al.*, IFN $\beta$  expression, which occurs through IRF3 activation, was not Nox2 dependent (Figure 2). Consistent with our findings that TLR7 activation did not result in an increase in endosomal ROS production in endothelial cells, imiquimod resulted in a small Nox2-independent increase in IL6 and CXCL10 expression in MLEC,

suggesting that contrary to what is seen in macrophages, TLR7 is not highly expressed in the endothelium. Pretreatment with catalase resulted in an increase in TLR7-induced expression of IL6, CXCL10, IFN $\beta$ , and TNF $\alpha$ . This is consistent with the finding of To, *et al.* (2017) who found a negative feedback loop in which TLR7 activation drove Nox2, but hydrogen peroxide deactivated TLR7 by oxidising a specific cysteine residue. Pretreatment with catalase, resulted in an increase in TLR3-induced IL6 and TNF $\alpha$  expression, suggesting a similar mechanism may be in place for TLR3. While the TLR7-induced expression of IL6, CXCL10, IFN $\beta$ , and TNF $\alpha$  in endothelial cells was shown to be catalase sensitive, this experiment didn't examine the source of ROS in this instance. Further experimentation is examining the source of TLR-induced ROS production in endothelial cells is required.

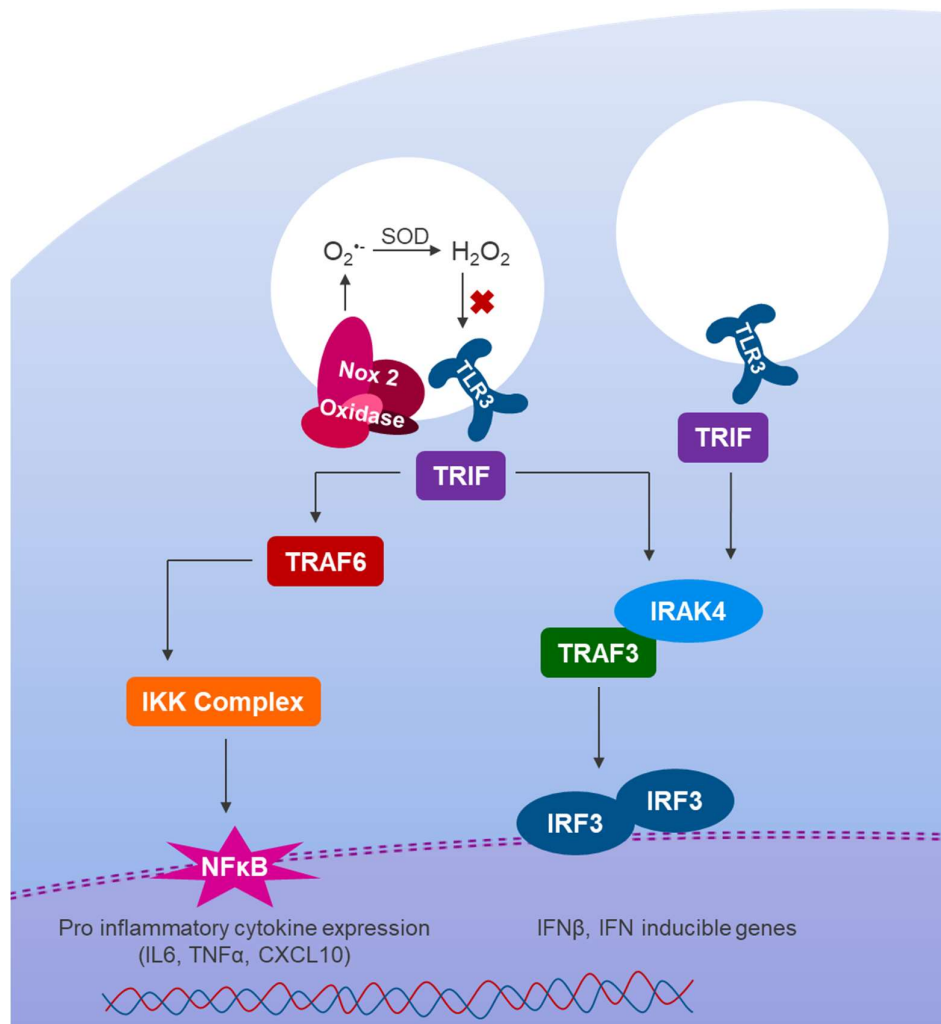


**Figure 2.** Proposed pathways by which TLR3 induces cytokine production, both dependently and independently of Nox2.

### **Chapter 3: Activation of TLR3 and TLR7 leads to vascular relaxation through distinct pathways**

Despite a large number of influenza-related deaths being due to cardiovascular complications (Dawood *et al.*, 2012), there has been very little literature on the cardiovascular effects of influenza infection. An important role of the endothelium is the regulation of vascular tone. Hypotension is a reported side effect of treatment with both TLR agonist imiquimod (Aldara product sheet, 2014) and with TLR3 agonists (Krown *et al.*, 1985; Stevenson *et al.*, 1985). This study sought to examine the effects of TLR3 and TLR7 activation on vascular tone, and to investigate the signalling pathways involved.

Treatment with TLR7 agonists imiquimod (3-300  $\mu\text{M}$ ), gardiquimod (3-300  $\mu\text{M}$ ) and resiquimod (3-300  $\mu\text{M}$ ) resulted in a concentration-dependent relaxation of pig coronary artery, with gardiquimod being slightly less potent. Imiquimod and gardiquimod both resulted in complete relaxation of the ring segments at 300  $\mu\text{M}$ . TLR7-induced relaxation of pig coronary artery was endothelium-independent. Pretreatment with eNOS inhibitor, L-NAME (100 $\mu\text{M}$ ), had no effect on TLR7-induced relaxation. Pretreatment with  $\text{K}^+$  (25mM) did inhibit TLR7-induced relaxation of pig coronary artery, suggesting that TLR7 activation results in relaxation through activation of potassium channels on the smooth muscle. Further investigation with specific potassium channel antagonists showed that TLR7-induced relaxation was not through inwardly rectifying potassium channels, intermediate or large conductance calcium activated potassium channels. Blocking small conductance calcium-activated potassium channels with apamin did partially decrease TLR7-induced relaxation. Pretreatment with catalase (500u/ml) resulted in a leftward shift of the concentration response curve, which is consistent with previous data in Chapter 2 and by To *et al.*, (2014) that showed hydrogen peroxide inhibiting TLR7. Interestingly, treatment with PEG-catalase (500u/ml) had no effect on TLR7-induced relaxation. Unconjugated catalase cannot pass through plasma membranes. This suggests that catalase must be taken into smooth muscle cells with *via* endocytosis to have an effect.

Treatment with TLR3 agonist, poly I:C (1-30 $\mu$ g/ml) also resulted in partial relaxation of pig coronary artery. Unlike TLR7, TLR3-induced relaxation was endothelium-dependent. While pre-treatment with K<sup>+</sup> (25mM) had no effect on TLR3-induced relaxation, pre-treatment with eNOS inhibitor L-NAME abolished this response. There was a strong trend for decreased TLR3-induced relaxation after pre-treatment with PEG-catalase (500u/ml), and a significant increase in TLR3-induced relaxation after treatment with PEG-SOD (600u/ml). This suggests that TLR3 induced relaxation involves hydrogen peroxide. Hydrogen peroxide has been shown to drive eNOS through phosphoinositide 3-kinase (Thomas *et al.*, 2002).

#### **Chapter 4: Endothelial Nox4 oxidase negatively regulates airway neutrophil infiltration and alleviates influenza virus pathology.**

Nox4 oxidase differs from Nox2 oxidase greatly in structure and function. Due to its unique structure Nox4 oxidase directly produces hydrogen peroxide and, unlike Nox2, is constitutively active. While Nox2 has been shown to exacerbate many inflammatory disorders, including influenza infection, Nox4 has been shown to have a protective role in atherosclerosis and ischemic stress. However, there has been one study examining the role of Nox4 in influenza A virus infection in epithelial cells. This study found that Nox4 increased viral replication in epithelial cells *in vitro* (Amatore *et al.*, 2015), however the antibody they used was unvalidated (Altenhöer, *et al.* 2012). Nox4 is a 100-fold times more expressed in the endothelium than Nox2, and not highly expressed in the epithelium.

Examining the role of endothelial Nox 4 *in vivo* is perhaps a more clinically relevant approach. Nox4 expression significantly decreased in the infected WT mice 3 and 7 days post infection. The current study investigated the role of endothelial Nox4 in influenza infection using the endothelial Nox4 overexpressing mice developed by Professor Ajay Shah. These transgenic mice were infected with influenza A virus strain X31 (10<sup>4</sup> PFU) for 3 and 7 days. Three days post infection, Nox4 TG mice lost less body weight, had a decrease in pulmonary oedema, measured as lung weight, superoxide production in BALF cells, a decrease in alveolar inflammatory cell infiltration, specifically of neutrophils, and a decrease in alveolitis and peribronchiolar inflammation compared to the WT mice.

Lung cytokine expression of CXCL10, CCL3, and CXCL2 was significantly decreased in Nox4 TG mice compared to the WT mice three days post infection. Despite the findings of Amatore, *et al.* that Nox4 was necessary for influenza replication, there was a trend for decreased viral titre three days post infection in the Nox4 TG mice compared to the WT mice. 7 days post infection, there was no significant difference in body weight, lung weight or in alveolar infiltration of inflammatory cells in the Nox4 TG mice compared to the Nox4 WT mice. However, there was a significant decrease in eosinophil infiltration and a strong trend in decreased neutrophil infiltration, a decrease in superoxide production in the BALF cells and a strong trend in decreased viral titre.

### **Expanding the paradigm: Influenza and the Vasculature**

The 2017 seasonal influenza epidemic was the worst Australia had seen since the 2009 pandemic, with 233 453 laboratory confirmed cases, an increase in the number of hospital admissions, and 745 deaths (Department of Health and Aging, 2017). The influenza vaccine proved ineffective this year, particularly against H3N2 strains (Sullivan *et al.*, 2017). Discovering more treatments, particularly treatments that do not cause resistance, is imperative.

There have been recent strides in understanding the mechanisms involved in influenza-induced inflammation and oxidative stress. However, despite many influenza patients presenting with potentially fatal cardiovascular complications (Dawood *et al.*, 2012), there has been very little research on the mechanisms involved. Additionally, the role of the endothelium in influenza pathology has only briefly been touched upon.

This thesis has examined previously unexplored pathways through which the endothelium and the vasculature contributes to influenza pathology. While endothelial cells had been shown to contribute to the influenza-induced “cytokine storm”, the mechanisms by which it does are unclear. Both TLR3 and Nox2 deletion reduces influenza-induced inflammation. Chapter 2 showed influenza infection and TLR3 activation resulted in an increase in endosomal ROS production in endothelial cells. This study also examined pathways by which TLR3 activation results in a Nox2-dependent and

independent increase in inflammatory cytokines, providing a better understanding of inflammatory signalling in influenza pathology and the role of the endothelium.

Hypotension is a sign of cardiopulmonary insufficiency in influenza patients (WHO, 2010), but there is no literature on how this occurs. Consistent with the effects of TLR7 and TLR3 agonists in human patients, Chapter 3 demonstrated that endothelial TLR3 activation resulted in eNOS activation and TLR7 activation causes relaxation of vascular smooth muscle through activation of small conductance calcium-activated potassium channels. Considering the role TLR3 and TLR7 play in influenza-induced inflammation, these pathways could potentially be involved in the cardiovascular complications presented by many influenza patients.

While the endothelium has been shown to be one of the sources of influenza-induced inflammation, Nox4, which is highly expressed in the endothelium, has been shown to have protective, anti-inflammatory and antioxidant effects. Chapter 4 was the first demonstration that endothelial Nox4 overexpression is protective against influenza induced morbidity, inflammation, and oxidative stress. Understanding how Nox4 signalling is protective against influenza infection could provide potential avenues for treatment.

As a whole, these studies shed light on the previously unstudied importance of the endothelium and the vasculature in influenza pathology.

### **Pharmacological Intervention**

These studies open up numerous possibilities in terms of potential influenza treatments. The endothelium could be specifically targeted by administering drugs intravenously. TLR3<sup>-/-</sup> mice had decreased influenza-induced lung damage and expression of IL6 and CCL5. Chapter 2 examined endothelial TLR3 signalling and Chapter 3 examined TLR3 induced relaxation of vascular smooth muscle. A TLR3 antagonist could be potentially be a treatment for reducing influenza-induced inflammation.

The protective effects of Nox4 could mean a nonspecific antioxidant would not be an effective treatment for influenza-induced inflammation and oxidative stress. To, *et al.* (2017) developed method of specifically targeting endosomal Nox2 using a specific Nox2 inhibitor, gp91ds-TAT, conjugated to cholestanol. This method proved effective in reducing alveolar inflammation, superoxide production and viral titre in X31 infected mice. Increasing Nox4 expression, potentially with gene therapy, may also prove an effective treatment against influenza infection.

### **Future directions**

More experiments need to be undertaken to better understand the pathways examined in this thesis. Chapter 2 uncovered a novel and important role for Nox2 in TLR3 signalling. However, whether or not TLR3-induced Nox2 activation in endothelial cells leads to induction of NF- $\kappa$ B and not IRF3 needs to be confirmed, potentially with reporter assays. Chapter 3 identified small conductance calcium-activated potassium channels as one of the channels involved in TLR7 mediated relaxation of vascular smooth muscle, but apamin treatment did not have a similar effect to treating with K<sup>+</sup> (25mM). Other potassium channels may also be involved and should be investigated. How TLR7 activates these channels is also unclear. Investigation of TLR7 signalling and calcium-dependent pathways may give us a better understanding. Determining if phosphoinositide 3-kinase and Akt are involved in TLR3 mediated vascular relaxation would solidify the study's findings. It is also necessary to examine TLR3 and TLR7-induced relaxation *in vivo*. This could be achieved using radiotelemetry or the tail cuff method in mice treated with imiquimod or poly I:C.

Chapter 4 established that Nox4 plays a protective role in influenza infection, but the exact mechanisms through which it does so remain unclear. Further experiments should focus on the signalling pathways down stream of Nox4. Other potential drug targets may come to light.

### **Concluding Remarks**

This thesis explores the critical and multifaceted role the endothelium and the vasculature play in influenza pathology. It further exemplifies the importance of redox signalling in influenza infection

and uncovers previously unknown information about the toll-like receptors. Targeting the pathways described in these studies could be the key to helping hundreds of thousands of patients.

## References

- Aldara product sheet (2014) iNova Pharmaceuticals
- Altenhöfer, S, Kleikers, PWM, Radermacher, KA, Scheurer, P, Hermans, JJR, Schiffers, P, *et al.* (2012). The NOX toolbox: Validating the role of NADPH oxidases in physiology and disease. *Cell. Mol. Life Sci.* **69**: 2327–2343.
- Amatore, D, Sgarbanti, R, Aquilano, K, Baldelli, S, Limongi, D, Civitelli, L, *et al.* (2015). Influenza virus replication in lung epithelial cells depends on redox-sensitive pathways activated by NOX4-derived ROS. *Cell. Microbiol.* **17**: 131–145.
- Dawood, FS, Iuliano, a D, Reed, C, Meltzer, MI, Shay, DK, Cheng, P-Y, *et al.* (2012). Estimated global mortality associated with the first 12 months of 2009 pandemic influenza A H1N1 virus circulation: a modelling study. *Lancet Infect. Dis.* **12**: 687–95.
- Department of Health and Aging (2017). Australian Influenza Surveillance Report - 2017 Season Summary
- Krown, SE, Kerr, D, Stewart, WE, Field, AK, Oettgen, HF (1985). Phase I trials of poly(I,C) complexes in advanced cancer. *J. Biol. Response Mod.* **4**: 640–649.
- Li, Q, Spencer, NY, Oakley, FD, Buettner, GR, Engelhardt, JF (2009). Endosomal Nox2 facilitates redox-dependent induction of NF-kappaB by TNF-alpha. *Antioxid. Redox Signal.* **11**: 1249–1263.
- Stevenson, HC, Abrams, PG, Schoenberger, CS, Smalley, RB, Herberman, RB, Foon, KA (1985). A phase I evaluation of poly(I,C)-LC in cancer patients. *J. Biol. Response Mod.* **4**: 650–655.
- Sullivan, SG, Chilver, MB, Carville, KS, Grant, KA, Higgins, G, Komadina, N, *et al.* (2017). Low interim influenza vaccine effectiveness , Australia , 1 May to 24 September 2017. *Eurosurveillance* **678**: 1–7.
- Thomas, S, Chen, K, Keaney, J (2002). Hydrogen peroxide activates endothelial nitric-oxide synthase

through coordinated phosphorylation and dephosphorylation via a phosphoinositide 3-kinase-dependent signaling pathway. *J. Biol. Chem.* **277**: 6017–6024.

To, EE, Broughton, BRS, Hendricks, KS, Vlahos, R, Selemidis, S (2014). Influenza A virus and TLR7 activation potentiate NOX2 oxidase-dependent ROS production in macrophages. *Free Radic. Res.* **48**: 940–947.

To, EE, Vlahos, R, Luong, R, Halls, ML, Reading, PC, King, PT, *et al.* (2017). Endosomal NOX2 oxidase exacerbates virus pathogenicity and is a target for antiviral therapy. *Nat. Commun.* **8**: 69.

Vlahos, R, Stambas, J, Bozinovski, S, Broughton, BRS, Drummond, GR, Selemidis, S (2011). Inhibition of Nox2 oxidase activity ameliorates influenza A virus-induced lung inflammation. *PLoS Pathog.* **7**: e1001271.

Yang, C-S, Kim, J-J, Lee, SJ, Hwang, JH, Lee, C-H, Lee, M-S, *et al.* (2013). TLR3-triggered reactive oxygen species contribute to inflammatory responses by activating signal transducer and activator of transcription-1. *J. Immunol.* **190**: 6368–6377.

## Appendix

To make up Krebs solution, the following chemicals were made up in distilled water.

Chemical	Final Concentration (mM)	Company
NaCl	118.9	Merck
KCl	4.69	Merck
MgSO <sub>4</sub> ·7H <sub>2</sub> O	1.16	Merck
KH <sub>2</sub> PO <sub>4</sub>	1.18	Ajax Finechem
NaHCO <sub>3</sub>	25	Sigma
CaCl <sub>2</sub>	2.5	Merck
Glucose	11.1	Merck

The stock solution was made up of NaCl, KCl, MgSO<sub>4</sub>·7H<sub>2</sub>O and KH<sub>2</sub>PO<sub>4</sub>, and stored at 4°C. When in use, the stock was then diluted 1:25, the NaHCO<sub>3</sub>, CaCl<sub>2</sub> and glucose were added, the solution was kept at 37°C and bubbled with carbogen.

To make up KPSS solution, the following chemicals were made up in distilled water.

Chemical	Final Concentration (mM)	Company
KCl	125	Merck
MgSO <sub>4</sub> ·7H <sub>2</sub> O	1.17	Merck
KH <sub>2</sub> PO <sub>4</sub>	1.18	Ajax Finechem
NaHCO <sub>3</sub>	25	Sigma
CaCl <sub>2</sub>	2.5	Merck
Glucose	6.06	Merck

The glucose, KCl, MgSO<sub>4</sub>·7H<sub>2</sub>O and KH<sub>2</sub>PO<sub>4</sub> were dissolved and stored at 4°C. When in use, the NaHCO<sub>3</sub> and CaCl<sub>2</sub> were added, the solution was kept at 37°C and bubbled with carbogen.